Aus der Medizinischen Klinik und Poliklinik IV der Ludwig-Maximilians-Universität München

Direktor: Prof. Dr. med. Martin Reincke

The Effects of Hyperuricemia on Sterile Inflammation during Chronic Kidney Disease

Dissertation

zum Erwerb des Doktorgrades der Humanbiologie

an der Medizinischen Fakultät der

Ludwig-Maximilians-Universität zu München

vorgelegt von

Qiuyue Ma

aus Henan, China

2019

Mit Genehmigung der Medizinischen Fakultät

der Universität München

Berichterstatter:	Prof. Dr. med. Hans-Joachim Anders
Mitberichterstatter:	Priv. Doz. Dr. Heike Pohla
Mitberichterstatter:	Priv. Doz. Dr. Ulrich Dendorfer
Mitberichterstatter:	Prof. Dr. Holger Schmid

Dekan: Prof. Dr. med. dent. Reinhard Hickel

Tag der mündlichen Prüfung: 04.12.2019

LMU LUDWIG-MAXIMILIANS-UNIVERSITÄT MÜNCHEN

Dean's Office
Faculty of Medicine

MMRS MUNICH MEDICAL RESEARCH SCHOOL

Affidavit

Ma,Qiuyue

Surname, first name

Street

Munich

Zip code, town

German

Country

I hereby declare, that the submitted thesis entitled

The Effects of Hyperuricemia on Sterile Inflammation during Chronic Kidney Disease

is my own work. I have only used the sources indicated and have not made unauthorised use of services of a third party. Where the work of others has been quoted or reproduced, the source is always given.

I further declare that the submitted thesis or parts thereof have not been presented as part of an examination degree to any other university.

Munich, 16.Dec.2019

Place, date

Qiuyue Ma

Signature doctoral candidate

Table of Contents

Zusammenfassung ..... **i**

Summary ..... **iii**

Abbreviations ..... **v**

1 Introduction **1**

1.1 Chronic kidney disease **1**

1.1.1 Classification of chronic kidney disease 1

1.1.2 Risk factors of CKD 2

1.1.3 Complications of CKD 3

1.1.4 The role of immune cells in CKD 4

1.2 Hyperuricemia **6**

1.2.1 Hyperuricemia and associations with diseases 6

1.2.2 Uric acid transport 10

1.2.3 Immunological effects of uric acid 12

1.3 Acute gouty arthritis **14**

1.3.1 Gout Risk factors and Management 14

1.3.2 Mechanisms of acute gouty arthritis 16

1.3.3 The role of immune cells in acute gouty arthritis 19

1.4 The prevalence of gouty arthritis in CKD **21**

2 Hypothesis **23**

3 Materials and methods **24**

3.1 Instruments and Reagents 24

3.2 Mouse models procedures 29

3.3 Assessment of mouse kidney injury and fibrosis 32

3.4 Measurement of cytokines via ELISA 32

3.5 Clinical study procedures 32

3.6 Human blood neutrophils and $CD14^+$ monocytes isolation 33

3.7 Preparation of soluble uric acid 33

3.8 Human neutrophil extracellular traps formation and quantification 34

3.9 Transwell migration assays 34

3.10 Human LFA-1 neutrophil activation assay 35

3.11 Human monocyte stimulation assay 35

3.12 THP-1 cell culture and stimulation 36

3.13 Small interfering RNA (siRNA) transfection 36

3.14 Uric acid uptake assay in THP-1 cells 36

3.15 RNA analysis 36

3.16 Flow cytometry 40

3.17 Statistical analysis 41

4 Results **42**

4.1 Establishment of a mouse model of Hyperuricemia with or without chronic kidney disease 42

4.2 Hyperuricemia contributes to CKD-related suppression of acute gouty inflammation 45

4.3 Hyperuricemia and CKD synergistically attenuate MSU-crystal-induced leukocyte

rolling, adhesion, and extravasation in vivo..... 50
4.4 Soluble UA inhibits human neutrophil activation, β2 integrin expression and transmigration in vitro..... 53
4.5 Hyperuricemia in uremic patients suppresses neutrophil migration..... 57
4.6 Uremia does not affect MSU crystal-induced NET formation in ESKD patients..... 62
4.7 Soluble UA suppresses the monocyte function..... 64
4.8 Soluble UA modulates monocyte function by intracellular uptake via SLC2A9/GLUT9. 71

5 Discussion..... 77
5.1 Overview..... 77
5.2 The suppressive effect of hyperuricemia on sterile inflammation..... 77
5.3 Hyperuricemia mediates neutrophil migration but not NET formation..... 79
5.4 Hyperuricemia mediates the inflammatory function of monocytes..... 82
5.5 Limitations of this study..... 85

6 Conclusions..... 87

7 Future directions in the context of hyperuricemia..... 89

8 References..... 91

9 Acknowledgements..... 103

10 Appendix..... 104

Declaration

I hereby declare that all of the present work embodied in this thesis was carried out by me from 10/2015 until 01/2019 under the supervision of Prof. Dr. Hans Joachim Anders and Dr. Stefanie Steiger, Nephrologisches Zentrum, Medizinische Klinik und Poliklinik IV, Innenstadt Klinikum der Universität München. This work has not been submitted in part or full to any other university or institute for any degree or diploma.

Part of the work was supported by others, as mentioned below:

1. Prof. Dr. med. Markus Sperandio, Ph.D. Monika Pruenster and Roland Immler Walter-Brendel-Center of Experimental Medicine Biomedical Center, Klinik III, Ludwig-Maximilians-Universität München, Munich, Germany.

   They have performed the intravital microscopy of postcapillary venules of the cremaster muscle for investigating leukocyte migration in living mice. The data are presented in the results section 4.3 of this thesis.

Date: …… Signature: ……..

Place: Munich, Germany (Qiuyue Ma)

Zusammenfassung

Die Hyperurikämie (HU), gekennzeichnet durch einen erhöhten Harnsäurewert im Blut (Serum Harnsäure ≥7.0 mg/dl bei Männern und ≥6.0 mg/dl bei Frauen), tritt häufig bei Patienten mit einer chronischen Niereninsuffizienz (CNI) / Niereninsuffizienz im Endstadium (ESKD) auf, und ist mit einer Vielzahl an Erkrankungen assoziiert. Jedoch ist die Kausalität der löslichen Harnsäure bei diesen Krankheiten umstritten. Unter bestimmten Bedingungen kann die lösliche Harnsäure zu Mononatriumurat (MSU)-Kristallen im Gelenk ausfallen und eine akute Entzündungsreaktion auslösen, bekannt als Gichtarthritis. Während eine persistierende HU stark mit der Gichtarthritis verbunden ist, kann eine rapide Reduzierung der HU mittels Harnsäure-senkender Therapie auch zu einem akuten Gichtanfall führen. Außerdem ist die Prävalenz akuter Gichtanfälle bei Patienten mit CNI viel niedriger als erwartet trotz persistierender HU. Das Ziel dieser Doktorarbeit war, zu untersuchen ob die lösliche Harnsäure eine immunmodulatorische Wirkung auf die MSU-Kristall-induzierte Entzündungsreaktion hat.

Um dies zu untersuchen, haben wir ein Tiermodell basierend auf dem Urat-Transporter Glut9 etabliert. Dazu wurden sechs Wochen alte Alb-creERT2/*Glut9*$^{lox/lox}$ Mäuse oder *Glut9*$^{lox/lox}$ Kontrollmäuse mit Tamoxifen injiziert, um die Glut9-Expression in Hepatozyten zu deaktivieren. Den transgenen Tieren wurde anschließend eine fettreiche- oder Standarddiät mit dem Purin Inosin verabreicht. Nach 22 Tagen entwickelten alle Alb-creERT2/*Glut9*$^{lox/lox}$ Mäuse nach Gabe der Inosin-angereicherten Diäten eine deutliche HU (Serum-Harnsäure: 10 – 15 mg/dl). Jedoch nur Alb-creERT2/*Glut9*$^{lox/lox}$ Mäuse entwickelten eine HU und CKD (Serum-Harnstoff: 110 mg/dl; Serum-Kreatinin: 2,0 mg/dl). Um eine akute Gichtarthritis nachzuahmen, injizierten wir diese Mäuse mit MSU-Kristallen in einen bereits vorhandenen Luftbeutel auf dem Rücken. Interessanterweise fanden wir heraus, dass die HU die Leukozytenrekrutierung nach MSU-Kristall-induzierter Entzündung in dem Luftbeutel beeinträchtigte. Intravitalmikroskopie des M. Cremaster zeigte, dass die HU speziell die Rollgeschwindigkeit der Leukozyten erhöhte, jedoch die Adhäsion und Rekrutierung ins Gewebe sowie die Leukozyten-bedingte Gewebeentzündung reduzierte. Die CKD-vermittelte Abschwächung der durch MSU-Kristalle-induzierte Entzündung war nach Behandlung von HU-Mäusen mit Rasburicase, einer rekombinanten Urat-Oxidase, welche die lösliche Harnsäure in das wasserlösliche Allantoin abbauen kann, vollständig reversibel.

In Neutrophilen, die aus dem Blut gesunder Individuen isoliert worden waren, verringerte die lösliche Harnsäure die β2 Integrin-Expression von LFA-1 und Mac-1, sowie die β2 Integrin-Aktivierung (die offene Konformation mit hoher Affinität), wodurch die lösliche Harnsäure die Migration der Neutrophilen in Richtung der Chemoattraktionsfaktoren IL-8, IL-1β und fMLP beeinträchtigte. Eine beeinträchtigte Migrationsfähigkeit wurde auch bei Neutrophilen von Patienten im CKD-Stadium G2-4 und G5D beobachtet. Ich konnte zudem zeigen, dass Seren von hyperurikämen ESKD-Patienten die Migrationsfähigkeit von Neutrophilen im Vergleich zu Seren von gesunden Individuen stark vermindert. Dieser Effekt war nach Vorbehandlung der Seren mit Rasburicase reversibel. Diese Daten verdeutlichten, dass die HU zu einer Beeinträchtigung der Migrationsfähigkeit von Neutrophilen von ESKD-Patienten beiträgt. Darüber hinaus schwächte die lösliche Harnsäure signifikant die durch LPS und MSU-Kristall-induzierte Toll-like- und TNF-α-Rezeptor-vermittelte Monozyten-Aktivierung, was zu einer reduzierten Freisetzung pro-inflammatorischer Zytokine führte. Dieser Prozess war stark von der intrazellulären Aufnahme der löslichen Harnsäure mittels des Urat Transporters SLC2A9 (GLUT9) in den Monozyten abhängig. Wir haben auch herausgefunden, dass die HU die Freisetzung von MSU-Kristall-induzierten Neutrophilen-extrazellulären DNA und toxischen Mediatoren (NETs) nicht direkt beeinflusst, stattdessen indirekt die NETs-Bildung durch freigesetzte pro-entzündliche, lösliche Mediatoren beeinflusste.

Zusammenfassend zeigen die Ergebnisse dieser Arbeit, dass die HU die sterile Entzündung unterdrückt, indem sie die Migration von Neutrophilen ins Gewebe und die durch den *pattern recognition* Rezeptor gesteuerte Monozyten-Aktivierung moduliert. Diese molekularen Mechanismen liefern eine mögliche Erklärung für die bislang ungeklärten klinischen Phänomene von akuten Gichtanfällen kurz nach rascher Korrektur der HU sowie die unerwartet niedrige Prävalenz von Gichtarthritis bei ESKD-Patienten trotz persistierender HU.

Summary

Hyperuricemia (HU), an excess of uric acid (UA) in the blood (serum UA ≥7.0 mg/dl for men and ≥6.0 mg/dl for women), is common in patients with chronic kidney disease (CKD)/end-stage kidney disease (ESKD) and associated with various diseases. However, the causality of soluble uric acid (sUA) remains controversial in these diseases. Under certain conditions, UA can precipitate into monosodium urate (MSU) crystals in joints, inducing an acute inflammatory response, known as acute gouty arthritis. While persistent HU is strongly associated with gouty arthritis, a rapid correction of HU with urate lowering therapy (ULT) can elicit acute gouty arthritis. In addition, only a minority of patients with advanced CKD-related HU experiences gouty arthritis. The aim of this thesis was to investigate whether sUA might exert immunomodulatory effects during sterile inflammation induced by MSU crystals.

To investigate this, we established an animal model based on the urate transporter Glut9. Six weeks old Alb-creERT2/*Glut9*$^{lox/lox}$ or *Glut9*$^{lox/lox}$ control mice were injected with tamoxifen to turn off Glut9 expression in hepatocytes and placed on a chow or high-fat diet enriched with the purine inosine. After 22 days, all Alb-creERT2/*Glut9*$^{lox/lox}$ mice fed with inosine developed HU (serum UA: 10-15mg/dl). Only Alb-creERT2/*Glut9*$^{lox/lox}$ mice on high fat diet with inosine developed HU+CKD (serum BUN: 110 mg/dl, creatinine: 2.0 mg/dl). To mimic acute gouty arthritis, those mice were injected with MSU crystals into a pre-existed air pouch. Interestingly, HU impaired leukocyte recruitment in response to MSU crystal-induced inflammation. Intravital microscopy of the cremaster muscle revealed that HU specifically increased leukocyte rolling velocity but reduced leukocyte adhesion, extravasation, and leukocyte-related tissue inflammation. The CKD-mediated attenuation of MSU crystal-induced inflammation was fully reversible by treating HU mice with rasburicase, a recombinant urate oxidase that can degrade UA into the water-soluble allantoin.

In blood neutrophils isolated from healthy individuals, sUA diminished β2 integrin expression (LFA-1 and MAC-1) and activation (the open conformation with high affinity), hence sUA impaired neutrophil migration towards the chemoattractants IL-8, IL-1β and fMLP. An impaired migratory capability was also observed in neutrophils from CKD stage G2-4 or G5D patients. Sera from hyperuricemic ESKD patients impaired the migratory capability of neutrophils compared to sera from healthy individuals. This effect was reversible after pre-treating sera with rasburicase. These further indicated that HU contributes

to the impaired ability of neutrophils from ESKD patients to migrate. Moreover, sUA attenuated LPS and MSU crystal-induced Toll-like and TNF-α receptor-mediated monocyte activation, resulting in less pro-inflammatory cytokines release, a process strongly dependent on the intracellular uptake of sUA via the urate transporter SLC2A9/GLUT9. In addition, HU did not directly affect MSU crystal-induced neutrophil extracellular traps (NETs) formation, but instead indirectly affected NET formation via monocyte-derived soluble mediators.

In summary, the results of this thesis indicate that HU suppresses sterile inflammation by modulating neutrophil migration and pattern recognition receptor-driven monocyte activation. This process provides a molecular explanation for the previously unexplained clinical phenomena of gouty arthritis flares early after rapidly correcting HU as well as the unexpectedly low prevalence of gouty arthritis in ESKD patients despite persistent HU.

Abbreviations

ABCG	ATP-binding cassette sub-family G member
AKI	Acute kidney disease
BMI	Body Mass Index
BUN	Blood urea nitrogen
CCL	Chemokine (C-C motif) ligand
CD	Cluster of differentiation
CKD	Chronic kidney disease
CXCL	Chemokine (C-X-C motif) ligand
DAPI	4′,6-diamidino-2-phenylindole
DC	Dendritic cells
ELISA	Enzyme-linked immunosorbent assay
ESKD	End-stage of kidney disease
FBS	Fetal bovine Serum
fMLP	N-formyl-methionyl-leucyl-phenylanine
GFR	Glomerular filtration rate
GLUT9	Glucose transporter 9
GWAS	Genome-wide Association Study
HU	Hyperuricemia
IL	Interleukin
KIM-1	Kidney injury marker-1
LFA-1	Lymphocyte function-associated antigen 1
LPS	Lipopolysaccharides
MAC-1	Macrophage-1 antigen

MFI	Mean fluorescence intensity
MPO	Myeloperoxidase
mRNA	Messenger Ribonucleic Acid
MRP	Multidrug-resistance proteins
MSU	Monosodium urate
NE	Neutrophil elastase
NETs	Neutrophil extracellular traps
NFKB	Nuclear factor kappa-light-chain-enhancer of activated B cells
NLRP3	NOD-like receptor family, pyrin domain containing 3)
OAT	Organic anion transporter 1
PAS	Periodic acid Schiff staining
PMA	Phorbol myristate acetate
PSGL-1	P-selectin glycoprotein ligand-1
RNA	Ribonucleic acid
ROS	Reactive oxygen species
RPTECs	Renal proximal tubules cells
RT-PCR	Reverse transcription polymerase chain reaction
SLC22A	Organic anion transporter
sUA	Soluble uric acid
TLRs	Tool like receptors
TNF-α	Tumor necrosis factor alpha
UA	Uric acid
VLA-4	Very Late Antigen-4

1 Introduction

1.1 Chronic kidney disease

1.1.1 Classification of chronic kidney disease

Chronic kidney disease (CKD), formerly known as chronic kidney injury is a global public health problem affecting almost 10% of the world population. In Latin America, Europe, East Asia and the Middle East, the prevalence of CKD increases even up to approximately 12%. In contrast, South Asia and Sub-Saharan Africa report the lowest prevalence with 7% and 8%, respectively[1]. The incident of CKD also varies due to age, ethnicity, economic status and other factors[2].

CKD is a progressive loss of kidney function, which is characterized by a persistent abnormality in the function of the kidney [glomerular filtration rate (GFR) below 60 ml/min/ 1.73 m^2] over a period of three months[3]. GFR and albuminuria are well-established indicators for CKD because the GFR is used for evaluating kidney excretory function and albuminuria for kidney permeability. The different severity stages of CKD based on GFR and albuminuria are classified in the kidney disease improving global outcomes (KDIGO) guidelines, as shown in Figure 1.

Low risk
Moderately increased risk
High risk
Very high risk

GFR categories (ml/min per 1.73 m2) Description and range				**Persistent albuminuria categories** Description and range		
				A1	A2	A3
				Normal to mildly increased	Moderately increased	Severely increased
				<30 mg/g <3 mg/mmol	30–300 mg/g 3–30 mg/mmol	>300 mg/g >30 mg/mmol
	G1	Normal or high	≥90			
	G2	Mildly decreased	60-89			
	G3a	Mildly to moderately decreased	45-59			
	G3b	Moderately to severely decreased	30-44			
	G4	Severely decreased	15-29			
	G5	Kidney failure	<15			

Figure 1: The KDIGO classification of CKD. Summary of KDIGO 2012 CKD Guideline: Behind the scenes, need for guidance, and a framework for moving forward.[4] Reproduced with permission.

1.1.2 Risk factors of CKD

Modern lifestyles, such as unhealthy diets, lack of exercise, smoking and drinking, are direct causes of obesity, diabetes, and elevated hypertension, which in turn arises the risk for developing CKD. Hypertension, diabetes and obesity have become the main causes of CKD. In addition, in developing countries infections and heavy metal or pesticides exposures play a big role in contributing to CKD.

Hypertension

Hypertension is closely related to various causes of CKD. As kidney function declines, blood pressure tends to increase, which in turn impairs kidney function[5]. In 2000, more than 25% of the adult population have high blood pressure, which is expected to increase to 60% by 2025[6]. Blood pressure severity is directly related to the risk of end-stage kidney disease (ESKD) in both men and women[7]. One study including 3612 adults with CKD shows that the prevalence of hypertension was 86%, while only 29% in the general population[8].

Diabetes

Regardless of income, diabetes is a major cause of CKD all over the world. Among all types of CKD, diabetic nephropathy accounts for 30-50%. In most developed countries, diabetes is the leading cause of ESKD, and the prevalence of ESKD in the world has increased significantly. Notably, 285 million (about 6.4%) of adults worldwide have diabetes, and the global prevalence of diabetes is expected to reach 642 million by 2040. Therefore, improving outcomes for patients with diabetes and CKD have critical health and economic implication[9].

Obesity

Obesity, the largest epidemic in the near history carries a markedly increased risk for CKD. Between 1978 and 2013, the proportion of overweight and obese adults (body mass index (BMI) above 25kg/m^2) worldwide increased from 28.8% to 36.9% among men, and from 29.8% to 38.0% among women[10]. In particular, the obesity rate in the Middle East and North America is more than 30%[2]. Meanwhile, patients with ESKD in North America who underwent dialysis had a much higher incidence of obesity than the general population[11], and a survey of the European populations found that high levels of BMI were among the most dangerous factors in new-onset long-term kidney disease[12]. However, it is still not clear whether obesity affects the development of early kidney disease.

Obesity not only aggravates the risk of CKD directly but also influences other chronic diseases such as diabetes and high blood pressure, which indirectly impair CKD[13]. Especially, obesity is known to be a frequent cause of type 2 diabetes and diabetic kidney disease[14]. In obese people with a high salt and protein intake, the oxidative stress level, kidney damage and inhibited glomerular auto-regulation will increase[15]. Changes in renal hemodynamics and adipose tissue-derived adipokines play a key role in obesity-associated nephropathy[16].

Other factors

Acute kidney injury (AKI) episodes are also a risk factor for CKD. If AKI is not treated promptly and effectively, it can cause damage to the kidneys by irreversible nephron loss, thus exacerbating the development of CKD[2]. Men are more likely to develop CKD than women, and have a higher chance of ESKD[1]. Infectious diseases, e.g. hepatitis B and hepatitis C infection affect about 500 million population in the world, and they are associated with severe kidney disease[17]. Certain populations, such as Australian natives, African Americans, South Asian and Pacific Islanders, are at higher risk than others, which implies the importance for genetic factors in increasing the risk of developing CKD[18]. Studies have shown that variants in the *APOL1* gene are almost exclusively present in people of West African origin and that these variants are strongly linked to increased risk of human immunodeficiency virus-associated nephropathy[19,20]. Environmental factors, heavy metals and organic compounds in the soil, such as pesticides, can also cause kidney damage[21]. Air pollution with elevated levels of fine particles at aerodynamic diameter above 2.5 μm (PM2.5) are significantly associated with risk of incident CKD, eGFR decline, and ESKD[22].

1.1.3 Complications of CKD

The kidney is related to a variety of critical processes of body homeostasis. The outcomes of CKD are complex and related with other diseases. Cardiovascular disease, anemia, hypertension, mineral bone disorder, infections, volume overload, electrolyte, and acid-base abnormalities are well defined CKD complications[23].

Cardiovascular disease

Cardiovascular disease is a class of diseases that pertain to the blood vessels of the heart, e.g. hypertension, coronary artery disease, heart attack, and stroke, are leading causes of death and closely interrelated with CKD[24]. In CKD, studies have shown the prevalence of vascular calcification ranges from 47%-92%[25]. It is estimated that patients with a GFR below 60ml/min/1.73 m^2 have 57% higher mortality and 33% higher risk of a non-fatal myocardial

infarction than people without CKD[26]. When it comes to micro-albuminuria, the mortality and risk of non-fatal myocardial infarction are even higher, 63% and 48%, respectively[27]. A large analysis of 83 studies found an inverse linear association between GFR and risk of stroke, the risk increased by 7% for every 10ml/min/1.73 m^2 decrease in GFR[28].

Anemia

Anemia is one of the common characteristics of CKD and the incidence increases as GFR declines. The reduction of renal erythropoietin reduced lifespan of red blood cells, iron deficiency and repetitive blood loss contribute to anemia in CKD[29]. The overall prevalence of CKD-related anemia is around 50%[30]. The severity of CKD is also associated with the prevalence of anemia, 25% with CKD stage 1, 50% with CKD stage 2, 3 and 4, and 75% of CKD patients starting dialysis suffer from anemia[30].

CKD Mineral and Bone Disorders

CKD mineral and bone disease is another common complication of CKD. It occurs when impaired kidney function and irregular hormone levels cause alterations in bone mineral metabolism, calcium and phosphate homeostasis. Changes start in the early stage of CKD and will progress when GFR declines[31].

Infections

Infections represent an important cause for the increased morbidity and mortality among uremic patients, especially ESKD patients, mainly as a result of the altered functions of neutrophils, monocytes, dendritic cells (DCs) and T cells, which are linked with higher risk of infection[32]. Disabled immune response and infection susceptibility seen in peritoneal dialysis patients also can to be triggered by impaired maturation of T helper lymphocytes[33].

1.1.4 The role of immune cells in CKD

CKD leads to multifaceted changes in the immune system. On the one hand, CKD patients have significantly increased blood levels of inflammatory cytokines, e.g. interleukin (IL)-10, IL-6, tumor necrosis factor (TNF)-α, mainly due to decreased renal clearance, uremic toxins, oxidative stress and elevated inflammatory cytokines originated from CKD complications[34]. On the other hand, uremia and the imbalance of the internal environment suppresses immune cells function. Under healthy conditions, immune cells such as neutrophils, monocytes/macrophages, and lymphocytes maintain homeostasis and are effective to combat any inflammatory or infectious immune response, for example clearing of pathogens or dying

cells. In CKD patients, however, these immune defense mechanisms are impaired, leading to a higher susceptibility to infections[35]. One immune mechanism is the inappropriately high rate of dying cells (e.g. apoptotic cell death) under uremic conditions, which attenuates the immune response[36,37]. This defective immune response in uremia is associated with an imbalance between pro-inflammatory and anti-inflammatory mediators such as cytokines, and pro-apoptotic and anti-apoptotic factors[35].

Neutrophils in CKD

Neutrophils are polymorphonuclear leukocytes and have a short life span in human and mouse circulation[38]. Neutrophils can be found in the bone marrow, blood, spleen, liver and lung under physiological conditions[39]. In the absence of an inflammatory signal, neutrophils die via apoptosis and are cleared by macrophages in the bone marrow and other tissues[39]. During inflammation or infection, however, neutrophils are the first cells to enter the site of inflammation, where they are able to remove debris and pathogens through various mechanisms, such as releasing neutrophil extracellular traps (NETs), secreting proteases, and producing reactive oxygen species (ROS). Neutrophils dysfunction will lead to an increased risk of bacterial infection.

CKD leads to an impaired renal metabolic function resulting in the production of numerous metabolic waste and toxic substances, which then accumulate throughout the body. Neutrophils isolated from uremic patients show functional changes, such as reduced chemotactic activity, lower cellular phagocytic response and reduced oxidative metabolism leading to intracellular killing[40]. Neutrophils chemotactic function is critical for appropriate recruitment to the sites of inflammation. Uremic toxins, such as urea, granulocyte inhibitory protein[41], modified ubiquitin[42], leptin[43], glucose-modified serum protein and free immunoglobulin light chain[37,44], resistin[45], parathyroid hormone[46], medium molecular weight uremic toxin and endogenous polyamine, all are inhibitors that can suppress neutrophils chemotactic activity.

Uremia also accelerates neutrophil apoptotic cell death, which may explain the low-grade of chronic inflammation in patients with ESKD[37]. Interestingly, some uremic components have also been found to delay neutrophils apoptosis, e.g. Ig light chains[47], advanced glycation end products[44], oxidized low-density lipoproteins[48], and TNF-α[49]. When apoptosis is delayed, neutrophils survive longer and enhance their ability to fight against infections. However, such neutrophils are more prone to necrosis, leading to a low-grade chronic inflammation by

releasing pro-inflammatory cytokines[32]. In addition, initiation of apoptosis will reduce necrosis-induced inflammation, hence attenuating the response to infection[50]. Further studies are needed to explore the pro-inflammatory and anti-inflammatory properties of uremia.

Monocytes in CKD

Monocytes also play an essential role in the immune system. The three main functions of monocytes are phagocytosis of invading pathogens and dying cells, presenting antigens to T lymphocytes, and cytokine and chemokine production. Monocytes circulate in the bloodstream for about one to three days before migrating into tissues, where they differentiate into macrophages or dendritic cells (DCs)[51]. Monocytes also contribute to tissue repair,[52] further illustrating their relevance to health and disease. Similar to some other primary and progenitor cells, monocytes are heterogeneous and plastic, with context-dependent functions attributed to different subpopulations[53].

The effects of uremia on monocytes are multifaceted, which is associated with dysfunction and distribution of the different monocyte subsets[54]. Monocyte dysfunction has traditionally been characterized by an overexpression of pro-inflammatory cytokines, such as IL-6 and TNF-α, that were found increased in the serum of ESKD patients[55]. Importantly, an increase in plasma levels of pro-inflammatory cytokines is associated with higher mortality in dialysis patients[56]. When cultured with uremic serum, healthy monocytes and monocyte-derived DCs exhibit decreased endocytosis and impaired maturation, similar to monocytes directly isolated from ESKD patients.[57] Besides that monocytes from hemodialysis patients were also reported with decreased antigen presentation activity[58], which might be related to the defective immune response to infection. However, opposite to the pro-inflammatory function, Ando M, *et al.* found that monocytes isolated from CKD patients on peritoneal dialysis release less IL-1β and TNF-α in response to lipopolysaccharide (LPS) compared to healthy controls[33], and they explained this might be due to the reduced monocyte expression of toll-like receptor (TLR)4[59].

1.2 Hyperuricemia

1.2.1 Hyperuricemia and associations with diseases

Uric acid (UA) is a metabolic breakdown product of purine nucleotides[60]. Birds and reptiles mainly excrete UA in a crystalline form. In most mammals including rodents, UA can be

degraded via the enzyme uricase into the more water soluble allantoin, a metabolite that is freely excreted by the urine. Therefore, the serum UA levels are extremely low < 0.5-1 mg/dl. However, humans and other higher primates lost uricase activity during evolution, as a consequence, UA is the end product of the purine metabolism[61]. In addition, the continuous UA production and the reabsorption during renal excretion, result in high serum UA levels in humans, of above ~6.0 mg/dl for adult males[62].

The excretion of UA depends mainly on three factors. First, the number of nephrons; Second, the expression levels of various UA transporters in the renal tubules, such as urate transporter 1 (SLC22A12 / URAT1), glucose transporter 9 (SLC2A9 / GLUT9), ATP-binding cassette transporter subfamily G member 2 (ABCG2), organic anion transport proteins (OAT) 1, 3, 4 and 10; and Third, the absence of other solutes that compete for secretion through these transporters[63] (discussed further in section UA transporter 1.2.2). An increase in UA production and a decline in the excretion contribute to continuously elevated serum UA levels in humans, better known as hyperuricemia (HU). Potential risk factors for HU are the environment, dietary intake, impaired kidney function and genetic-related factors.

A reduced UA excretion occurs following GFR decline (decreased kidney filtration) due to renal glomerular or tubular injury. Some diuretics, especially thiazide diuretics and other drugs such as aspirin, pyrazinamide, levodopa, ethambutol, ethanol, etc. can also interfere with the reabsorption of UA via renal tubules[64]. Organic acids, such as ketoacids and lactic acid, can competitively inhibit renal tubular UA secretion[65].

Furthermore, excessive UA production is common during the treatment of bone marrow and lymphocyte-proliferative disorders. In leukemic patients that receive chemotherapy and radiotherapy, a large number of cells dies and the nucleic acid metabolism accelerates, leading to secondary HU[66]. Excessive production of endogenous UA may also result from a purine-rich diet. Indeed, serum UA levels increase along with purine consumption in the diet[67].

Associations of hyperuricemia with diseases:

Kidney disease

Hyperuricemia is recognized as a risk factor for the development of AKI. This is clearly shown during tumor lysis syndrome where enormous tumor cell death happens during chemotherapy for haematological malignancies[68]. The tumor cell contents which are released

into the blood stream can causes an increase in serum UA levels and severe renal nephropathy[69]. Rasburicase has been approved for preventing and treating tumor lysis syndrome because it can catalyzes UA into the more water-soluble allantoin[70]. However, it is still not clear whether a decline of serum UA with rasburicase therapy will be beneficial for decreasing kidney-related problems in the long-term[71]. Epidemiological and animal studies have shown that in CKD persistent HU can lead to the deposition of UA crystals causing renal inflammation and interstitial fibrosis, better known as chronic urate nephropathy[72]. However, it is difficult to separate the independent effects of raising serum UA levels from other pathologies associated with HU and kidney disease. As such, definitive causation has not yet been proven in humans[73].

Lesch-Nyhan syndrome

Lesch-Nyhan syndrome is a congenital anthraquinone metabolic deficiency disease of X-linked recessive inheritance, characterized by the absence of hypoxanthine-guanine phosphoribosyltransferase. A defect in this enzyme impairs hypoxanthine and guanine degradation into inosine monophosphate and guanosine monophosphate but rather produce UA, which induces formation of kidney stones early in life[74].

Hypertension and cardiovascular disease

A number of epidemiological studies confirmed serum UA as an independent risk factor for the onset of hypertension. When serum UA levels increase up to 59.5μmol/L, the relative risk of hypertension onset increases to 25%[75]. Clinical studies found that 90% of patients with essential hypertension have HU, compare to only 30% of patients with secondary hypertension[76]. In addition, urate-lowering therapy (ULT) has been shown to reduce essential hypertension[77]. However, it is still a matter of debate whether increased serum UA levels lead to hypertension. For example, the association between hypertension and HU will decrease due to aging patients and the duration of hypertension[78,79].

The association of HU with heart disease is rather weak, and this link could potentially be explained by the contribution of HU with hypertension. Studies have shown that HU can induce endothelial dysfunction, an independent predictor of cardiovascular disease, by decreasing eNOS activity in endothelial cells[80] that can precede the development of atherosclerosis[81]. Thus, HU is regarded as a risk factor for cardiovascular disease progression and stroke (serum UA levels above 357 μmol/L and 416.5 μmol/L)[82]. This link is supported

by a study demonstrating that as per 1 mg/dl increase in serum UA level, the risk of cardiovascular death increases by 39%[83].

Metabolic Syndrome, Type 2 diabetes and obesity

Metabolic syndrome is characterized by hyperinsulinemia, insulin resistance and low-grade chronic inflammation. HU has been shown to be associated with the development of type 2 diabetes, but whether HU significantly contributes to the metabolic syndrome and diabetes epidemic is still a debate[84]. Similar to cardiovascular disease, a recent study showed that the contribution of HU with type 2 diabetes might be due to endothelial dysfunction and low-grade chronic inflammation[85]. In contrast, another study showed a direct effect of sUA on inhibiting pancreatic β-cells growth *in vitro* by inducing intracellular oxidative damage[86]. Insulin resistance enlarged serum UA production during the glycolysis process and free fatty acid metabolism, which directly leads to HU by increasing renal reabsorption of UA[87].

Obesity can be classified as either metabolically healthy or unhealthy, with the later being a risk factor for the development of cardiovascular disease[88]. Interestingly, HU was regarded as one of the main predictors of unhealthy obesity. In addition, obesity can contribute to the increased level of serum UA by promoting purine metabolism within adipose tissue[89]. It is difficult to clarify whether HU contribute to the disease or the disease contributes to HU.

Gouty arthritis

One metabolic disorder which has been definitely related to HU, is gouty arthritis. Gout is caused by the formation of MSU crystals in joints and periarticular spaces[90], where they induce a severe, self-limiting auto-inflammatory response[91]. As the crystallization event is critical to the pathophysiology of gout, it is clear that HU is only a risk factor for gouty arthritis, while the crystallization of UA and the ensuing auto-inflammation is the cause. This is an important distinction, as it defines the immunological action of crystalline UA as functionally different from sUA (discussed further in section 1.2.3). Although elevated serum UA levels increase the risk of an acute gout attack[92,93], only a minority of people with HU (about 25%) develop gouty arthritis in their life time[94,95].

Taken together, persistent HU is the core pathogenesis of gouty arthritis and chronic urate nephropathy, as well as Lesch-Nyhan syndrome. In addition, epidemiological studies document associations between persistent HU and cardiovascular disease, obesity or CKD progression, but whether these associations involve causal relationships remains unclear.

1.2.2 Uric acid transport

UA homeostasis depends on the balance of three factors: UA production, renal tubule secretion and reabsorption, and intestine excretion. In gout patients, renal under-excretion is the main cause for the development of HU[96]. It is estimated that the kidney accounts for approximately 70% of urate excretion and the intestine for about 30%[97]. Proximal tubular cells are the main cells involved in urate elimination from the plasma to the urine. Studies on renal urate transport have been investigating this for many years[60].

Urate transporters in the proximal renal tubule include the organic anion transporters (SLC22A family: URAT1/SLC22A12, OAT4/SLC22A11 and OAT10/SLC22A13, OAT1/SLC22A6 and OAT3/SLC22A8), multidrug-resistance proteins (MRP2/ABCC2, MRP4/ABCC4, ABCG2), sodium-phosphate transporters (NPT1/SLC17A1 and NPT4/SLC17A3), and the reabsorptive urate transporter Glut9/SCL2A9 (see Figure 2). Among those, SLC2A9, URAT1, OAT1 and OAT3 seem to be the main transporters of renal urate regulation, while the secretory transporter ABCG2 is more important for the intestinal UA transport.

GLUT9/SLC2A9

GLUT9 is a member of the SLC2 family transporters and was initially identified as a class II glucose/fructose transporter[98]. Recently, four genome-wide association studies (GWAS) found that the *SLC2A9* gene has a major effect on increased serum UA levels[99–102]. Two isoforms of Glut9 were found strongly expressed in renal proximal tubular cells (RPTECs), the long isoform Glut9a (-L) expressed on basolateral membranes and the short isoform Glut9b (-S) expressed on apical membranes (Figure 2)[103].

URAT1

URAT1 belongs to the SLC22A family and is expressed on the apical membranes of RPTECs, where it is responsible for the urate-anion exchange of UA into the cell and the export of small anionic counterions, such as lactate, out of the cell. Hypouricemic patients have high urinary UA concentrations but lower UA levels in the serum indicating a mutation in URAT1[104].

OAT1 and OAT3

Like URAT1, OAT1 and OAT3 also belong to the SLC22A family and are secretory anion-exchange transporters. They are highly expressed in the basolateral surface of RPTECs and well-known as major multi-specific drug transporters. They can transport a variety of organic anion drugs, classic physiological probes, as well as many metabolites and signaling molecules[105].

ABCG2

The urate secretory transporter ABCG2, an ATP-binding cassette sub-family G member2, is expressed in the apical membranes of RPTECs and intestinal epithelia. Unlike most other urate transporters, which largely mediate renal tubular handling of UA, the expression of ABCG2 in the intestine is much higher than in the kidney, implying that this gene mainly account for intestinal secretion of UA[106]. Lower gut excretion and higher serum UA level were found in ABCG2 knockout mice[107].

Currently, there are three mechanisms through which UA levels can be pharmacologically manipulated: 1), Xanthine oxidoreductase (XOR) inhibitors such as allopurinol and febuxostat; 2), Recombinant uricases such as rasburicase and pegloticase, and 3), Uricosuric drugs to increase renal UA excretion such as lesinurad and probenecid to target URAT1, OAT1, OAT3 and OAT4[108,109], and benzbromarone for URAT1[110]. There are also secondary uricosurics that are primarily used in patients with other comorbidities, such as losartan for hypertension and fenofibrate for hyperlipidemia, both inhibiting URAT1.

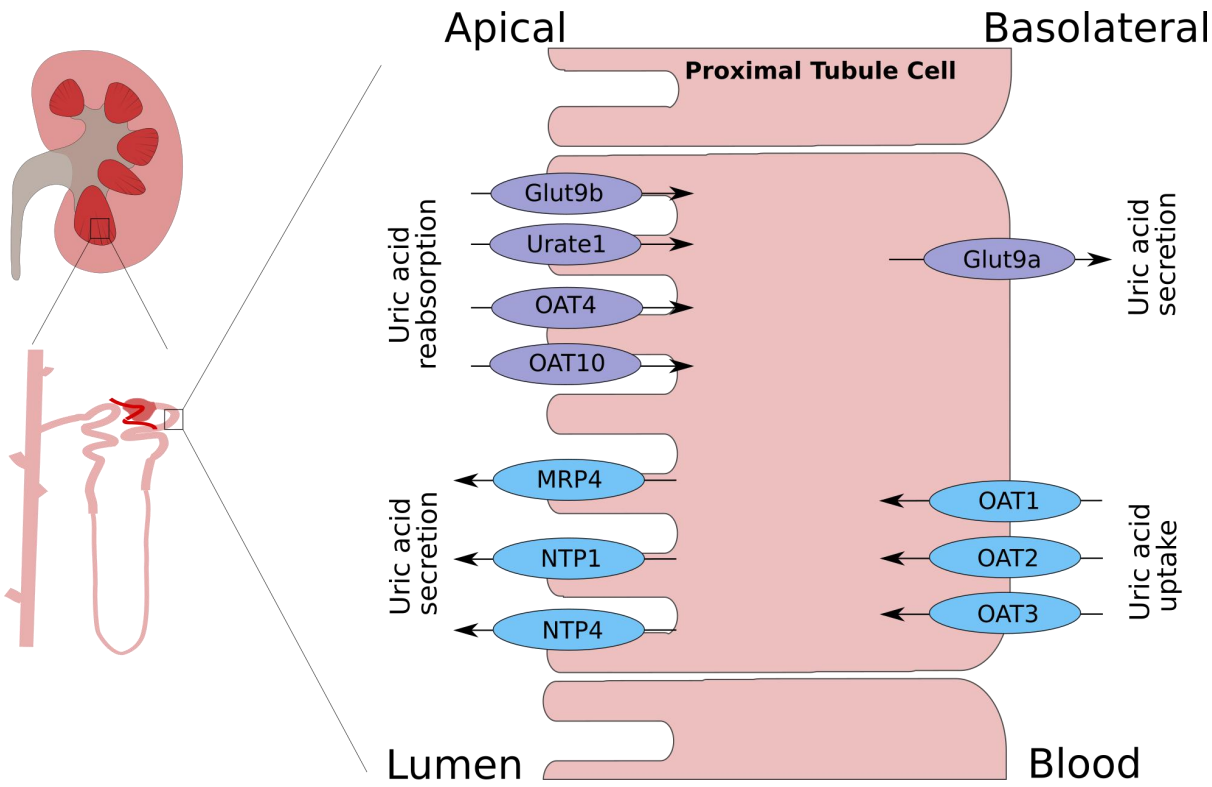

Figure 2: Urate transporters in the proximal tubule of the kidney. Transporters involved in reabsorption of urate from tubule lumen into blood are shown in violet, and those involved in secretion of urate from blood into tubule lumen are shown in blue. Abbreviations: Glut, glucose transporter; OAT, organic anion transporter; URAT, urate transporter; NPT, sodium phosphate transporter; MRP, multidrug resistant protein.

1.2.3 Immunological effects of uric acid

Crystalline monosodium urate (MSU)

MSU crystals are the causative agent for gouty arthritis, because they activate the NLRP3 inflammasome leading to IL-1β maturation from its precursor and release[111]. This in turn is a characteristic feature of an acute inflammatory response to MSU crystals within the joints (discussed further in section 1.3). In addition, MSU crystal deposits in the kidney can also induce chronic inflammation, interstitial fibrosis and glomerulosclerosis[112].

In a study by Shi, *et al.*[113], the authors show that UA acts as a strong endogenous immune adjuvant that is released from dying cells. They found that UA not only can improve adaptive immune responses but also could potentiate the generation of CD8 T-cell responses *in vivo*, indicating that MSU crystals are responsible for this adjuvant effects. Accordingly, effect of MSU crystals as an adjuvant has been studied in a murine cancer model wherein MSU crystals and *M. smegmatis* co-injection promoted tumor progression through the rapid

induction of monocyte-derived DCs[114]. Most studies have focused on the crystalline form of UA; however, the functional role of sUA remains less clear.

Soluble UA

Soluble UA has powerful antioxidant properties similar to ascorbic acid [62,115]. For example, sUA acts as a scavenger for peroxyl and hydroxyl radicals, singlet oxygen and oxygen radicals[62]. It can chelate metal ions to prevent catalyse free-radical reactions, e.g. iron ion-mediated ascorbic acid oxidation or Cu^{2+}- mediated LDL oxidation[115,116]. These antioxidant effects together may constitute protective effects of UA in aging and cancer[62]. Human studies further emphasize neuroprotective effects of high serum UA levels as an antioxidant, for example HU protects against the progression of Parkinson's disease and other kind of neurodegenerative diseases[117–119]. Furthermore, in human macrophages, sUA reduces LPS-induced TNF-α production and increases IL-10 production. The authors speculated that the pathological concentration of UA in mice do not induce an immune response in human immune cells, thus sUA exhibits anti-inflammatory activity rather than pro-inflammatory properties in human macrophages[120].

On the other hand, sUA has been identified as a danger signal that can alert the immune system to dying cells[121]. *In vitro* studies have shown that sUA inhibits IL-1Ra function in human peripheral blood mononuclear cells, leading to TLRs activation and pro-inflammatory cytokine production[122], and activates the AKT-PRAS40 autophagy pathway in human monocytes[123]. In a mouse model of unilateral ureteral obstruction (UUO), sUA activates the NLRP3 inflammasome in bone marrow-derived macrophages and aggravates kidney fibrosis[120]. Besides immune cells, sUA also has the ability to activate adipocytes with enlarged ROS production and oxidative stress[124], and decreased anti-inflammatory adipokine adiponectin production[125]. Another study showed that sUA also activates NFκB and MAPK signaling, and cell proliferation in vascular smooth muscle cells[80,126,127]. These results would suggest that sUA directly contributes to oxidative stress and inflammation.

Taken together, elevated levels of sUA seem to be a "double-edged sword" depending on the clinical context. The effects of sUA can be on one hand protective and on the other hand pro-inflammatory. Further studies are needed to unravel the exact molecular mechanisms because an association does not necessarily imply causality. Therefore, well-designed clinical studies and animal models are needed.

1.3 Acute gouty arthritis

Gout is one of the most common arthritis diseases and characterized by MSU crystals deposition in episodic joints and soft tissues. Acute gouty arthritis is triggered when MSU crystals interact with resident synoviocytes, like macrophages, which elicit an acute inflammatory response, but it is self-limited and will be resolved within a few days or 1 to 2 weeks[128]. The prevalence of gout increased globally over the last half century. For example, from 1970 to 1990 in England, gout rates rose from 0.3% to 1.0%[129] and from 1990 to 1999 in the US, from 2.1% to 4.1% on men above 75 years old[130]. In eastern China, the incidence is 1.14% in 2008 compared to the rare case in 1980[131].

1.3.1 Gout Risk factors and Management

Gout is a complex disorder, which is induced by multiple risk factors. The central element of gout is MSU crystal. Thus, risk factors contributing to HU and MSU crystal nucleation and growth are also risk factors for gout. Both non-genetic and genetic factors associate with progression of gout.

Non-genetic risk factors

Well-described dietary risks for HU and incidence of gout are: the high purines food (especially meat and seafood), soft drinks, fructose, and ethanol (beer and spirits)[132]. Both acute purine-rich foods intake and alcohol consumption increase recurrent gout attacks[133,134]. Sugars were also reported as a risk factor of both HU and gout by influencing serum UA level via the urate transporter GLUT9[135]. In contrast, coffee, dairy products and vitamin C were reported as UA lowering diet[136,137]. Why these foods affect the incidence of gout is still not fully understood. Currently, there are two possible explanations one being the increased generation of UA via hepatic metabolism[138] and the other modulating the function of UA transporters[104].

Aging causes a decline in kidney function associated with decreased excretion of UA, which can lead to HU and gout. One reason might be the alterations of connective tissues as people get older, which can serve as a nucleation spot for MSU crystals[94]. Men tend to have higher UA levels than women, especially compared to pre-menopausal women, following with 3 to 4 times higher gout risk in men[139]. Ljubojevic M, *et al*. showed that the estrogen has a uricosuric-like effect, which may explain the lower serum UA levels and less gout rate in young females[140].

Comorbid conditions, for example CKD, obesity, HU, anaemia, and hypertension are risk factors for HU (discussed in section 1.2.1) and were reported to increase the development of gout. Medications, e.g. diuretics, cyclosporine, tacrolimus, angiotensin-converting-enzyme inhibitors, non-losartan angiotensin II receptor blockers, β-blockers, pyrazinamide, ritonavir are also associated with the risk of gout[128]. In addition, factors facilitating MSU crystal formation, such as temperature, pH, salt concentration and cartilage matrix components are believed to be accountable for a higher incidence of gout attacks[141].

Genetic risk factors

Compared with environmental factors, genetic-related risk factors are more recognized recently by GWAS surveys. For example, genetic variations were identified focusing on the loci that are related to controlling urate levels (see in section 1.2.2). However, the loci that control MSU crystals formation and inflammatory response pathways are still poorly understood[142].

Gout Management

Gout management includes short-term treatment of acute inflammatory flares as well as long-term management. For acute gout attacks, a rapid and effective treatment of MSU crystal-induced inflammation is necessary to decrease joint pain and swelling in patients. There are three common anti-inflammatory drugs recommend: First, non-steroidal anti-inflammatory drugs (NSAIDs) including naproxen, ibuprofen, indomethacin and ketorolac, and non-selective inhibitors of cyclooxygenase; Second, colchicine, which will bind to neutrophils and hence inhibits the inflammatory response of neutrophils; and Third, glucocorticoids that are usually used for patients where the first two line treatment options do not provide enough pain release[143]. These drugs mentioned above can be used alone or in combination depending on the patient condition. In addition, anakinra[144], an IL-1 receptor blocker, is another potential drug being used to decrease IL-1β levels, because IL-1β is a critical pro-inflammatory cytokine released after MSU crystal-induced NLRP3 inflammasome activation[111], as well as the IL-1 blocking-related agents rilonacept and canakinumab[145].

For long-term gout management the central strategy is to lower serum UA levels to prevent recurrent gout attacks and to protect joint damage. Recently, the American college of Rheumatology guidelines suggest that UA levels should be below 6.0 mg/dl and if the signs continue, it should be lower than 5 mg/dl[146]. There are different strategies for ULT. The first recommended therapy from the American college of Rheumatology guidelines are xanthine

oxidase inhibitors, which include allopurinol (a purine analog) and febuxostat (a non-purine secective, non-competitive inhibitor), both prevent UA production. Secondly, uricosurics such as probenecid and benzbromarone, which are organic acids preventing UA reabsorption and increase kidney UA excretion. Thirdly, the uricoslytic drug pegloticase, a recombinant uricase, can convert UA into the more water-soluble allantoin. Other guidelines also suggest a reduction in fructose and alcohol consumption, avoiding high purine food, weight loss, increasing exercise, and eliminating unnecessary medications that are considered to benefit gout management[147].

1.3.2 Mechanisms of acute gouty arthritis

The synovial joint where the gout flare usually occurs consists of the synovial membrane and a variety of cellular components including fibroblasts, adipocytes, collagen fibers, proteoglycans and two main cell types: type A and type B synovial lining cells[148]. The type A cells are derived from monocytes known as tissue macrophage-like synoviocytes[149]. These macrophage-like cells can remove cellular and particulate debris like MSU crystals via phagocytosis. And the type B cells are connective tissue fibroblast-like cells, which origin from the mesenchyme[150]. The synovial membrane is also enriched with capillaries and postcapillary venules that together maintain joint homeostasis.

Monosodium urate crystallization

MSU crystals formation and precipitation in the synovial cavity is the dominant step for the induction of an acute gout attack (Figure 3)[151]. However, the mechanisms behind the crystallization process *in vivo* are still not fully understood. A decrease in UA solubility and MSU nucleation are critical steps for the priming of a gout attack[152]. Although the UA concentrations in gout patients are similar in plasma and synovial fluid, the plasma represents a better solvent for MSU[153]. Compared with the plasma environment, peripheral joints have a lower tissue temperature, ionic strength and pH, which may account for the lower solubility of UA[154]. Synovial fluid components, such as gamma globulin and type I collagen fibers, were also found to increase MSU nucleation, which was demonstrated in an *in vitro* study with synovial fluid from gout patients[152].

Acute immune response to MSU crystals

Not only is the solubility of UA influenced by its binding to plasma proteins, including inflammatory proteins, connective tissue and matrix proteins, apolipoproteins, histones, and adaptive immunity associated proteins like immunoglobulins IgG and complement[155], but

also its inflammatory potential. These protein-coated MSU crystals act as an inflammatory danger signal upon phagocytosis by resident macrophages, hence triggering cell membrane signals, for example the activation of the NOD-like receptor protein 3 (NLRP3) inflammasome. NLRP3 inflammasome activation leads to IL-1β maturation and release, as well as other multiple secondary inflammatory cytokines, chemokines and prostaglandins[111,155].

Amplified inflammation

Cytokines, especially IL-1β, released from macrophages and other cells[156], act as chemotactic factor, and subsequently leads to a rapid recruitment of neutrophils to the site of MSU crystals deposition amplifying the inflammatory response[91]. This neutrophil-centered process also includes mast cell degranulation[157], complement activation[158] and the expression of endothelium-derived selectins[159]. Once migrated in the joint, neutrophils interact with MSU crystals, inducing inflammatory mediators like nitric oxide, ROS, leukotriene B4, prostaglandins and other mediators that can damage tissue and cause pain[91]. MSU crystal-induced neutrophil activation also promotes monocyte/macrophages recruitment and activation (Figure 3).

Resolution of gouty arthritis

One characteristic feature of acute gouty arthritis, which differs from other acute inflammatory responses, is that a gout flare usually resolves within a few days or several weeks even in the absence of treatment[160]. Some negative mediators were found in synovial fluid during acute flares that might be involved in resolving inflammation, such as transforming growth factor-β, IL-10, IL-1R antagonist, TNFR-I/II, suppressors of cytokine signaling 3 and cytokine inducible SH2-containing protein[161]. In addition, inflammatory mediators and cells deactivation, apoptotic neutrophils clearance by recruited monocytes or resident macrophages, and enhanced expression of anti-inflammatory receptors also contribute to suppressing MSU crystal-induced inflammation[91]. The changed physical properties of MSU crystals may also comprise the resolution stage[152]. A recent *in vivo* study showed that aggregated NETs due to a high density of neutrophils can have a positive role in favoring the resolution of MSU crystal-induced inflammation by degrading cytokines and chemokines (Figure 3)[162].

Current therapies for managing gout are designed to suppress the different phases and stages of MSU crystal-induced inflammation[146]. Although the mechanisms of gout are well known

and effective management is available, many uncertainties still remain. For example, why does the acute attack self-resolve and why are MSU crystal deposits (also known as tophi) present within the synovium without inducing an inflammatory response? Why do MSU crystals form preferentially at certain sites? Why do tophi form in some individuals and not in others? All these observations would suggest that the existing mechanisms can modify the acute gout attack. So a better understanding of both the pro- and anti-inflammatory pathway may help to develop new strategies for the management of gout.

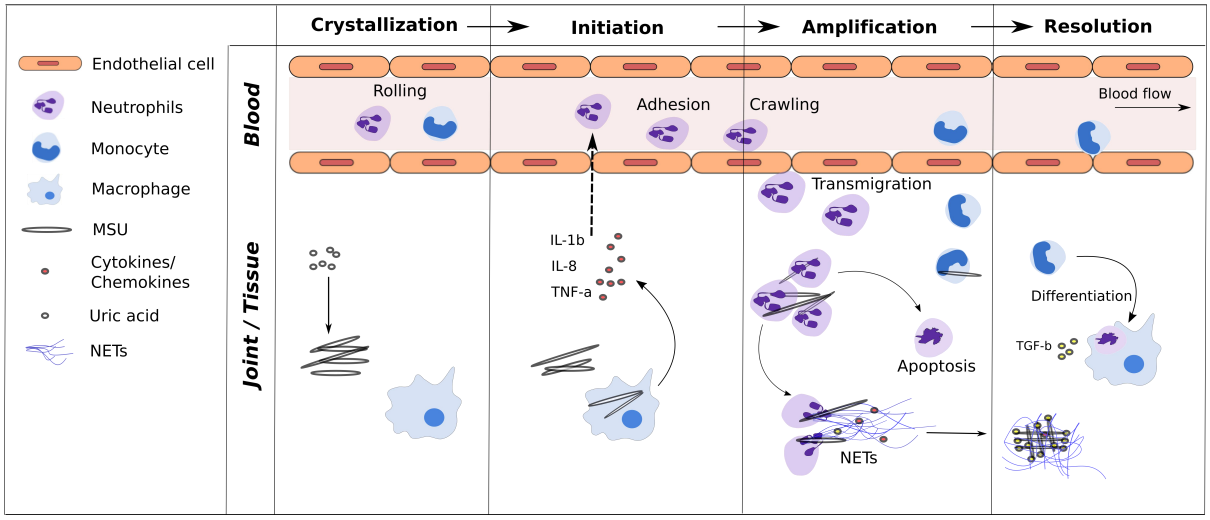

Figure 3: Mechanisms of acute gout attack. A decrease in UA solubility and MSU nucleation are critical steps for the priming of a gout attack. Deposited MSU crystals act as an inflammatory danger signal upon phagocytosis by resident macrophages, hence triggering cell membrane signals, for example the activation of the NOD-like receptor protein 3 (NLRP3) inflammasome. NLRP3 inflammasome activation leads to IL-1β maturation and release, as well as other multiple secondary inflammatory cytokines, chemokines and prostaglandins. These signals subsequently initiate a rapid recruitment of neutrophils to the site of MSU crystals deposition, where they generate superoxide and IL-8, and release NETs, amplifying the inflammatory response. MSU crystal-induced neutrophils activation also promotes monocyte/macrophages recruitment and activation. Recruited monocytes or resident macrophages take up apoptotic neutrophils and produce anti-inflammatory factors, such as TGF-β, contributing to the resolution. Recently, aggregated NETs were reported to have a positive role in favoring the resolution of MSU crystal-induced inflammation by degrading cytokines and chemokines. MSU, monosodium urate crystals; NETs, neutrophil extracellular traps; TGF, transforming growth factor; TNF, tumor necrosis factor; IL, interleukin.

1.3.3 The role of immune cells in acute gouty arthritis

During an acute gout attack, both innate immune cells (monocyte/macrophages, neutrophils, mast cells and NK cells[163]) and adaptive immune cells (T cells and B cells[164]) are involved. Among them, monocytes/macrophages and neutrophils play a key role during the inflammatory response to MSU crystals. This section will focus on what is currently known about the cellular response.

Monocytes and macrophages

The initiation of an acute gout attack is characterized by NLRP3 inflammasome activation and IL-1β release by resident macrophages[111]. Unlike monocytes, macrophages require two signals for MSU crystal-induced NLRP3 inflammasome activation: priming and activation signal. Subsequently, caspase-1 is recruited and activated, and promotes maturation of pro-IL-1β into active IL-1β[91]. The IL-1β-mediated inflammatory response is a key feature of acute gout arthritis[165].

Like neutrophils, monocytes also require adhesion molecules and chemokines, such as monocyte chemoattractant protein-1 (MCP-1) and IL-8[166] for their migration to the site of MSU crystal-induced inflammation. Furthermore, cyclooxygenase-2[167] and leukotriene B4[168] were reported to act as chemoattractants for monocyte recruitment. In a model of MSU crystal-induced peritonitis, monocytes infiltrated into the peritoneum after 4-8 hours[169]. Following their activation by MSU crystals, monocytes released pro-inflammatory mediators, such as IL-1β, TNF-α, IL-6 and CCL-2, and finally differentiated into a pro-inflammatory M1-like macrophage phenotype over time[157,169,170].

Apart from their role in the initiation phase, growing evidence shows that monocyte-derived macrophages also play a critical role during the resolution phase of acute gout. Human CD14+ monocyte-differentiated macrophages stimulated with MSU crystals in vitro have been shown to produce the anti-inflammatory cytokine transforming growth factor (TGF)-β but decreased levels of pro-inflammatory cytokines[171]. This indicated that macrophages switched from a pro-inflammatory into an anti-inflammatory phenotype. In addition, the phagocytosis of apoptotic neutrophils by macrophages triggers the production of TGF-β as well as the safe removal of MSU crystals[172]. The cellular characterization of gout tophi revealed that the tophus is composed of central MSU crystalline material with mast cells, B and T cells, and plasma cells surrounded by macrophages and multinucleated macrophage-

like cells[173], highlighting the importance of monocytes and macrophages during the resolution of gout.

Neutrophils

Neutrophils are well known for amplifying acute gouty inflammation and several mechanisms have already been reported. Inflammatory signals initiated by MSU crystals, activate the endothelium of blood vessels and induce a series of molecular processes on endothelial cells, for example, the expression of the neutrophil adhesion molecules ICAM-1, VCAM-1 and E-selectin[174]. This upregulation of neutrophil adhesion molecules on endothelial cells allows neutrophils to slowly roll and firmly adhere to the endothelium before migrating to the site of inflammation. Meanwhile, vascular dilatation and increased permeability also support neutrophil transmigration[175] along chemokine gradients, such as IL-8, nitric oxide, leukotriene B4 and IL-1[176].

Neutrophils represent a positive feedback loop whereby some extravasated neutrophils phagocytose MSU crystals leading to degranulation or direct crystal lysis of lysosomal[177], cell membrane ruptures, IL-8 release and further neutrophil recruitment. This in turn triggers the release of further inflammatory mediators, such as prostaglandin E2, nitric oxide, leukotriene B4, ROS, S100A8, S100A9, IL-1, and IL-8, as well as other mediators for tissue damage[178]. *In vitro* and *in vivo* studies showed that low concentrations of MSU crystals and culture supernatants from MSU crystal-stimulated neutrophils decreased the number of apoptotic neutrophil death[179], whereas at high concentrations MSU crystals cause NET formation, known as NETosis, associated with ROS production, autophagy and PI3K signaling[162,180–182].

Neutrophils were thought to contribute to the pathophysiology of sterile inflammation due to their cytotoxic potential. However, studies now showed that neutrophils also play an active role in resolving acute inflammation. As professional phagocytes, neutrophils are capable of phagocytosing apoptotic neutrophils, which triggers the production of TGF-β and suppresses superoxide production and IL-1β release by MSU crystal-activated neutrophils *in vitro*[183]. In response to MSU crystals, neutrophils form NET-like structures associated with the release of proteases that can trap and cleave pro-inflammatory cytokines[162]. These trapped pro-inflammatory cytokines and chemokines, such as TNF-α, IL-6 and MCP-1, are then degraded and inactivated[184]. Furthermore, Gagné and colleagues found that neutrophils once activated by MSU crystals down-regulate the myeloid inhibitory C-type lectin, which leads to

decreased IL-8 production[185]. As a result, decreased IL-8 production impaired neutrophils recruitment and thereby suppresses inflammation. This might be one possible mechanism for the self-limiting nature of gout.

1.4 The prevalence of gouty arthritis in CKD

Hyperuricemia and gout

Many epidemiological studies show that HU is strongly associated with gout and that the prevalence is increasing worldwide. In the UK and Germany, compared with those serum UA below 6mg/dl, the odds ratio in patients with serum UA between 6 to 7 mg/dl is 1.33 and 1.37, and in those with UA levels above 9 mg/dl 2.15 and 2.18, respectively[93]. In Israel, between 2000 to 2012, a follow up study found that asymptomatic HU (men above 7.0 mg/dl and women above 5.6 mg/dl) is significantly associated with the risk of developing gout, especially for men who have severe HU[186]. Recently, Dalbeth N, *et al.* included 18889 gout-free patients from four publicly available cohorts and calculated the incidence of gout based on the reference serum UA level, and they found that serum UA level is a strong non-linear concentration-dependent predictor for the incidence of gout[187]. Interestingly, only about half of those with serum UA concentrations ≥10mg/dl developed clinically evident gout over 15 years, indicating a role for prolonged HU and additional factors in the pathogenesis of gout[187]. There is no doubt that HU is a requisite for the precipitation of MSU crystals. However, it seems like that HU is not always the precursor of acute gout attack. A rapid correction of HU with allopurinol can trigger acute gout attacks in patients[188] and some patients even with normal serum UA levels (lower than 6.8mg/dl) can develop acute gout[189]. Furthermore, some individuals with persistent HU never experience gout attacks in their lives, especially those patients who suffer from CKD and HU[160]. This would indicate that HU alone is not essential for gout but rather implies a more complex role for HU in gout.

Hyperuricemia and gout in CKD

Hyperuricemia is common in CKD patients due to a decline in the excretory function of the kidneys[190]. Reduced GFR and the presence of albuminuria in CKD patients are associated with HU[191]. The cross-sectional study NHANES 2007-2010 in the US including 10,814 CKD patients with HU demonstrated that the prevalence of self-reported gout was 5.7% in CKD patients with an eGFR of 60-89 ml/min/1.73 m^2, 12.9% with an eGFR of 30-59 ml/min/1.73 m^2 and 29.8% in CKD patients with an eGFR <30 ml/min/1.73m^2[192].The German chronic

kidney disease (GCKD) study including 5,085 CKD patients also showed an increased prevalence of self-reported gout is common among patients with CKD and that lower eGFR (<30 ml/min/1.73 m^2) is strongly associated with gout (35.6%) and in CKD patients with an eGFR ≥60 ml/min/1.73 m^2 (16.0%)[193]. In patients with ESKD receiving maintenance dialysis the frequency of gouty arthritis decreases compared to CKD patients despite persistent HU possibly due to metabolic perturbations of uremia[194,195]. However, while only a minority of non-CKD individuals has HU[186,196], nearly all individuals with CKD/ESKD display persistent HU. This raises the question why do not all CKD/ESKD patients suffer from gouty arthritis? Currently, the molecular mechanisms are not well understood to why the prevalence of gouty arthritis is much lower than expected although all CKD/ESKD patients have persistent HU. It is intriguing to suggest that HU may rather act as a suppressor of the inflammatory response to MSU crystals in acute gouty arthritis.

Challenges of urate-lowering therapy in CKD

According to the 2012 ACR guidelines, ULT is recommended for patients with frequent acute gout flares (>1 per year)[146]. Pharmacological management of gout in patients with CKD is suboptimal. Whether HU contributes to the progression of CKD or is just an accidental event due to loss of renal function has been argued for many years[73,191,197,198]. Currently, there is no strong evidence recommending ULT in asymptomatic HU patients to delay the progression of CKD. Therefore, larger human trails on ULT in CKD and ESKD patients with a long follow up period are needed for a better understanding[199].

2 Hypothesis

Crystalline UA induces inflammation, and HU predisposes to MSU formation. Indeed, persistent HU is associated with gouty arthritis and it is also an important characteristic feature of CKD/ESKD. Nevertheless still only a minority of patients with persistent HU such as advanced CKD-related HU experiences gouty arthritis. Therefore, we hypothesized that HU not only is a substrate for MSU formation but also might exert independent immunomodulatory effects during sterile inflammation induced by MSU crystals.

Accordingly, the specific aims of this thesis were:

1. To investigate, whether HU has immunomodulatory effects on the acute inflammatory response *in vivo* during experimental gouty arthritis in CKD, e.g. the release of inflammatory mediators, the leukocyte rolling, adhesion and extravasation induced by MSU crystals.

2. To investigate the effect of sUA on human blood neutrophils from healthy volunteers and CKD/ESKD patients *ex vivo*, e.g. the functional impact of sUA on human neutrophil activation and migration, as well as NET formation (DNA, MPO and NE release) in response to MSU crystals.

3. To evaluate the immune-modulatory role of sUA on the inflammatory function of human blood CD14+ monocytes from healthy volunteers and CKD/ESKD patients *ex vivo* and on human monocytic THP-1 cells *in vitro*, e.g. the uptake of sUA and the associated phenotype changes regarding the release of inflammatory mediators.

3 Materials and methods

3.1 Instruments and Reagents

3.1.1 Instruments

Analytic Balance, BP 110 S	Sartorius, Göttingen, Germany
Mettler PJ 3000	Mettler-Toledo, Greifensee, Switzerland
Type B5060 EC-CO2	Heraeus Sepatech, München, Germany
Leica DC 300F	Leica Microsystems, Cambridge, UK
Olympus BX51	Olympus Microscopy, Hamburg, Germany
Tecan, GENios Plus	Tecan, Crailsheim, Germany
Heraeus, Minifuge T	VWR International, Darmstadt, Germany
Heraeus, Biofuge primo	Kendro Laboratory GmbH, Hanau, Germany
ABI prism ™ 7700 sequence detector	PE Biosystems, Weiterstadt, Germany
qRT-PCR syber green LC-480	Roche, Mannheim, Germany
Beckman DU® 530	Beckman Coulter, Fullerton, CA, USA
Nanodrop	PEQLAB, Erlangen, Germany
Cryostat RM2155	Leica Microsystems, Bensheim, Germany
FACSCalibur	BD Biosciences, CA, USA
Homogenizer ULTRA-TURRAX T25	IKA GmbH, Staufen, Germany
Microtome HM 340E	Microm, Heidelberg, Germany
pH meter WTW	WTW GmbH, Weilheim, Germany
Thermomixer 5436	Eppendorf, Hamburg, Germany
Vortex Genie 2™	Bender & Hobein AG, Zürich, Switzerland
Water bath HI 1210	Leica Microsystems, Bensheim, Germany

3.1.2 Reagents

Antibodies	**Source**
Anti-human PSGL-1	BioLegend, Fell, Germany
Anti-human VLA-4a	BioLegend, Fell, Germany
FITC linked Anti-mouse Ly6G	BioLegend, Fell, Germany
PE linked Anti-mouse Ly6C	BioLegend, Fell, Germany
PE/Cy5 linked Anti-mouse CD45	BioLegend, Fell, Germany
APC linked Anti-mouse CD11b	BioLegend, Fell, Germany
FITC linked Anti-human CD11b	BioLegend, Fell, Germany
PE linked Anti-human CD66b	eBiosciences, Germany
APC linked Anti-human CD15	eBiosciences, Germany
FITC linked Anti-human CD14	BioLegend, Fell, Germany
PE linked Anti-human CD15	BioLegend, Fell, Germany
APC linked Anti-human CD16	BioLegend, Fell, Germany
Cit. histone H3, red	Cell Signaling, Danvers,MA
FcR block	BD Biosciences, Germany
Neutrophil elastase, green	Santa Cruz biotechnology, San Cruz, CA
Anti-DNA	Roche, Germany
Anti-human MPO	AbD Serotec, Raleigh, North Carolina
mAB24 (clone 24)	Gallios, Beckman Coulter
LFA (clone HI111)	BioLegend, Fell, Germany
MAC-1 (clone ICRF44)	BioLegend, Fell, Germany
Anti-human TNF-α	BioLegend, Fell, Germany
Anti-human IL-6	BioLegend, Fell, Germany

Kits	Source
mouse IL-6	Ray Biotech, norcross, USA
mouse IL-1β	Ray Biotech, norcross, USA
mouse CXCL-1	EBiosciences, Germany
mouse TNF-α	Biolegend, San Diego, CA
PicoGreen dsDNA kit	Fisher Scientific, Schwerte, Germany
Creatinine FS	DiaSys Diagnostic System, Holzheim, Germany
Urea FS	DiaSys Diagnostic System, Holzheim, Germany
Uric acid	BioAssay Systems, Hayward, USA
RNA extraction Kit	Qiagen GmbH, Düsseldorf, Germany

Drugs and Treatment	Source
MSU	Invivogen, SanDiego, USA
Uric acid	Sigma-Aldrich, Taufkirchen, Germany
Rasburicase	EBiosciences, Germany
PMA	Sigma-Aldrich, Taufkirchen, Germany
fMLP	Immunotools, Friesoythe, Germany
Human CXCL8	Immunotools, Friesoythe, Germany
Human IL-1β	Immunotools, Friesoythe, Germany
LPS	Sigma-Aldrich, Taufkirchen, Germany
GolgiPlug	BD Biosciences, Germany
Human TNF-α	Sigma-Aldrich, Taufkirchen, Germany

Cell culture	Source
RPMI-1640 medium	GIBCO/Invitrogen, Paisley, Scotland, UK
FCS	Biochrom KG, Berlin, Germany
Dulbecco's PBS (1×)	PAN Laboratories GmbH, Cölbe, Germany
Trypsine/EDTA (1×)	PAN Laboratories GmbH, Cölbe, Germany
HBSS	GIBCO/Invitrogen, Paisley, Scotland, UK
Fetal bovine serum	Biochrom, Berlin, Germany
Glutamine	Gibco, Invitrogen, Grand Island, NY, USA
Penicillin/Streptomycin (100×)	PAN Laboratories GmbH, Cölbe, Germany
3-um Transwell filter	Sigma-Aldrich, Taufkirchen, Germany
HEPES buffer	Sigma-Aldrich, Taufkirchen, Germany

Chemicals	Source
AEC Substrate Packing	Biogenex, San Ramon, USA
Beta mercaptoethanol	Roth, Karlsruhe, Germany
Bovines Serum Albumin	Roche,Diagnostics,Mannheim, Germany
Calcium chloride	Merck, Darmstadt, Germany
Calcium dihydrogenphosphate	Merck, Darmstadt, Germany
Dextran	Sigma-Aldrich, Taufkirchen, Germany
DMSO	Merck, Darmstadt, Germany
EDTA	Calbiochem, SanDiego, USA
Ethanol	Merck, Darmstadt, Germany
HCl (5N)	Merck, Darmstadt, Germany

Monopotassium phosphate	Merck, Darmstadt, Germany
Penicillin	Sigma, Deisenhofen, Germany
Potassium chloride	Merck, Darmstadt, Germany
Sodium azide	Roche, Germany
Sodium dihydrogenphosphate	Merck, Darmstadt, Germany
Streptomycin	Sigma, Deisenhofen, Germany
Trypan Blue	Sigma, Deisenhofen, Germany
Xylol	Merck, Darmstadt, Germany
4% Formalin	Merck, Darmstadt, Germany

Miscellaneous	**Source**
RT-PCR primers	Metabion, Munich, Germany
HumanCD14 microbeads	Miltenyi Biotec, Bergisch Gladbach, Germany
AccuCheck counting beads	Thermo Fisher Scientific, München, Germany
RNAlater^{TM} Soln	Invivogen, SanDiego, USA
Distilled water (DNAse/RNase free)	GIBCO/Invitrogen, Paisley, Scotland, UK
Sunflower seed oil	Sigma, Deisenhofen, Germany
Inosine	Sigma, Deisenhofen, Germany
Tamoxifen	Sigma, Deisenhofen, Germany

3.2 Mouse models procedures

3.2.1 Maintenance and ethical approvals

All animal experiments were performed in accordance with the directive 2010/63/EU of the European parliament and upon approval by the local government authorities Regierung von Oberbayern (reference number: ROB-55.2-2532.Vet_02-15-189). The experimental mice were housed in groups of maximum five in filter-top cages with bedding and pulp, 22.2 °C and a 12 hours light/dark cycle. Mice had free access to food and water ad libitum. Cages, litter, nest lets, houses, food and water were sterilized by autoclaving at 120 °C and 1 bar pressure for 20 minutes.

3.2.2 Mouse model of hyperuricemia and chronic kidney disease

Six-weeks old Alb-creERT2;Glut9$^{lox/lox}$ mice and Glut9$^{lox/lox}$ control mice (kindly provided by Frédéric Preitner and Bernhard Thorens, University of Lausanne, Center for Integrative Genomics, Lausanne, Switzerland) were injected with tamoxifen every alternate day for one week[200]. Then the Alb-creERT2;*Glut9*$^{lox/lox}$ mice were randomized into two groups: one group (n=7) received a high-fat diet enriched with inosine (Research Diets Inc., New Brunswick, USA) to induce hyperuricemia with chronic kidney disease (HU+CKD) and the second group (n=7) received a chow diet with inosine (Ssniff, Soest, Germany) to induce only hyperuricemia (HU) without any renal impairment for 22 days. The *Glut9*$^{lox/lox}$ mice (n=7) received only chow diet with inosine for 22 days and served as control group (healthy), as shown in Figure 4.

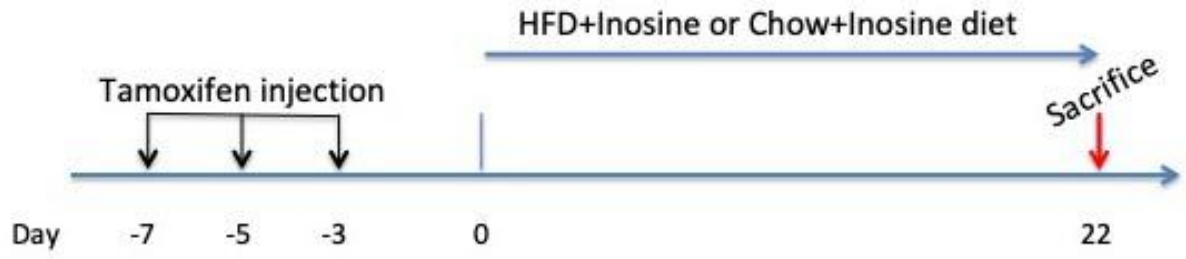

Figure 4: Flow chart of mouse model of HU with and without CKD.

3.2.3 Air pouch model of acute gouty arthritis

Alb-creERT2;*Glut9*$^{lox/lox}$ (n=18) and *Glut9*$^{lox/lox}$ (n=10) mice were injected with tamoxifen. Then the Alb-creERT2;*Glut9*$^{lox/lox}$ mice were randomized into two groups: the HU+CKD group (n=10) was fed a high-fat diet with inosine and the HU group (n=8) a chow diet with inosine. The *Glut9*$^{lox/lox}$ control mice (n=10) were fed a chow diet enriched with inosine. All the groups of mice were injected with MSU crystals (5 mg per mouse, Invivogen, San Diego, USA) into a pre-existing air pouch on day 21, a well-established mouse model of acute gouty arthritis[162]. After 12 hours, all three groups of mice (healthy, HU and HU+CKD) were sacrificed and blood, kidneys, and air pouch fluid collected for further analysis, as shown in Figure 5. To lower the UA levels in the blood, Alb-creERT2;*Glut9*$^{lox/lox}$ mice (n=20) were injected with tamoxifen and placed on a high-diet with inosine for 22 days. Then the mice were randomized into four groups: the rasburicase treated two groups were administered intravenously with rasburicase on day 16, 18 and 20 (10 mg/kg body weight) prior to MSU crystal (n=6) or vehicle (n=6) injection into the air pouch, the non-treated two groups with MSU crystals (n=4) or vehicle (n=4) injection has the same procedure as shown in Figure 6.

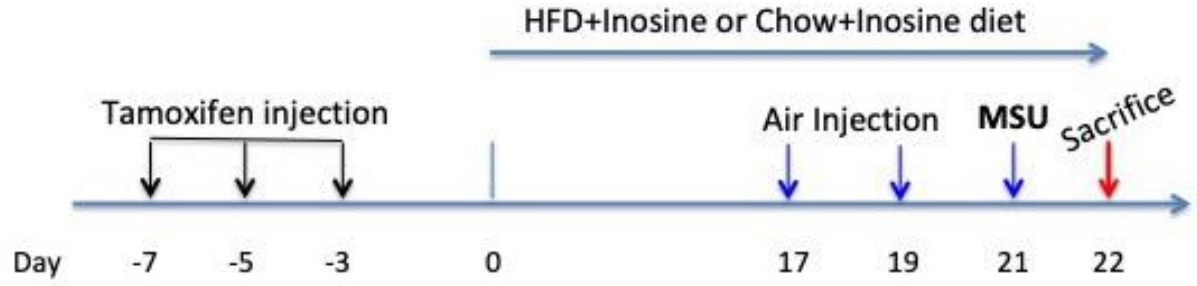

Figure: 5: Flow chart of air pouch model of acute gout in hyperuricemic mice with and without CKD.

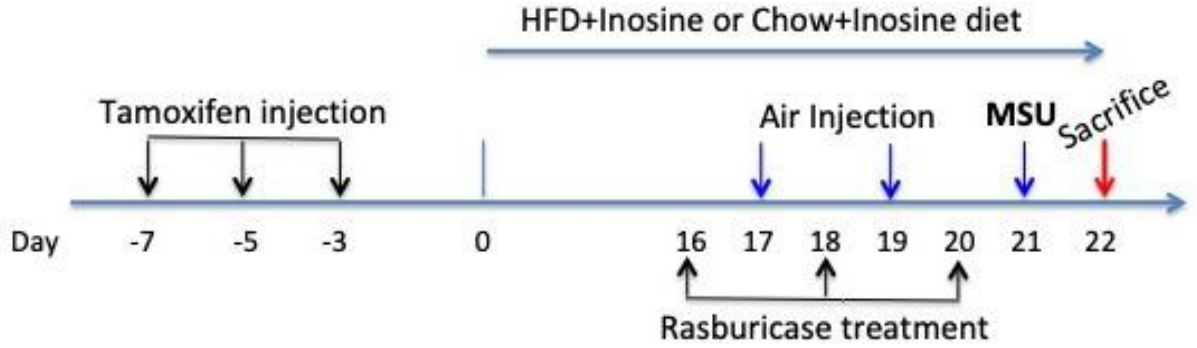

Figure 6: Flow chart of rasburicase treatment in the air pouch model in hyperuricemic mice with and without CKD.

3.2.4 Intravital microscopy of the cremaster muscle

Intravital microscopy was conducted on an OlympusBX51 WI upright microscope, equipped with a 40x water immersion objective (Olympus, 0.8NA) and a CCD camera (KAPPA CF 8 HS) as previously reported[201]. To induce inflammation, male Alb-creERT2;*Glut9*$^{lox/lox}$ (n=8) and *Glut9*$^{lox/lox}$ (n=3) mice were injected with tamoxifen. The Alb-creERT2;*Glut9*$^{lox/lox}$ mice were randomized into two groups: the HU+CKD group (n=4) was fed a high-fat diet with inosine and the HU group (n=4) a chow diet with inosine. The *Glut9*$^{lox/lox}$ control mice (n=3) were fed a chow diet enriched with inosine. After 22 days, all the groups of mice were received an intrascrotal injection of 0.5 mg MSU crystals per mouse 4 hours prior to exteriorization of the cremaster muscle, as shown in Figure 7. During the observation, the muscle was constantly superfused with thermo-controlled and gased superfusion bicarbonate buffer[202,203] and up to 6 postcapillary venules were recorded for later analysis. Centerline velocities of every recorded vessel were measured with a dual photodiode and converted to mean blood flow velocities (Circusoft Intrumentation). Rolling flux fraction, leukocyte adhesion and leukocyte rolling velocities were analyzed offline on the basis of the recorded movie sequences using FIJI software (Schindelin 2012) (n = 13 vessels of healthy mice, n = 23 vessels of HU mice, n = 22 vessels of HU+CKD mice). To assess leukocyte extravasation, exteriorized cremaster muscles were removed after intravital microscopy, fixed in 4% of paraformaldehyde, stained with Giemsa (Merck, Darmstadt, Germany) and mounted using Eukitt mounting medium (Sigma-Aldrich) (n = 5 M. cremasters of healthy mice, n = 4 M. cremasters of HU mice, n = 5 M. cremasters of HU+CKD mice). Number of perivascular leukocytes was blind analyzed at the core facility Bioimaging of the Biomedical Center with a Leica DM2500 microscope, equipped with a 100x objective (Leica, 1.4NA, oil immersion) and a Leica DMC2900 CMOS camera.

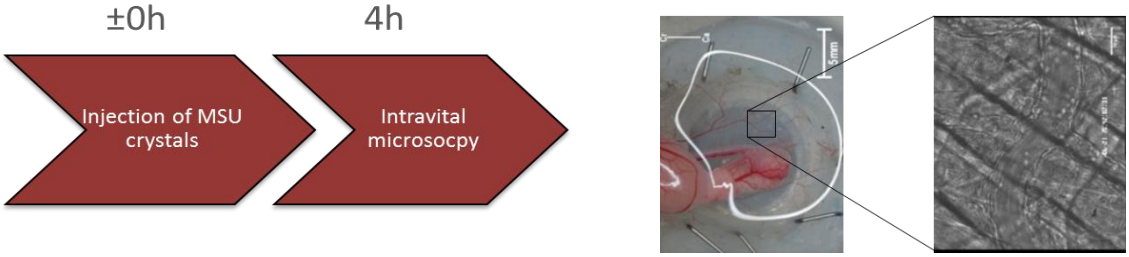

Figure 7: Schematic represents of the experimental setup of intravital microscopie of the cremaster muscle.

3.3 Assessment of mouse kidney injury and fibrosis

Serum blood urea nitrogen (BUN) and creatinine (DiaSys, Holzheim, Germany), and serum UA (BioAssay Systems, Hayward, USA) levels were measured using commercially available kits as per manufacturer's protocol. Kidneys from mice were harvested after sacrifice. One kidney was used for flow cytometric analysis and the other was divided into two equal parts. One part was kept in RNA later solution at -80°C for RNA isolation and the second part fixed in 4% formalin to be embedded in paraffin for histology analysis. Periodic acid-Schiff (PAS) and Sirius red reagents were used to assess kidney injury on 2 μm thick kidney sections.

3.4 Measurement of cytokines via ELISA

Concentrations of mouse IL-6, CXCL-1 and IL-1β in air pouch extracts were measured using the mouse ELISA kits for IL-6 and IL-1β (Ray Biotech, Norcross, USA) and CXCL-1 (EBiosciences, Germany) according to manufacturers' protocols. The absorbance was measured on a Multiskan EX reader (Thermo Electron Corporation, Germany). Briefly,

a) coat 96-well immune plate with diluted capture antibody, incubate overnight at 4°C.
b) wash plate 3 times with PBST, then incubate with assay diluent for 1 hour.
c) wash 3 times, add the standards, samples and sample diluent (blank) into each wells, incubated at room temperature (RT) for 2 hours.
d) wash 5 times, add diluted secondary antibody, incubated at RT for 1 hour.
e) wash 5 times, add Avidin-HRP, incubated at RT for 1 hour.
f) wash 5-7 times, add 100 μl of substrate, incubated for 20-30 minutes in the dark.
g) add 50 μl of 2 M H_2SO_4.
h) measured at 450 nm (reference wavelength 620 nm) using a spectrophotometer (TECAN-Genios Plus).

3.5 Clinical study procedures

The study included 10 patients with CKD (CKD, CKD stage G2-4; male/female: 6/4; mean age: 57.13 ± 5.89 years), 18 patients with ESKD that were on hemodialysis (ESKD, G5D; male/female: 11/7; mean age: 57.28 ± 3.74 years) and 15 healthy individuals without renal impairment (healthy, CKD stage G0) (male/female: 7/8; mean age: 44.50 ± 4.84 years). There was no significant difference in age between the groups. We excluded 8 patients due to the intake of immunosuppressive drugs e.g. cyclosporine, and urate lowering drugs, e.g. allopurinol, febuxostat (Figure 18). Blood was collected, centrifuged at 8000 rpm for 8 minutes and plasma transferred into 1.5 ml plastic Eppendorf tubes, and stored at -20°C until

analysis. Plasma creatinine, BUN and UA levels were measured using the creatinine FS kit, urea FS kit and the UA assay kit according to the protocol provided by the manufacturer. The study to obtain whole blood samples from healthy volunteers and uremic patients was approved by the local Ethical Review Board of the Medical Faculty at the Klinikum der Universität München (369-15). Informed consent was obtained from all subjects prior to inclusion in the study.

3.6 Human blood neutrophils and CD14$^+$ monocytes isolation

Neutrophils were isolated from human healthy individuals and CKD/ESKD patients using standard dextran sedimentation followed by Ficoll–Hypaque density centrifugation procedures[204]. Briefly, the collected whole blood was mixed with 1.25% dextran at 1:1 and after 10-20 minutes in 4 °C the red blood cells settled down, and the supernatants which contain white blood cells (WBCs). The cells were washed with D-PBS, and the WBCs were lysed with 10 ml cold distilled water for 20 seconds and the reaction was stopped using 4 ml of 0.6 M potassium chloride (KCl) buffer. The cells were then washed with DPBS, re-suspended in 4 ml DPBS and 4 ml Ficoll gradient solution added on the top. The cell solution was centrifuged for 30 minutes at 1500 rpm at 4 °C without break. After centrifugation, the peripheral blood mononuclear cells (PBMCs) layer in the middle and the neutrophil pellet at the bottom of the tube were collected.

Human PBMCs were isolated from healthy individuals and CKD/ESKD patients and CD14$^+$ monocytes purified by magnetic activated cell sorting (MACS) with human CD14 microbeads (Miltenyi Biotec, Bergisch Gladbach, Germany), according to manufacturer's protocol. Briefly, PBMCs were re-suspended in magnetic separation buffer and mixed with CD14 microbeads. After 15 minutes of incubation at 4 °C, the cells were washed and re-suspended in magnetic buffer, then cells suspension was applied onto the magnetic column, which was already placed on a magnetic cell separator. After three times of washing, the column was removed from the separator and 5 ml buffer added onto the column, the CD14$^+$ monocytes were flushed out by firmly pushing the plunger.

3.7 Preparation of soluble uric acid

UA (Sigma-Aldrich, Taufkirchen, Germany) was solubilized in 4N NaOH. Afterwards the pH was adjusted to 7.4 by adding 6N HCl and the UA stock solution (0.01M sUA) filtered sterile using a 0.22 µm filter. The concentration of sUA was examined by commercial UA assay kit, then split and stored in -20 °C for further use.

3.8 Human neutrophil extracellular traps formation and quantification

Neutrophils from healthy individuals and ESKD patients were pre-incubated with or without 10 mg/dl sUA for 1 hour prior to stimulation with PMA (25 nM; Sigma-Aldrich) or MSU crystals (200 µg/ml) for an additional 3 hours. For indirect NET formation via soluble mediators, supernatants from activated monocytes (as indicated above) were added to the neutrophil culture for 3 hours. Afterwards, neutrophils were fixed with 4% paraformaldehyde and NETs stained for citrullinated histone 3 (cit. histone H3, Cell Signaling, Danvers, MA), neutrophil elastase (NE, Santa Cruz Biotechnology, Santa Cruz, CA) and DAPI as previously described[204]. The % area of cit. histone H3 and NE and were quantified for NET formation using ImageJ software. NETs were quantified in supernatants with the MPO-DNA sandwich ELISA using an anti-DNA (Roche, Germany) and anti-human MPO antibody (AbD Serotec, Raleigh, North Carolina), as previously described[205], or with the PicoGreen dsDNA Assay Kit (Fisher Scientific, Schwerte, Germany) according to manufacturer's instruction.

3.9 Transwell migration assays

Migration assays were carried out in 24-well transwell plates using hanging chamber inserts with 3-µm pore transwell filters (Sigma-Aldrich, Taufkirchen, Germany). Neutrophils (2×10^5 cells/transwell) from healthy individuals or ESKD patients were isolated and pre-treated with or without 0.6 mM sUA for 30 minutes, or 20% serum from healthy individuals, CKD and ESKD patients (with or without 0.1 µg/ml rasburicase), and added in the upper chamber. The chemoattractants N-formyl-methionyl-leucyl-phenylanine (fMLP) (50 ng/ml), human IL-8 (100 ng/ml) or human IL-1β (250 ng/ml) (Immunotools, Friesoythe, Germany) were added to RPMI media in the bottom chamber and incubated for 3 hours at 37°C and 5% CO_2, as shown in Figure 8. Total number of migrated neutrophils/µl in the bottom chamber was quantified using AccuCheck counting beads (Thermo Fisher Scientific, München, Germany) by flow cytometry (FACSCalibur, USA).

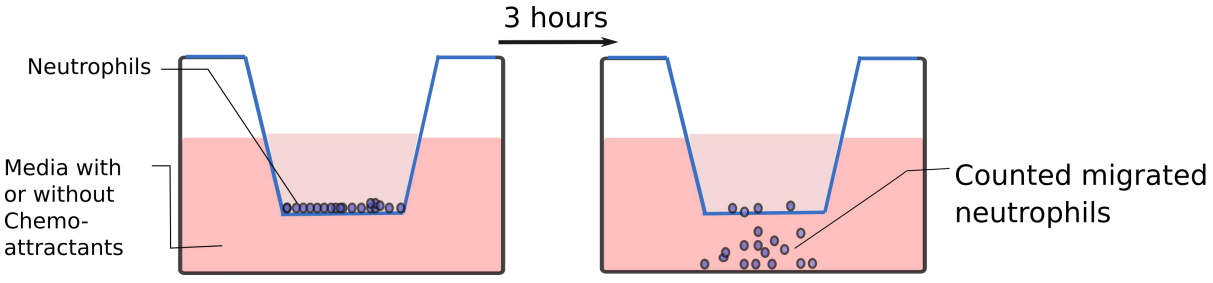

Figure 8: Schematic showing the transwell migration assay of human neutrophils.

3.10 Human LFA-1 neutrophil activation assay

β_2 integrin activation in neutrophils was assessed as previously described[206]. Briefly, isolated human neutrophils from healthy blood donors (using Polymorphprep; AXIS-SHIELD PoC AS) were incubated with sUA (0.6 mM) or carrier substance, respectively for 30 minutes at 37°C (in HBSS buffer, containing 0.1% of glucose, 1 mM $CaCl_2$, 1 mM $MgCl_2$, 0.25% of BSA, and 10 mM HEPES (Sigma-Aldrich), pH7.4) and then stimulated for 5 minutes at 37°C with CXCL8/IL-8 (0.1 mg/ml; Peprotech). Integrin activation was stopped by adding ice cold FACS lysing solution (BD Bioscience). Fully activated β_2 integrins were detected using mAB24 antibodies (clone 24) and flow cytometry (Gallios, Beckman Coulter). Human neutrophils were defined as CD15 (clone W6D3), CD66b (clone G10F5) double positive cells. In addition to that, total surface expression levels of LFA-1 (clone HI111) and MAC-1 ($\alpha_M\beta_2$ integrin; CD11b/CD18; clone ICRF44; all Biolegend) were quantified. Flow cytometry data was analyzed using Kaluza Flow analysis Software (Beckman Coulter).

3.11 Human monocyte stimulation assay

$CD14^+$ monocytes were isolated and pretreated with 10 mg/dl sUA or 20% serum from CKD or ESKD patients or healthy individuals in the presence of absence of rasburicase (0.1 µg/ml) for 1 hour, and then stimulated either with 10 µg/ml LPS (Sigma-Aldrich, Taufkirchen, Germany) or 500 µg/ml MSU crystals or left untreated (medium control). After one or four hours, total monocyte mRNA was isolated for RT-PCR, or prepared for surface marker and intracellular cytokine staining by flow cytometry, or supernatants collected for NET formation assays.

After pretreatment with 10 mg/dl sUA or medium alone, $CD14^+$ monocytes were stained with the surface antibodies: anti-human CD162 (PSGL-1), anti-human CD49d (VLA-4a) (BioLegend, Fell, Germany). For intracellular cytokine staining, $CD14^+$ monocytes were incubated with GolgiPlug for 15 minutes to avoid release of intracellular cytokines prior to stimulation. Cells were then harvested, washed and resuspended in cell fixation/permeabilization buffer for 15 minutes and washed in permwash buffer. Intracellular antibodies for anti-human TNF-α and anti-human IL-6 (BioLegend, Fell, Germany) were added for 40 minutes at 4°C. After incubation, cells were washed with PBS and reconstituted in fresh wash buffer (0.1% BSA, 0.01% sodium azide in PBS). Flow cytometric analysis was performed using the BD FACSCalibur and analyzed using the software FlowJo 8.7 (Tree Star Inc., Ashland, OR).

3.12 THP-1 cell culture and stimulation

Human monocytic leukemia THP-1 cell line was purchased from American Type Culture Collection (ATCC) and grown in RPMI-1640 culture medium supplemented with 10% fetal bovine serum (Biochrom, Berlin, Germany), 2 mM glutamine (Gibco, Invitrogen, Grand Island, NY, USA), 1 mM sodium pyruvate, 10 mM HEPES, and 1% penicillin/streptomycin (PAA Laboratories, Pasching, Austria). Cells were incubated at 37°C (with humidity) in 5% CO_2.

THP-1 cells were cultured in 6-well plates (Costar, Corning Incorporated, Corning, NY, USA) at a cell density of 1×10^6 cells/well and pre-incubated with 0.6 mM sUA for 1 hour prior to stimulation with 10 µg/ml LPS or 100 ng/ml TNF-α for another 4 hours. Cells were harvested for RNA preparation and real-time quantitative PCR (*NFKB-p50*, *NLRP3*, *ASC*, *IL-6*, *TNF-alpha*), and culture supernatants were collected and stored at -80°C until analysis.

3.13 Small interfering RNA (siRNA) transfection

SLC2A9 (GLUT9) and control siRNAs were purchased from RIBOXX (Radebeul, Germany). THP-1 cells (1×10^6 /well) were transiently transfected with 120 nM of siRNA control and SLC2A9 using the Neon™ transfection system (Thermo Fisher Scientific, Germany) with the following electroporation parameters: Pulse voltage 700 v, Pulse width 40 ms and Pulse number 4, plain RPMI medium was changed with complete RPMI medium (10% of FBS) after 4 hours post transfection. 48 hours post transfection, the cells were pre-incubated with 10 mg/dl sUA for 1 hour prior to stimulation with 10 µg/ml LPS or 100 ng/ml TNF-α for another 4 hours.

3.14 Uric acid uptake assay in THP-1 cells

Human monocytic leukemia THP-1 cells were pretreated with or without 10 mg/dl sUA for 1 hour in serum-free RPMI media and then treated with 10 µg/ml LPS or 100 ng/ml TNF-α for another 4 hours. The culture supernatants were collected after 4 hours, and the cells harvested, washed with PBS and digested. The concentration of sUA in cell culture supernatants and cytosol were measured by commercial UA assay kit and the intracellular sUA uptake rate was determined by adjusting the UA levels to cell number ($1x10^6$ cells) in each sample.

3.15 RNA analysis

The RNA extraction kit from Qiagen (Düsseldorf, Germany) was used to isolate total RNA from mouse kidneys (n = 5 per group) or human blood monocytes as well as THP-1 cells

following the manufacturer's instructions. RNA quality was assessed using a Nano drop (PEQLAB Biotechnology GmbH, Erlangen, Germany) and agarose gels before being transcribed into cDNA using reverse transcriptase (Superscript II) (Invitrogen, Carlsbad, CA). To get the cDNA, the master mix that contained RNA (Table1) was incubated at 42^0C for 1 hour and 30 minutes, then 90^0C for 5 minutes. Real-time RT-PCR was performed using SYBR Green PCR master mix (Table 2) and analyzed with a Light Cycler 480 (Roche, Mannheim, Germany). All gene expression values were normalized using *18s rRNA* or *GAPDH* as a housekeeping genes. All mouse and human primers used for amplification were purchased from Metabion (Martinsried, Germany) and are listed in Table 3.

Table 1: RNA to cDNA master mix

Reagent	Volume (µl)
RNA+ DEPC treated water	30 (contain 2 ug RNA)
5x buffer	9
25 mM dNTP	1
0.1 M DTT	2
Lin Acrylamid	0.5
40U/ µl RNAsin	1
Hexanucleotide	0.5
Superscript	1

Table 2: the RT-PCR master mix

Reagent	Volume (µl)
SYBR green master mix	10
Forward primer	0.6
Reverse primer	0.6
Taq polymerase	0.16
DEPC treated water	6.64
cDNA (1:10)	2

Table: 3. Oligonucleotide primer sequences used in the study

Mouse Genes	Primer sequences
KIM-1	Forward 5‘-TCAGCTCGGGAATGCACAA-3‘ Reverse 5‘-TGGTTGCCTTCCGTGTCTCT-3‘
Tnfα	Forward 5‘-CCACCACGCTCTTCTGTCTAC-3‘ Reverse 5‘-AGGGTCTGGGCCATAGAACT-3‘
Col1α-1	Forward 5‘-ACATGTTCAGCTTTGTGGACC-3‘ Reverse 5‘-TAGGCCATTGTGTATGCAGC-3‘
Fibronectin 1	Forward 5‘-GGAGTGGCACTGTCAACCTC-3‘ Reverse 5‘-ACTGGATGGGGTGGGAAT-3‘
18s RNA	Forward 5‘-GCAATTATTCCCCATGAACG-3‘ Reverse 5‘-AGGGCCTCACTAAACCATCC-3‘
Human Genes	**Primer sequences**
NLRP3	Forward 5‘-CTTCTCTGATGAGGCCCAAG-3‘ Reverse 5‘-GCAGCAAACTGGAAAGGAAG-3‘
ASC	Forward 5‘-AGCTCACCGCTAACGTGCTGC-3‘ Reverse 5‘-GCTTGGCTGCCGACTGAGGAG-3‘
IL-6	Forward 5‘-ACAAATTCGGTACATCCTC-3‘ Reverse 5‘-GCAGAATGAGATGAGTTGT-3‘
TNF-alpha	Forward 5‘-CTTCTCCTTCCTGATCGTGG-3‘ Reverse 5‘-GCTGGTTATCTCTCAGCTCCA-3‘
NFKB-p50	Forward 5‘-GCAGCACTACTTCTTGACCACC-3‘ Reverse 5‘-TCTGCTCCTGAGCATTGACGTC-3‘
IL-12p40	Forward 5‘-GACATTCTGCGTTCAGGTCCAG-3‘ Reverse 5‘-CATTTTTGCGGCAGATGACCGTG-3‘
CCL2	Forward 5‘-TAGATACAGAGACTTGGGGAAATTGC-3‘ Reverse 5‘-TGATTCTTGCAAAGACCCTCAAAAC-3‘
IL-10	Forward 5‘-CTGTGAAAACAAGAGCAAGGC-3‘ Reverse 5‘-GAAGCTTCTGTTGGCTCCC-3‘
SLC2A9 (GLUT9)	Forward 5‘-GCTCTTGGAGAAGCACAACGAG-3‘ Reverse 5‘-ACACCAGGCGGATGCTCCTCT-3‘
SLC22A12 (URAT-1)	Forward 5‘-TTGATTGGCAGGAGGTGA CC-3‘ Reverse 5‘-GGTTAAGTGGAGTCGGTCAG-3‘
SLC22A6 (OAT1)	Forward 5‘-CCACCTCTTCCTCTGCCTCTCCAT-3‘ Reverse 5‘-GTCTGTTTCCCTTTCCTGCTCTCC-3‘
SLC22A11 (OAT4)	Forward 5‘-CAGACCAAGCACTTCAGGAGCT-3‘ Reverse 5‘-TCCTTCACGCTGGACATCAGCA-3‘
SLC22A13 (OAT10)	Forward 5‘-TTTCCGCAACTGGAGGCTCCTT-3‘ Reverse 5‘-GTTGTATCGCCTCGTCCATCCT-3‘
GAPDH	Forward 5‘-GTCTCCTCTGACTTCAACAGCG-3‘ Reverse 5‘-ACCACCCTGTTGCTGTAGCCAA-3‘

3.16 Flow cytometry

3.16.1 Flow cytometric analysis of murine samples

Blood and air pouch fluids were collected from mice. Blood was collected in tubes containing EDTA and red blood cells lysed using ammonium chloride for 10 minutes at room temperature. White blood cells were washed in PBS buffer, centrifuged and reconstituted in wash buffer (0.1% BSA, 0.01% sodium azide in PBS). After blocking the FcR with anti-mouse CD16/32 (2.4G2) for 5 minutes, cells were stained with the surface antibodies FITC anti-mouse Ly6G, PE anti-mouse Ly6C, PE/Cy5 anti-mouse CD45 and APC anti-mouse CD11b (all antibodies obtained from BioLegend, Fell, Germany) for 30 minutes. After staining, cells were washed with wash buffer and stored at 4 °C for flow cytometric analysis.

Air pouch fluid was harvested by injecting 1 ml cold PBS into the air pouch. Air pouch extracts were retrieved with a 1 ml syringe and centrifuged at 1200 rpm for 5 minutes. Supernatants were collected and stored at -20 °C for further cytokine and chemokine analysis by Enzyme-linked immune-sorbent assay (ELISA). Air pouch extracts were suspended in wash buffer and FcR blocked for 5 minutes before staining with the surface antibodies FITC anti-mouse Ly6G, PE anti-mouse Ly6C, PE/Cy5 anti-mouse CD45 and APC anti-mouse CD11b for 30 minutes. After incubation, cells were washed with PBS and reconstituted in 1 ml fresh wash buffer. Flow cytometric analysis was performed using the BD FACSCanto II and data analyzed with the software. For determining the number of cells/µl, Invitrogen AccuCheck counting beads were used and the absolute cell counts calculated according to manufacturer's instruction.

3.16.2 Flow cytometric analysis of human samples

Neutrophils were identified as $CD15^+CD11b^+CD66b^+$ by flow cytometry and had a purity of approximately 99% (Figure 19A). The antibodies used were FITC anti-human CD11b (BioLegend, Fell, Germany), PE anti-human CD66b, APC and anti-human CD15 (both from eBiosciences, Germany) (Figure 19A). Neutrophils were suspended in RPMI ($0.5*10^6$ cells per 300 µL or $1*10^6$ cells/ml) and seeded onto eight-well microslides (Ibidi, Martinsried, Germany) or 24-well plates in a 5% carbon dioxide atmosphere at 37 °C for 30 minutes before stimulation.

Human $CD14^+$ monocytes were identified using the antibodies FITC anti-human CD14, PE anti-human CD15 and APC anti-human CD16 by flow cytometry with a purity of 88%

(Figure 22A). Monocytes were suspended in RPMI ($1*10^6$ cells/ml) and seeded onto 24-well plates in a 5% carbon dioxide atmosphere at 37 °C for 30 minutes before stimulation.

3.17 Statistical analysis

Prior to the application of any other statistical methods, the Shapiro-Wilk Normal distribution test, the Levene homoscedasticity test and the Grubb outlier test applied to the data set. Student's t-test was only used for the comparison of two normally distributed datasets. Alternatively, in the case of two non-normally distributed datasets, the Wilcoxon-Mann-Whitney test was used.

For more than two datasets, the normally distributed and homoscedastic datasets were evaluated by using one-way analysis of variance (ANOVA) with Tukey's post-test. In the case of heteroscedasticity, the post-hoc Games Howell test was used. When using two parameters with multiple groups, two-way ANOVA with Bonferroni's comparison post-hoc test was carried out.

Statistical analyses were performed using GraphPad Prism 7 (CA, USA). Unless otherwise indicated, data are presented as mean values ± standard error of the mean (SEM). Differences were considered significant if $p<0.05$; non-significant differences (ns) are indicated accordingly. Sample sizes were indicated in each corresponding figure legend.

4 Results

4.1 A mouse model of hyperuricemia with or without chronic kidney disease

Recently, the glucose transporter family member GLUT9 (encoded by *SLC2A9* gene) was reported to be a UA transporter[63]. In human and mice, GLUT9 is mainly expressed in proximal renal tubular cells and responsible for reabsorbing UA from the urine into the blood. However, in mice, SLC2A9 is also expressed in the basolateral membrane of hepatocytes and mediates the UA uptake in hepatic cells, which can be degraded via the enzyme uricase into the more water soluble allantoin, a metabolite that is freely excreted by the urine[207]. To investigate the impact of HU and CKD on sterile inflammation, we used a mouse model of HU with or without CKD by inducing liver-specific Glut9 deficiency with tamoxifen in Alb-creERT2;*Glut9*$^{lox/lox}$ mice[207] and as well as control *Glut9*$^{lox/lox}$ mice. Both mouse strains were either fed a high-fat diet enriched with the purine inosine, a precursor of UA, or a standard chow diet with inosine for 22 days.

Compared to *Glut9*$^{lox/lox}$ control mice (healthy), the serum UA levels significantly increased in all Alb-creERT2;*Glut9*$^{lox/lox}$ mice exposed to both diets indicating that the Alb-creERT2;*Glut9*$^{lox/lox}$ mice developed HU, similar to serum UA levels observed in humans (Figure 9A). However, only the Alb-creERT2;*Glut9*$^{lox/lox}$ mice on a high-fat diet had elevated blood urea nitrogen (BUN) and creatinine levels compared to the Alb-creERT2;*Glut9*$^{lox/lox}$ mice on chow+inosine diet or *Glut9*$^{lox/lox}$ control mice (Figure 9B, C).

Furthermore, PAS staining showed tubular injury and diffused tubular atrophy in HU+CKD mice but not in healthy and HU mice (Figure 9D). This was confirmed by an increased renal mRNA expression of the kidney injury marker *KIM-1* in mice with HU+CKD (Figure 9E). Intrarenal mRNA expression of the inflammatory marker *Tnfα* revealed that the HU+CKD mice had increased *Tnfα* mRNA expression levels compared to the other two groups (Figure 9F). This was in line with a significant higher number of infiltrating CD45$^+$ cells (Figure 9G) and neutrophils (Figure 9H) into the kidneys of HU+CKD mice, which implied that hyperuricemic mice with CKD showed increased tubular injury and inflammation associated with an impaired renal function compared to hyperuricemic mice without CKD or healthy mice.

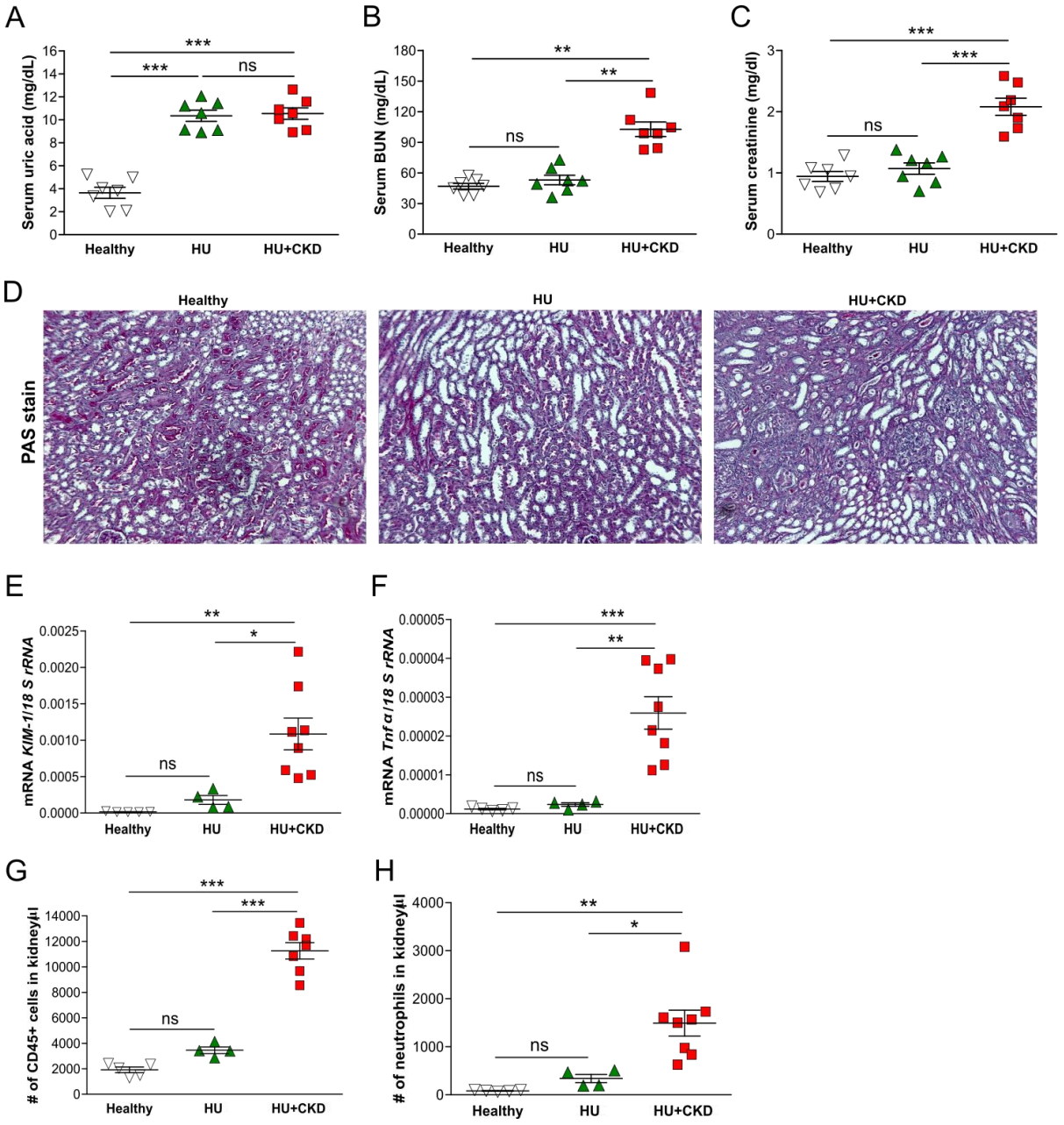

Figure 9: A mouse model of HU with or without CKD. Alb-creERT2;*Glut9*$^{lox/lox}$ mice and *Glut9*$^{lox/lox}$ control mice were injected intraperitoneal with tamoxifen. Both groups were fed either a high-fat diet enriched with inosine or a standard chow diet with inosine for 22 days. (**A** to **C**) Serum uric acid (UA) (**A**), blood urea nitrogen (BUN) (**B**) and creatinine (**C**) levels of *Glut9*$^{lox/lox}$ mice with chow diet and inosine (healthy), Alb-creERT2;*Glut9*$^{lox/lox}$ mice with chow diet (HU) and high-fat diet with inosine (HU+CKD) on day 22 (n = 7 mice per group). (**D**) Periodic acid-Schiff (PAS) staining (original magnification 100x). (**E** to **F**) Intrarenal mRNA expression levels of kidney injury marker *KIM-1* (**E**) and inflammation marker *Tnfα* (**F**) (n = 4-8 per group, one-way ANOVA). (**G to H**) Flow cytometric analysis of infiltrating CD45+ leukocytes (**G**) and neutrophils (**H**) in kidneys with absolute numbers (n = 4-8 per group, one-way ANOVA). Data are mean ± SEM. * $p<0.05$; ** $p<0.01$; *** $p<0.001$; ns = not significant.

CKD is characterized by a gradual loss of kidney function associated with glomerulosclerosis, vascular sclerosis and tubulointerstitial fibrosis. Sirius Red staining, a specific fibrosis staining for collagen type I and III, showed that only hyperuricemic mice with CKD showed interstitial fibrosis compared to healthy and hyperuricemic mice on kidney sections (Figure 10A). Consist with the fibrosis staining mRNA levels of the kidney fibrosis marker *Col1α-1* and *Fibronectin 1* were also increased in the HU+CKD mice (Figure 10B and C). Taken together, the data show a mouse model of HU with or without CKD.

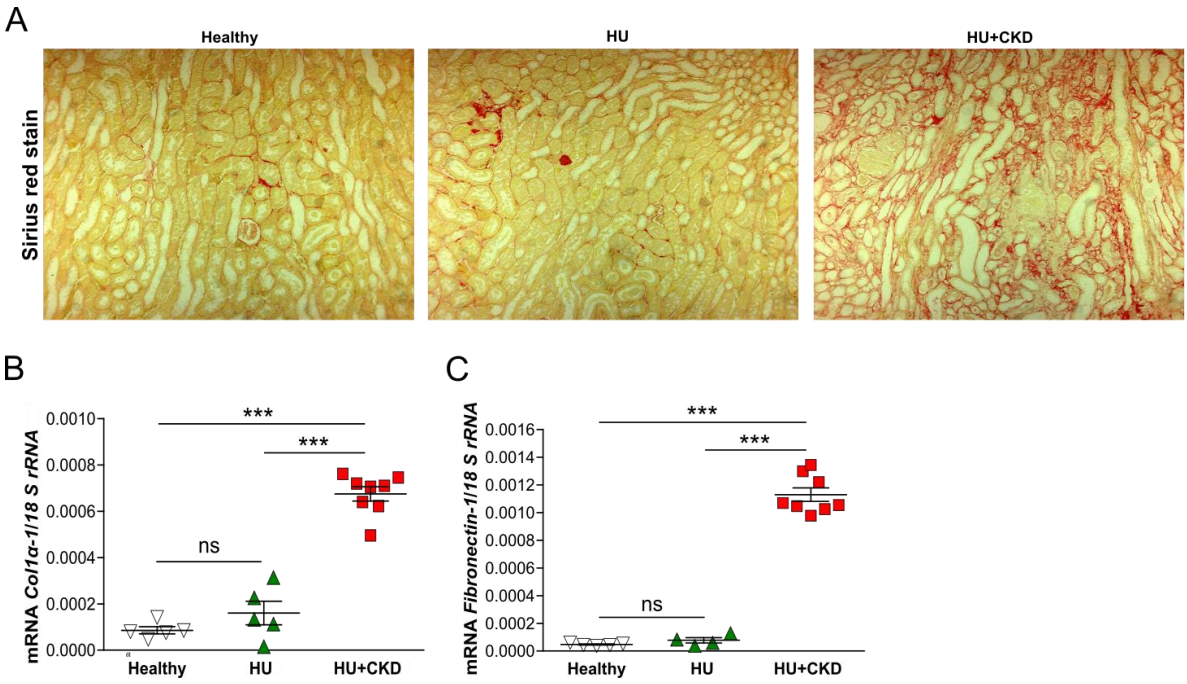

Figure 10: Alb-creERT2;*Glut9*$^{lox/lox}$ mice on high-fat diet with inosine developed kidney fibrosis. Alb-creERT2;*Glut9*$^{lox/lox}$ mice and *Glut9*$^{lox/lox}$ control mice were injected intraperitoneal with tamoxifen. Both groups were fed either a high-fat diet enriched with inosine or a standard chow diet with inosine for 22 days. (**A**) Sirius red staining of *Glut9*$^{lox/lox}$ control mice with chow diet and inosine (healthy), Alb-creERT2;*Glut9*$^{lox/lox}$ mice with chow diet (HU) and high-fat diet with inosine (HU+CKD) on day 22. (original magnification 100x); (**B** to **C**) Intrarenal mRNA expression level of the kidney fibrosis marker *Col1α-1* (**B**) and *Fibronectin 1* (**C**) (n = 5-8 per group, one-way ANOVA). Data are mean ± SEM. * p<0.05; ** p<0.01; *** p<0.001; ns = not significant.

4.2 Hyperuricemia contributes to CKD-related suppression of acute gouty inflammation

The first of our three objectives was to investigate whether HU has immunomodulatory effects on the acute inflammatory response *in vivo* during experimental gouty arthritis in CKD, e.g. the release of inflammatory mediators, the leukocyte rolling, adhesion and extravasation induced by MSU crystals. In addition, rasburicase treatment in HU mice with CKD was further tested to determine the putative contribution of HU during gout.

4.2.1 Hyperuricemia and CKD synergistically attenuate MSU crystal-induced gouty arthritis-like sterile inflammation

To mimic acute gouty arthritis[162], twice sterile air (on day17 and day 19) was injected into the intra-scapular area of the back of all three groups mice (HU+CKD, HU and healthy). The pouch primarily consists of macrophage- and fibroblast-like cells, which is similar to the synovial cavity[208]. Afterwards, 5mg MSU crystals or vehicle (on day 21) was injected into the preexisting air pouch in all three groups of mice. Twelve hours later after MSU injection, the air pouch lavage was collected. The numbers of infiltrated leukocytes were analyzed by flow cytometry and the levels of cytokines examined by ELISA.

In all three groups of mice, MSU crystal aggregates were observed as shown in Figure 11A. Flow cytometry analysis revealed a significant increase in the number of infiltrating $CD45^+$ cells, neutrophils, and monocytes in all three groups of mice that were injected with MSU crystals compared to vehicle (Figure 11B to D). However, compared to healthy mice, the number of infiltrating $CD45^+$ cells, neutrophils and monocytes into the air pouch after MSU crystal injection significantly decreased in HU mice (Figure 11B to D). This effect of impaired leukocyte infiltration was even more pronounced in HU+CKD mice (Figure 11B to D). The findings suggested that HU and CKD suppressed MSU crystal-induced leukocyte recruitment.

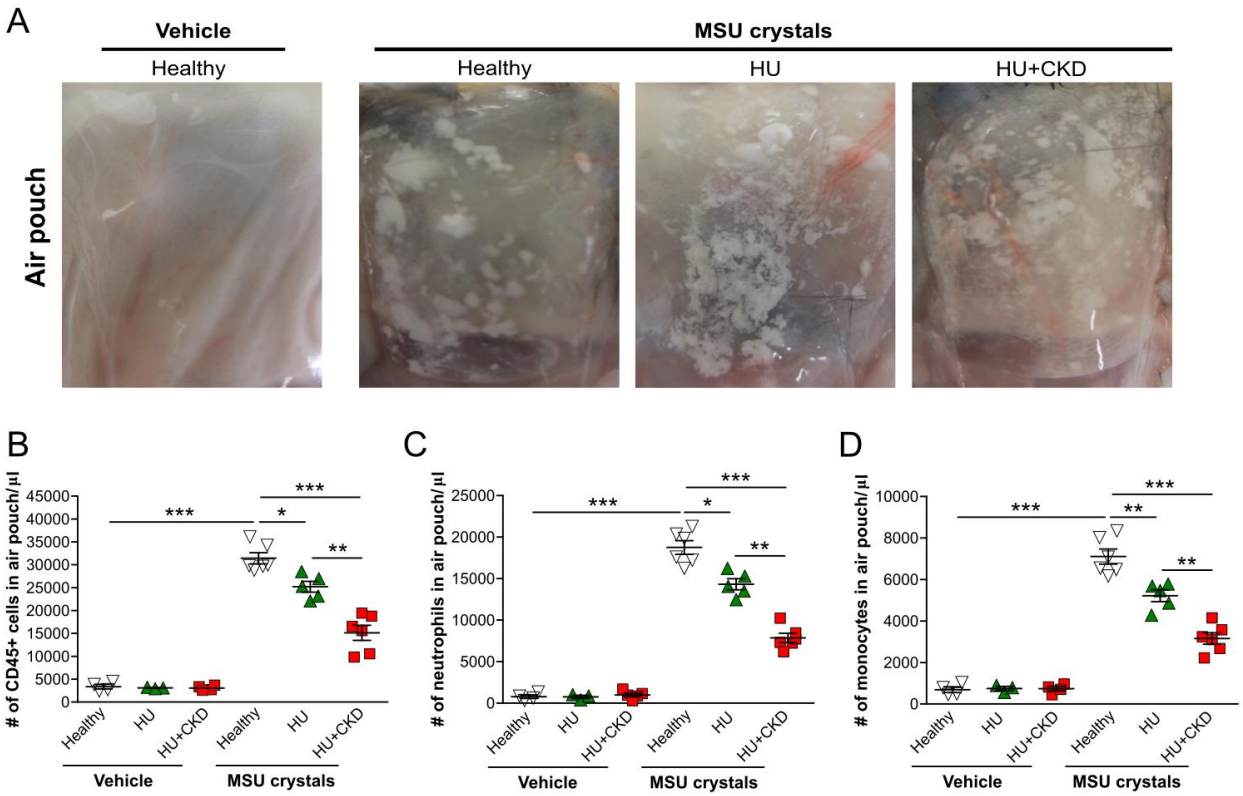

Figure 11: Hyperuricemia and CKD attenuate MSU crystal-induced leukocyte recruitment. Alb-creERT2;*Glut9*$^{lox/lox}$ mice and *Glut9*$^{lox/lox}$ control mice were injected with tamoxifen. Both groups were fed either a high-fat diet enriched with inosine or a standard chow diet with inosine for 22 days. On day 21, mice received a s.c. injection of MSU crystals or vehicle into a pre-existing air pouch, and sacrificed 12 hours later. (**A**) Representative images of vehicle and MSU crystals injected into the air pouch. (**B** to **D**) Numbers of CD45^{+} cells (**B**), neutrophils (**C**) and monocytes (**D**) in air pouch per µl from mice with or without MSU crystals determined by flow cytometry (n = 3-6 per group). Data are mean ± SEM. * $p<0.05$; ** $p<0.01$; *** $p<0.001$; ns = not significant by two-way ANOVA.

An acute gout attack is characterized by the infiltration of leukocytes and the production of inflammatory mediators including pro-inflammatory cytokines and chemokines[172]. To test the effect of HU and CKD on the inflammatory mediators also in this model, the levels of the pro-inflammatory cytokines IL-1β and IL-6, as well as the chemoattractant CXCL-1 levels in the air pouch fluid were measured. As shown in Figure 12, MSU crystal injection significantly increased the levels of IL-1β (Figure 12A), IL-6 (Figure 12B) and CXCL-1 (Figure 12C) in all three groups of mice compared to vehicle-treated mice. Consist with the flow cytometry results, the cytokine and chemokine levels were lower in hyperuricemic mice compared to healthy mice. This difference was even more significant in mice with HU and CKD (Figure 12A to C). Together, HU and CKD suppressed MSU crystal-induced leukocyte recruitment and attenuated gouty arthritis-like sterile inflammation. However, how exactly HU impairs leukocyte recruitment to the site of still needs to be explored in more detail.

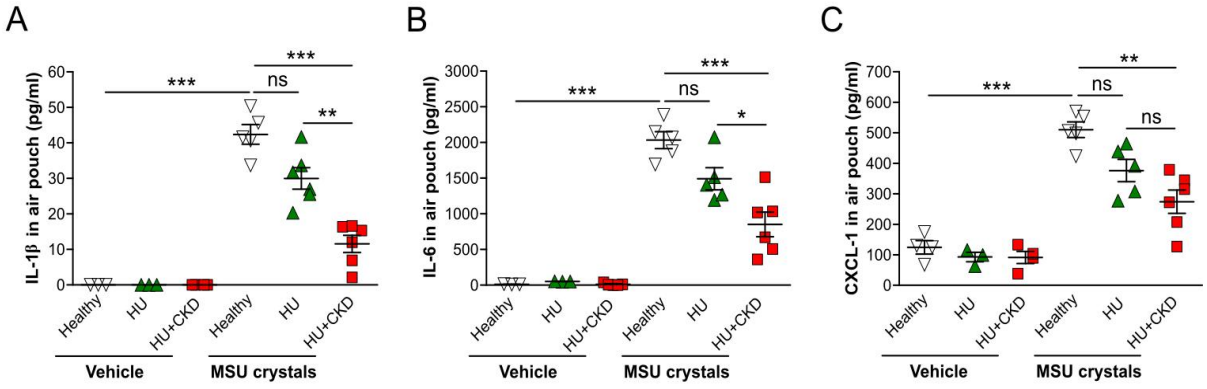

Fig. 12: Hyperuricemia and CKD attenuate MSU crystal induced inflammatory cytokines and chemokines production. Alb-creERT2;*Glut9*$^{lox/lox}$ mice and *Glut9*$^{lox/lox}$ control mice were injected with tamoxifen. Both groups were fed either a high-fat diet enriched with inosine or a standard chow diet with inosine for 22 days. On day 21, mice received a s.c. injection of MSU crystals or vehicle into a pre-existing air pouch, and sacrificed 12 hours later. (**A** to **C**) Concentrations of IL-1β (**A**), IL-6 (**B**) and CXCL-1 (**C**) measured in the air pouch fluid via ELISA (n = 3-6 per group). Data are mean ± SEM. * $p<0.05$; ** $p<0.01$; *** $p<0.001$; ns = not significant by two-way ANOVA.

4.2.2 Rasburicase treatment reversed the suppressive effect of HU

As demonstrated in section 4.2.1, HU and CKD suppressed MSU crystal-induced leukocyte recruitment and attenuated the inflammatory response. To test the putative contribution of HU during gout, the HU+CKD mice were treated with rasburicase or vehicle prior to MSU crystal injection (details in methods 3.2.3 and Figure 6). Rasburicase is a FDA-approved and commercially available recombinant urate oxidase that can degraded UA into allantoin resulting in lower serum UA levels in humans and mice[70]. Rasburicase treatment significantly decreased the serum UA levels from 10 mg/dl to 6 mg/dl compared to the vehicle-treated group (Figure 13A) without affecting the BUN levels (Figure 13B), indicating that rasburicase treatment did not improve kidney function. Importantly, rasburicase did not alter the MSU crystal deposition in the air pouch (Figure 13C).

Flow cytometry analysis showed that rasburicase treatment significantly increased the number of infiltrating $CD45^+$ cells and neutrophils after MSU crystal injection into the air pouch, while rasburicase itself did not influence the number of leukocytes in the vehicle-treated group (Figure 13D and E). In addition, the levels of IL-1β, IL-6, and CXCL-1 increased after rasburicase treatment compared to vehicle-treated HU+CKD mice upon MSU crystal injection (Figure 13F to H). These findings suggested that HU mediated in part the immunosuppressive effect of CKD during acute gouty arthritis.

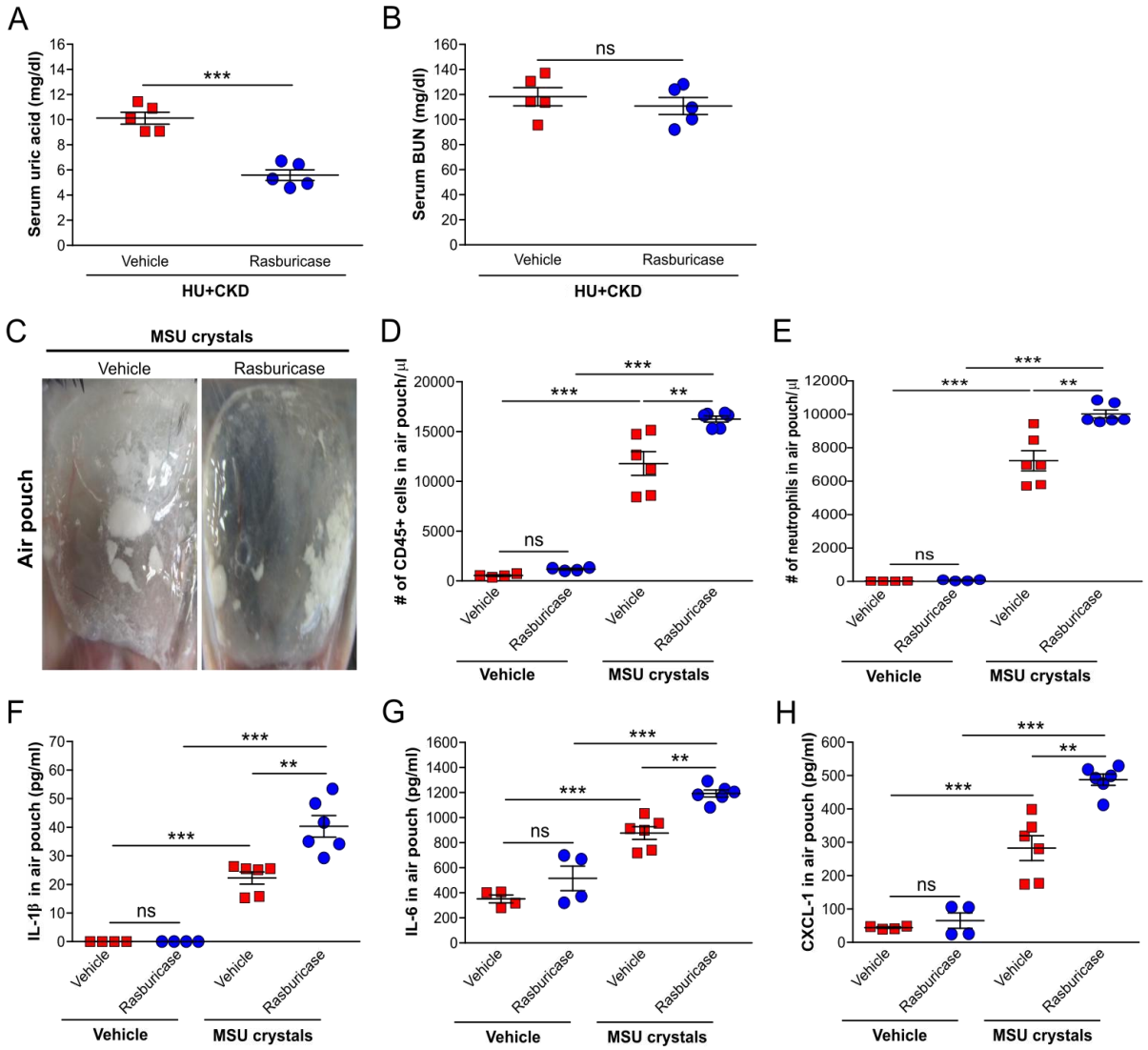

Figure 13: Rasburicase treatment increases MSU crystal-induced leukocyte recruitment and inflammation in mice with HU and CKD. Alb-creERT2;*Glut9*$^{lox/lox}$ mice were injected with tamoxifen and placed on a high-fat diet with inosine (HU+CKD) for 22 days. Mice received vehicle or rasburicase treatment prior to injection of vehicle or MSU crystals into a preexisting air pouch, and sacrificed after 12 hours. (**A** to **B**) Serum UA (**A**) and BUN (**B**) levels of HU+CKD mice with rasburicase or vehicle treatment (n = 5 per group, Student's t-test). (**C**) Representative images of MSU crystal injection into the air pouch with or without rasburicase. (**D** to **E**) Flow cytometry analysis of infiltrating CD45+ cells (**D**) and neutrophils (**E**) into the air pouch from mice with or without MSU crystals and/or rasburicase treatment (absolute numbers) (n = 4-6 per group). (**F** to **H**) Concentrations of IL-1β (**F**), IL-6 (**G**) and CXCL-1 (**H**) from air pouch fluid measured via ELISA (n = 4-6 per group). Data are mean ± SEM. * p<0.05; ** p<0.01; *** p<0.001; ns = not significant by two-way ANOVA.

4.3 Hyperuricemia and CKD synergistically attenuate MSU-crystal-induced leukocyte rolling, adhesion, and extravasation in vivo

The recruitment of neutrophils from the circulation to the site of inflammation occurs in four steps: the rolling, adhesion, crawling, and transmigration[209]. In the previous section we found that HU and CKD contribute to impaired neutrophil migation during acute gouty inflammation. To investigate the effect of HU and CKD on the different steps of the leukocyte recruitment cascade, we performed intravital microscopy of postcapillary venules in the cremaster muscles of mice from all three groups 4 hours after intramuscular injection of MSU (500 μg) crystals (see methods and materials, section 2.2.4). Intravital microscopy of postcapillary venules of the cremaster muscle is a widely used method for investigating leukocyte migration in living mice[210].

As shown in Table 1, microvascular hemodynamic parameters including vessel diameter (μm), center line velocity (μm/s) and shear stress rate (s^{-1}) were identical in all three groups of mice. We choose postcapillary venules with a diameter between 30-40 μm, because the red blood cells were easier to distinguish from leukocytes by their nuclei. The microcirculatory conditions, such as the blood flow velocity and the shear rate, normally do not have much difference.

Table 4: Hemodynamic parameters of the cremaster muscle.

Descriptive Data	Healthy	HU	HU+CKD	P value
n (mice)	3	4	4	
n (vessels)	13	23	22	
Diameter (μm)	32±2	31±1	32±1	ns (p=0.7744)
Centerline velocity (μm/s)	1577±167	1787±114	1745±149	ns (p=0.6192)
Shear rate (s^{-1})	1280±167	1438±81	1351±103	ns (p=0.6192)

Next, we analyzed the functional parameters related to leukocytes migration. The rolling leukocyte flux fraction, which indicates the percentage of leukocytes that travel across each micro-vessel[211], was higher in vessels of HU and HU+CKD mice compared to vessels of healthy mice (Figure 14A). In addition, the mean rolling velocity of the interacting leukocytes (Figure 14B) as well as the cumulative frequency (Figure 14C) was significantly increased in vessels of HU mice and even higher in HU+CKD mice. Representative images are shown in Figure 14D.

In contrast, HU significantly reduced the number of adherent cells/mm^2, an effect that was even stronger in HU+CKD mice (Figure 14E), indicating that HU mainly affects leukocytes in their transition from rolling into firm arrest during the interaction with endothelial cells. Because extravasation is a downstream event of leukocyte adhesion, we also quantified the number of perivascular leukocytes on whole mount Giemsa-stained cremaster muscles. Consistent with the reduced number of adherent leukocytes, HU also significantly decreased the number of perivascular leukocytes, which further decreased in HU+CKD mice (Figure 14F). Differential cell counts displayed that the majority of perivascular cells were neutrophils, and other cells including monocytes and eosinophil (Figure 14 G). These findings demonstrated that HU and CKD synergistically modulate leukocyte rolling, adhesion, and extravasation towards the site of MSU crystal-induced inflammation.

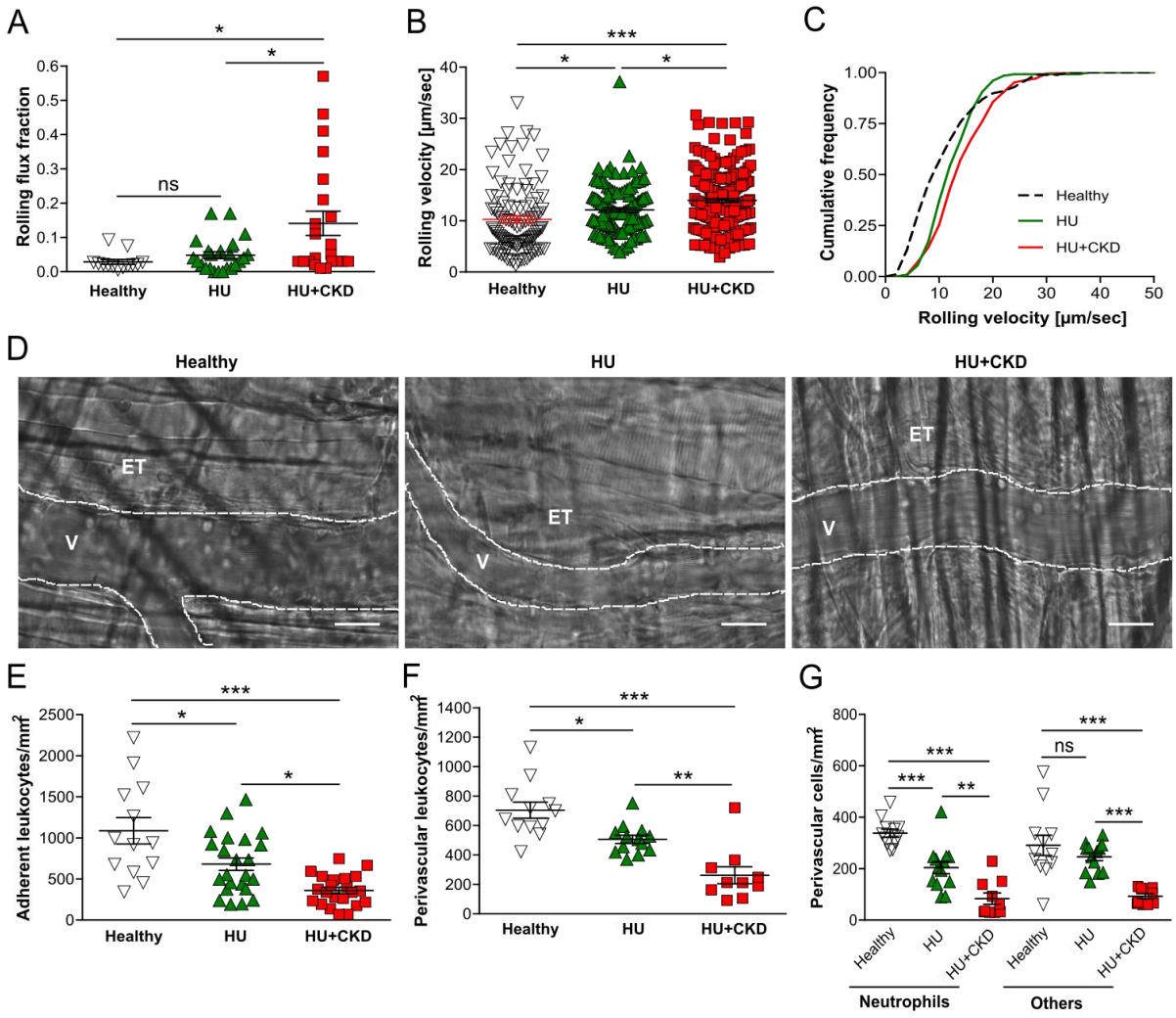

Figure 14: Decreased leukocyte adhesion and extravasation in MSU crystal-stimulated cremaster muscle venules in hyperuricemic mice with or without CKD. Alb-creERT2;Glut9$^{lox/lox}$ and Glut9$^{lox/lox}$ control mice were injected with tamoxifen and placed on a chow or high-fat diet with inosine (n = 3-4 mice per group). After 22 days, mice were injected intrascrotal with MSU crystals (500 µg per mouse) for 4 hours and intravital microscopy carried out. (**A** to **C**) Rolling flux fraction (**A**), rolling velocity (**B**), and cumulative frequency (**C**) (n = 13 venules of healthy mice, n = 23 venules of HU mice, n = 22 venules of HU+CKD mice). (**D**) Representative images of venules of the cremaster muscles from all three groups (indicated by white dotted lines). V=vessels, ET=extravascular tissue. (**E** to **G**) Quantification of the total number of adherent leukocytes/mm^2 (**E**), the total number of perivascular leukocytes/mm^2 (**F**) on the microvessel wall surface, and distribution of extravasated neutrophils and other cell subsets (**G**) (n = 10-13 vessels). Data are mean ± SEM. * p<0.05; ** p<0.01; *** p<0.001; ns = not significant by one-way ANOVA.

4.4 Soluble UA inhibits human neutrophil activation, β2 integrin expression and transmigration in vitro

The ability of immune cells to migrate through the endothelium to the site of inflammation depends on selectins, chemokine receptors, adhesion molecules and β2 integrins such as (CD11/CD18)[212]. The β2 integrin is well studied in the field of neutrophil recruitment and its dysfunction can cause impaired neutrophil migration[213]. As shown in section 4.3, HU and CKD modulate leukocyte rolling, adhesion, and extravasation in a mouse model of MSU crystal-induced inflammation.

4.4.1 Soluble UA inhibits β2 integrin expression on healthy human neutrophils

To study whether sUA can also affect adhesion molecule expression and β2 integrin activation in human neutrophils will be investigated in this section, blood neutrophils from healthy individuals were isolated and stimulated for 30 minutes with 0.6 mM sUA or vehicle (control) followed by 5 minutes stimulation with IL-8 to activate β2 integrins and adhesion molecules *in vitro*. The total surface expression of LFA-1 and MAC-1 subunits of β2 integrin was quantified by flow cytometry.

While activation of healthy neutrophils with IL-8 alone did not affect total LFA-1 expression, pre-incubation with sUA significantly reduced the total amount of LFA-1 as compared to control (Figure 15A). This effect could not be reversed by additional IL-8 stimulation (Figure 15A). Soluble UA stimulation also showed a trend towards reduced total MAC-1 expression (Figure 15B), although this was not significant. Compared to vehicle or sUA alone, the total amount of MAC-1 expression significantly increased upon IL-8 stimulation (Figure 15B). Nevertheless, the presence of sUA reduced MAC-1 expression in IL-8-activated neutrophils (Figure 15B).

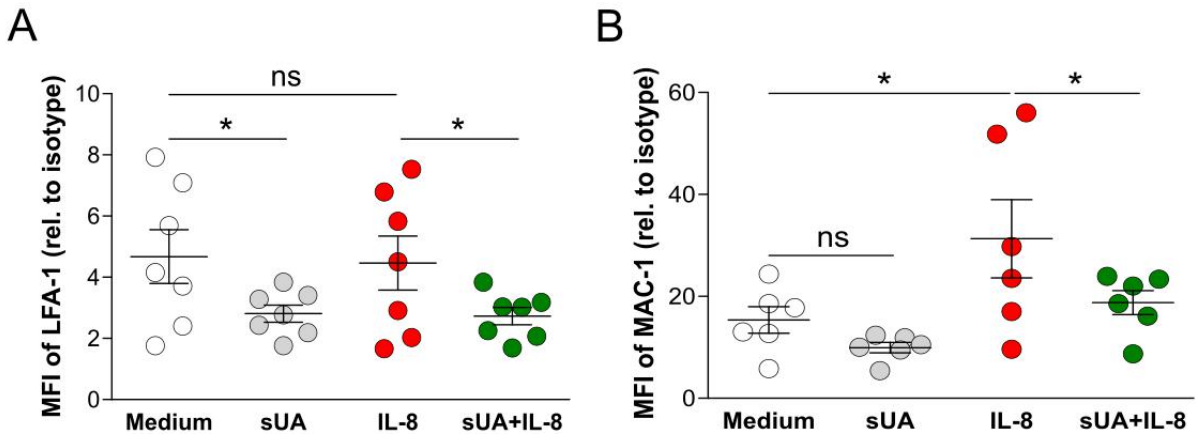

Fig. 15: Soluble UA affects β2 integrin expression levels on neutrophils. Human neutrophils were isolated from healthy individuals and pre-incubated with or without 0.6mM sUA for 30 minutes prior to stimulation with human IL-8. (**A to B**) The expression levels of LFA-1 (**A**) and MAC-1 (**B**) shown as mean fluorescence intensity (MFI) relative to isotype control (n = 6-7) were quantified by flow cytometric analysis. Data are mean ± SEM and values are representative of two independent experiments. * $p<0.05$; ** $p<0.01$; *** $p<0.001$; ns = not significant by one-way ANOVA.

4.4.2 Soluble UA inhibits β2 integrin activation on healthy human neutrophils

The signaling cascade through β2 integrin on leukocytes can be distinguished in three different conformation stages, as illustrated in Figure 16A. First, a bent form (V shape) with the ligand-binding head (I domain) is close to the membrane, which represents inactive integrin. Second, an extended form in a 'switchblade-like' motion with the ligand-binding head away from the membrane represents intermediate integrin affinity. Third, the extended form is in an open conformation and represents high integrin affinity[212]. Upon close interaction between the β-subunit (ligand-binding I domain) and the α-subunit (the extended form), the activation status of leukocytes can be tested using the high affinity β2 integrin activation marker mAB24. Stimulation with IL-8 induced β2 integrin activation as indicated by increased mAB24 binding and MFI compared to medium (Figure 16B and C). Consistent with the previous findings, sUA also reduced mAB24 expression in IL-8-activated neutrophils, indicating that sUA impaired β2 integrin activation (Figure 16C).

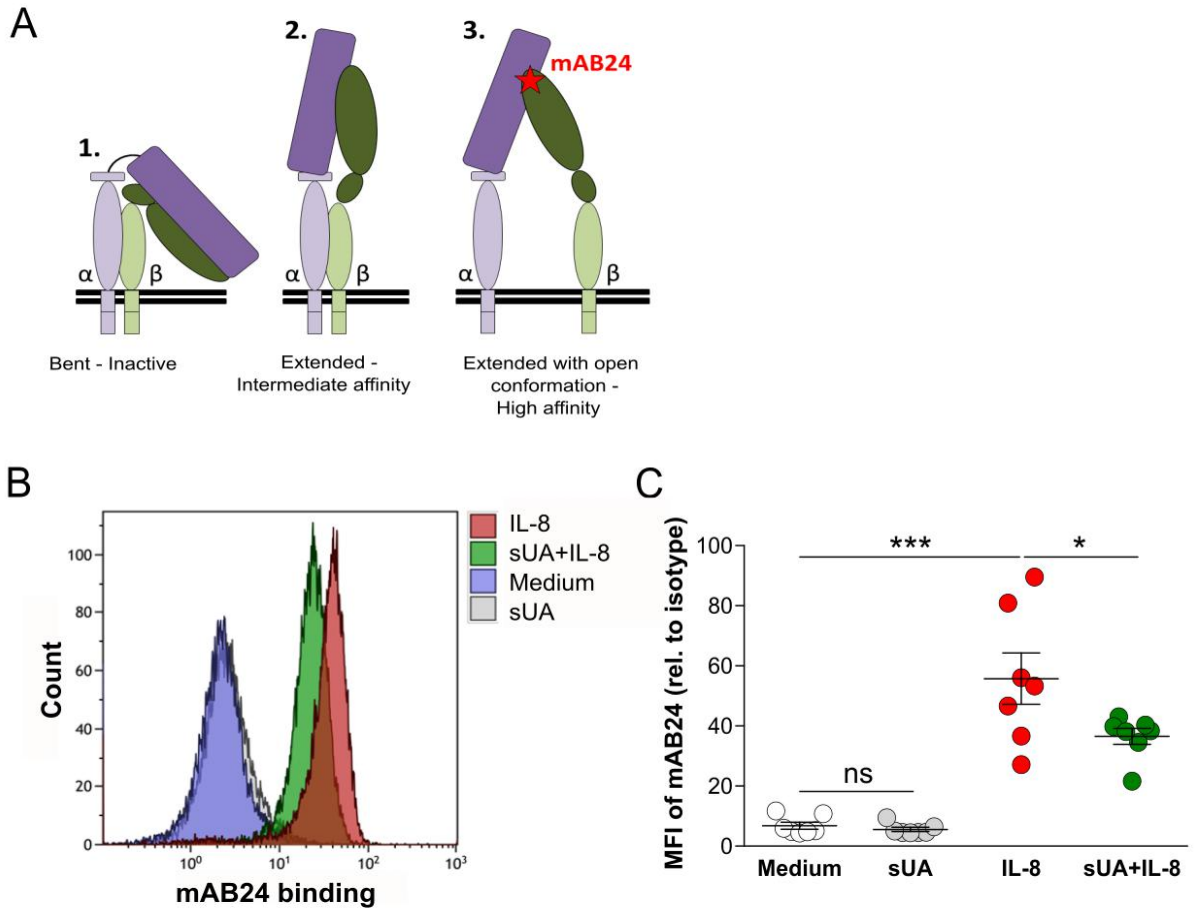

Fig. 16: Soluble UA affects β2 integrin activation on neutrophils. Human neutrophils were isolated from healthy individuals and pre-incubated with or without 0.6mM sUA for 30 minutes prior to stimulation with human IL-8. (**A**) Schematic of three β2 integrin conformations that reflect the different stages of cell activation: 1. The bent form – inactive; 2. The extended from with a closed ligand-binding head of intermediate affinity; 3. The extended form enabling the ligand-binding for mAB24 with high affinity (adopted from Evans, *et al*[212]). (**B** and **C**) mAB24 binding illustrated as histogram (**B**) and the expression levels of mAB24 (**C**) determined by flow cytometry (n = 6-7). Data are mean ± SEM. Data are mean ± SEM and values are representative of two independent experiments. * $p<0.05$; ** $p<0.01$; *** $p<0.001$; ns = not significant by one-way ANOVA.

4.4.3 Soluble UA prevents healthy human neutrophil migration in transwell assay

Soluble UA inhibits β2 integrin expression and activation in healthy human neutrophils. To test the effect of sUA on neutrophil sensing chemokine gradients, neutrophils from healthy individuals were pre-incubated with vehicle (control) or sUA for 30 minutes and allowed to migrate across a transwell filter in the presence or absence of different chemokines and cytokines for 3 hours. As shown in Figure 17A to C, the presence of sUA attenuated the migratory capability of neutrophils towards IL-8, IL-1β, and fMLP. However, sUA itself did not alter the ability of human neutrophils to migrate compared to medium control alone (Figure 17 A to C). These findings demonstrate that sUA impaired the activation status and therefore the migratory ability of neutrophils along chemokine gradients, which might be an explanation for the impaired leukocyte recruitment observed *in vivo* (section 4.2 and 4.3).

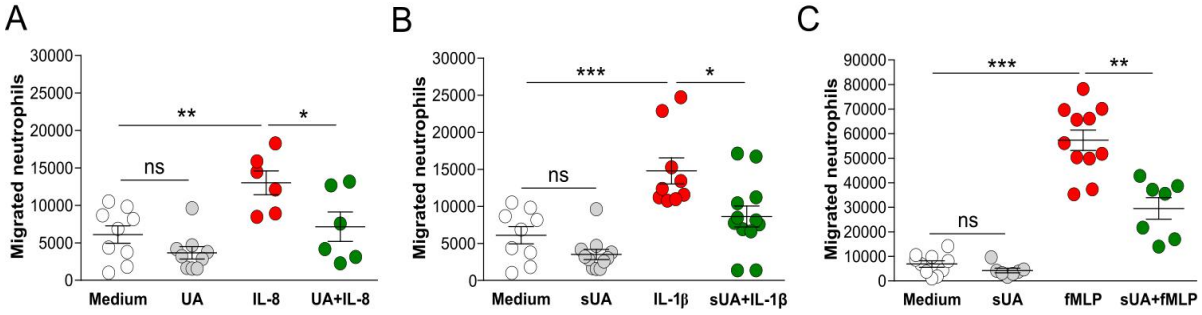

Figure 17: Soluble UA prevents healthy human neutrophil migration in transwell assay. (**A** to **C**) Transwell migration assays were carried out and the number of neutrophils per µl that migrated towards the chemoattractants human IL-8 (**A**), human IL-1β (**B**) and fMLP (**C**) was determined after 3 hours by flow cytometry (n = 6-12). Data are mean ± SEM and values are the pooled from three independent experiments. * $p<0.05$; ** $p<0.01$; *** $p<0.001$; ns = not significant by one-way ANOVA.

4.5 Hyperuricemia in uremic patients suppresses neutrophil migration

Neutrophils from uremic patients were reported to have a reduced chemotactic activity[214] and a variety of uremic toxins may contribute to this process (see introduction section 1.1.4). It has shown in section 4.4 that sUA inhibits β2 integrin expression and activation in healthy human neutrophils. To investigate the role of HU on the functional properties of neutrophils from uremic patients, neutrophils were isolated from patients with different stages of CKD, i.e. CKD stage 2-4 (CKD) and CKD stage 5 on dialysis (ESKD) as well as healthy individuals.

4.5.1 Study design, clinical, and demographical characteristics

In this study, 51 patients were included and 8 of them were excluded due to the intake of immunosuppressive drugs e.g. cyclosporine, and urate lowering drugs, e.g. allopurinol and/or febuxostat. The 43 patients included were then divided into three groups: 10 patients with CKD (CKD stage G2-4; male/female: 6/4; mean age: 57.13 ± 5.89 years), 18 patients with ESKD that were on dialysis (ESKD, stage G5D; male/female: 11/7; mean age: 57.28 ± 3.74 years) and 15 healthy individuals without renal impairment (healthy, CKD stage 0) (male/female: 7/8; mean age: 44.50 ± 4.84 years), as illustrated in Figure 18.

There was no significant difference in age between the three groups (Table 5). Plasma urea, creatinine and UA levels were significantly higher in patients with CKD and ESKD compared to healthy subjects (Table 5). The renal pathologies of the uremic patients were diverse and included: hypertensive nephritis, diabetic kidney disease, minimal change disease, microscopic polyangiitis, proteinuria, hyperaldosteronism, and polycystic kidney disease for CKD patients, and diabetic kidney disease, hypertensive nephritis, IgA nephropathy, lupus nephritis with focal segmental glomerulosclerosis (FSGS), membranous glomerulonephritis, myeloma kidney disease, and contrast-induced nephropathy for ESKD patients (Table 6).

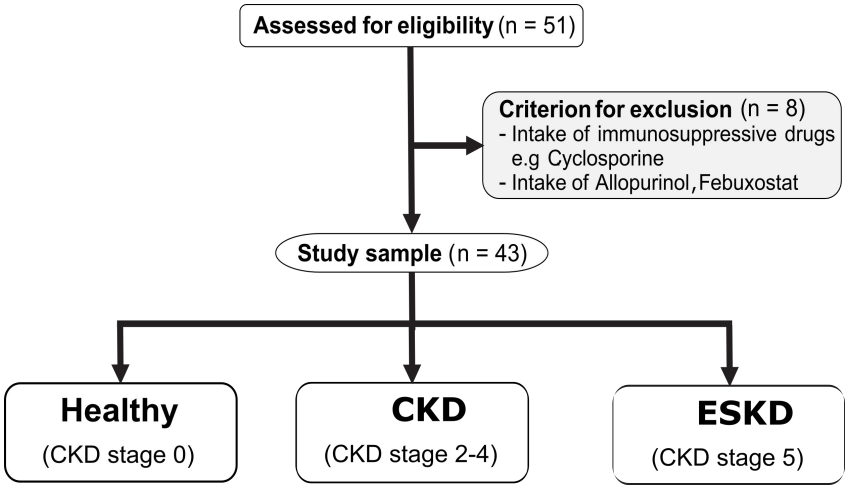

Fig. 18: Schematic of study design. Out of 51 individuals, 8 patients were excluded due to the intake of immunosuppressive drugs e.g. cyclosporine, and urate lowering drugs e.g. allopurinol, febuxostat. Of the remaining, 10 patients represented with CKD (CKD stage G2-4), 18 patients with ESKD that were on dialysis (CKD stage G5) and 15 healthy individuals without any renal pathologies (healthy, CKD stage G0).

Table 5: Clinical and demographic characteristics.

Descriptive Data		Healthy n=15	CKD n=10	ESKD n=18
Age (years)	Mean	44.50 ± 4.84	57.13 ± 5.89	57.28 ± 3.74
	P		0.120	0.061
Gender	Male	7	6	11
	Female	8	4	7
Plasma urea (mg/dl)	Mean	30.28 ± 3.83	59.12 ± 8.59	111.5 ± 8.07
	P		0.01	0.001
Plasma creatinine (mg/dl)	Mean	1.51 ± 0.09	2.57 ± 0.46	9.25 ± 0.62
	P		0.426	0.001
Plasma uric acid (mg/dl)	Mean	4.27 ± 0.26	8.93 ± 0.46	10.25 ± 0.55
	P		0.001	0.001

Table 6: Main human pathological diagnoses.

Descriptive Data	Healthy	CKD	ESKD
Kidney pathology	None	Hypertensive nephritis,	Diabetic kidney disease,
		Diabetic kidney disease,	Hypertensive nephritis,
		Minimal change disease,	IgA nephropathy,
		Microscopic polyangiitis,	Lupus nephritis with FSGS,
		Proteinuria,	Membranous glomerulonephritis,
		Hyperaldosteronism,	Myelom kidney disease,
		Polycystic kidney disease	Contrast-induced nephropathy

4.5.2 Neutrophil number does not differ between uremic patients and healthy controls

To investigate the effect of HU on the functional properties of neutrophils from uremia patients, neutrophils were isolated from healthy individuals, CKD and ESKD patients (see methods and materials for the isolation process). Neutrophils were identified as $CD15^{+}CD11b^{+}CD66b^{+}$ by flow cytometry (see gating strategy) and had a purity of approximately 99% (Figure 19A). Neutrophil counts revealed no significant difference between CKD and ESKD patients compared with healthy individuals (Figure 19B).

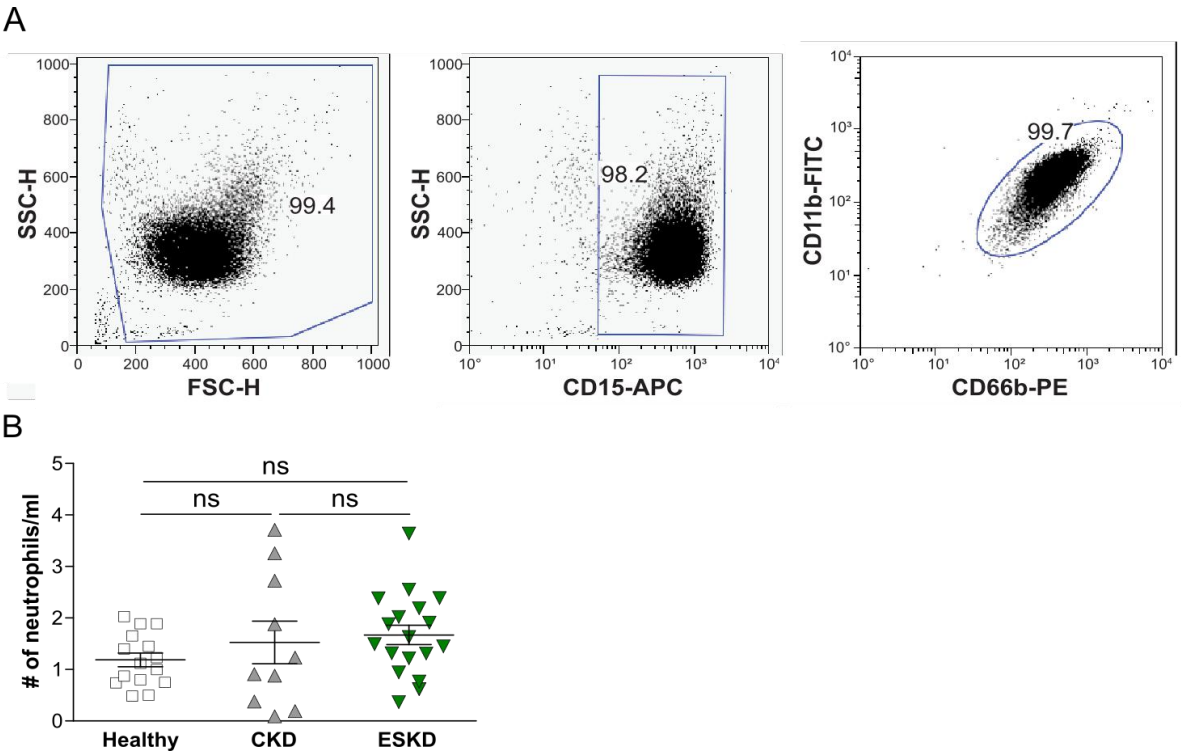

Figure 19: No difference in number of neutrophils between uremic patients and healthy controls. (**A**) Human neutrophils were isolated (see methods and materials) and identified as $CD15^{+}CD11b^{+}CD66b^{+}$ by flow cytometry with a purity of approximately 99%. (**B**) The number of isolated neutrophils per ml from CKD and ESKD patients as well as healthy individuals. Data are mean ± SEM (healthy, n = 15; CKD, n = 10; ESKD, n = 18; one-way ANOVA); ns = not significant.

4.5.3 Hyperuricemia in uremic patients suppresses neutrophil migration

Neutrophils from healthy individuals showed decreased β2 integrin expression and activation after treatment with sUA (see section 4.4). To investigate the role of HU on the functional properties of neutrophils from uremia patients, the surface marker expression of L-selectin (CD62L) and αM subunit of β2 integrin (MAC-1) were determined by flow cytometry. The data revealed that neutrophils from ESKD patients showed significantly lower surface expression of CD62L and MAC-1 compared to neutrophils from healthy controls (Figure 20A and B). Next, the ability of sUA-stimulated neutrophils to sense chemokines were quantified by performing transwell migration assays as before. Compared to neutrophils from healthy individuals, neutrophils from ESKD patients migrated in significantly lower numbers towards human IL-8 and fMLP (Figure 20C and D).

In addition, leukocytes from CKD patients have an impaired migratory capability and respond less to inflammatory danger signals due to the uremic environment, in particular uremic toxins[43,45,214]. To test whether sUA in uremic serum contributes to the intrinsic dysfunction of neutrophils from uremic patients, neutrophils from healthy subjects were isolated and pre-incubated with serum from either CKD and ESKD patients as well as healthy individuals. These sera contained sUA levels as follows: CKD (7.93 ± 0.93 mg/dl), ESKD (9.94 ± 1.3 mg/dl), and healthy (4.17 ± 0.46 mg/dl). CKD and ESKD serum decreased the ability of healthy donor neutrophils to migrate towards IL-8 as well as fMLP compared to neutrophils incubated with serum from healthy subjects (Figure 20E). Interestingly, this effect was entirely reversible by pre-incubating the sera with rasburicase as indicated by an increased number of migrating neutrophils (UA was undetectable in the serum after rasburicase treatment) (Figure 20E). This further confirmed that HU contributed to the impaired ability of neutrophils from uremic patients to migrate.

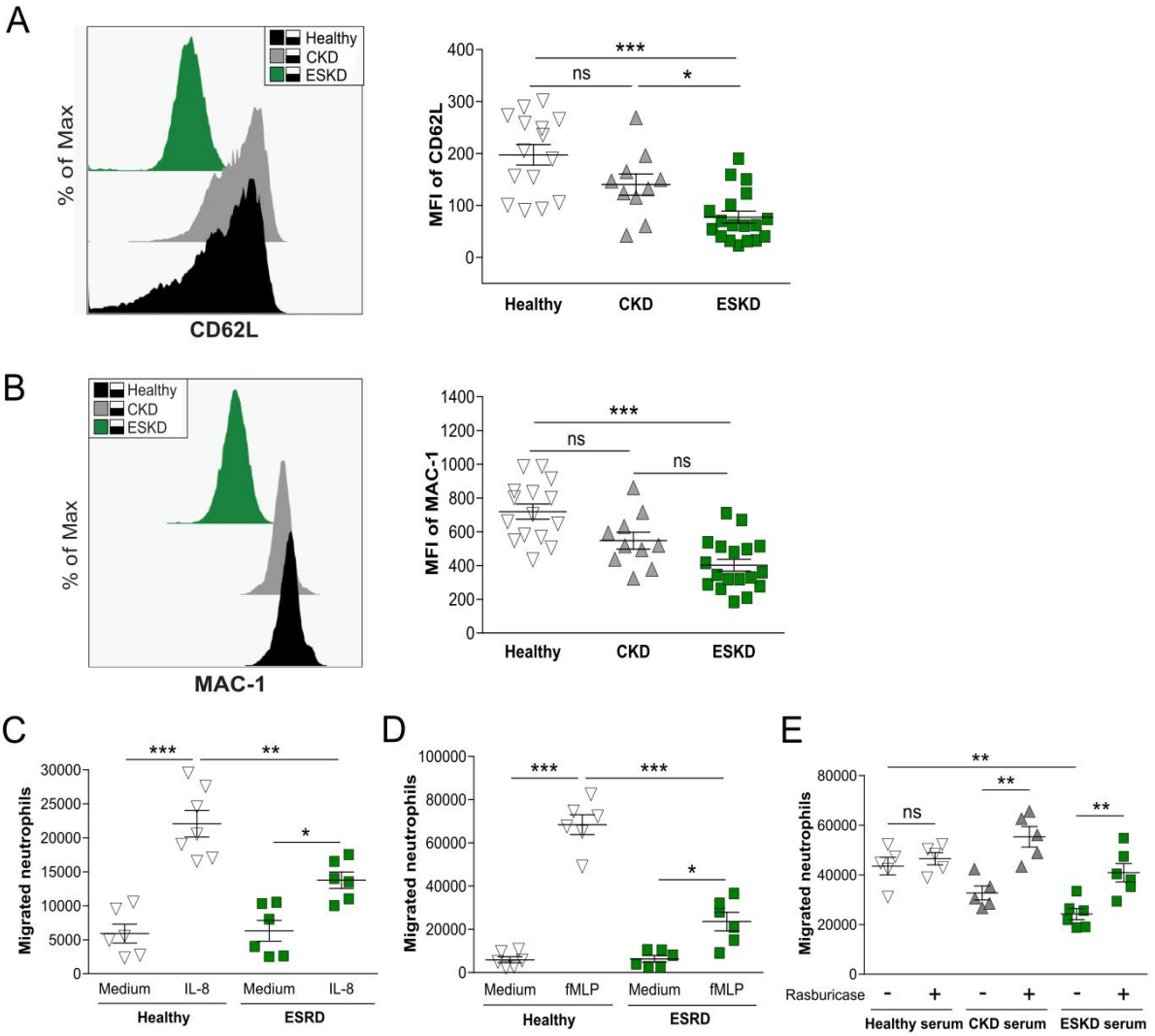

Fig. 20: Uremia impairs neutrophil migration in ESKD patients. Human neutrophils were isolated from CKD and ESKD patients as well as healthy individuals. (**A** to **B**) Expression (MFI) of CD62L (**A**) and MAC-1 (**B**) determined by flow cytometry (healthy, n = 15; CKD, n = 10; ESKD, n = 18; one-way ANOVA). (**C** to **D**) Number of neutrophils per µl isolated from healthy individuals and ESKD patients that migrated though the transwell membrane towards the chemoattractants human IL-8 (**C**) and fMLP (**D**) (healthy, n = 6-7; ESKD, n = 6; two-way ANOVA) were determined by flow cytometry after 3 hours. (**E**) Healthy neutrophils were incubated with serum from healthy individuals, CKD or ESKD patients in the absence or presence of rasburicase, and the number of neutrophils per µl that migrated towards fMLP was determined by flow cytometry after 3 hours (n = 5-6; two-way ANOVA). Data are mean ± SEM. * $p<0.05$; ** $p<0.01$; *** $p<0.001$; ns = not significant.

4.6 Uremia does not affect MSU crystal-induced NET formation in ESKD patients

NETs are released by neutrophils, which initially were identified as an antimicrobial, net-like structure that consist of histone and other antimicrobial proteins[215]. Growing evidence imply that NETs are also involved in sterile inflammation-related diseases, such as rheumatoid arthritis[216], atherosclerosis[217], vasculitis[218] and lupus[219]. Schauer C, *et al*. have previously shown that MSU crystals can induce NET formation and NETosis as well as aggregated NETs[162]. Another report showed that NET formation is increased in uremic patients[220]. To investigate whether this is also the case in this patients cohort, neutrophils from healthy volunteers and ESRD patients were stimulated with MSU crystals or phorbol myristate acetate (PMA), as positive control[221] and quantified NET formation by staining with neutrophil elastase (NE) and cit. histone H3 antibodies. Immunofluorescence microscopy illustrated that neutrophils from healthy volunteers and ESKD patients released significantly more NE and cit. histone H3 (% area) upon MSU crystal or PMA stimulation compared to untreated (medium control) (Figure 21A). However, we did not observe any difference regarding NE or histone H3 release between healthy volunteer and ESKD patients (Figure 21A).

Furthermore, DNA-MPO and DNA release are known to predominantly be released during NET formation[222]. As shown in Figure 21B and C, DNA-MPO and DNA release were significantly increased in both MSU crystal- and PMA-stimulated healthy neutrophils compared to unstimulated healthy neutrophils. However, stimulated neutrophils from CKD and ESKD patients showed a trend towards more DNA-MPO and DNA release compared to medium, but not significant. In addition, there was no significant difference in the DNA-MPO and DNA release observed in neutrophils between CKD and ESKD patients and healthy volunteers (Figure 21B and C). Together, the findings suggested that CKD- and ESKD-related HU had no effect on MSU crystal and PMA-induced NET formation.

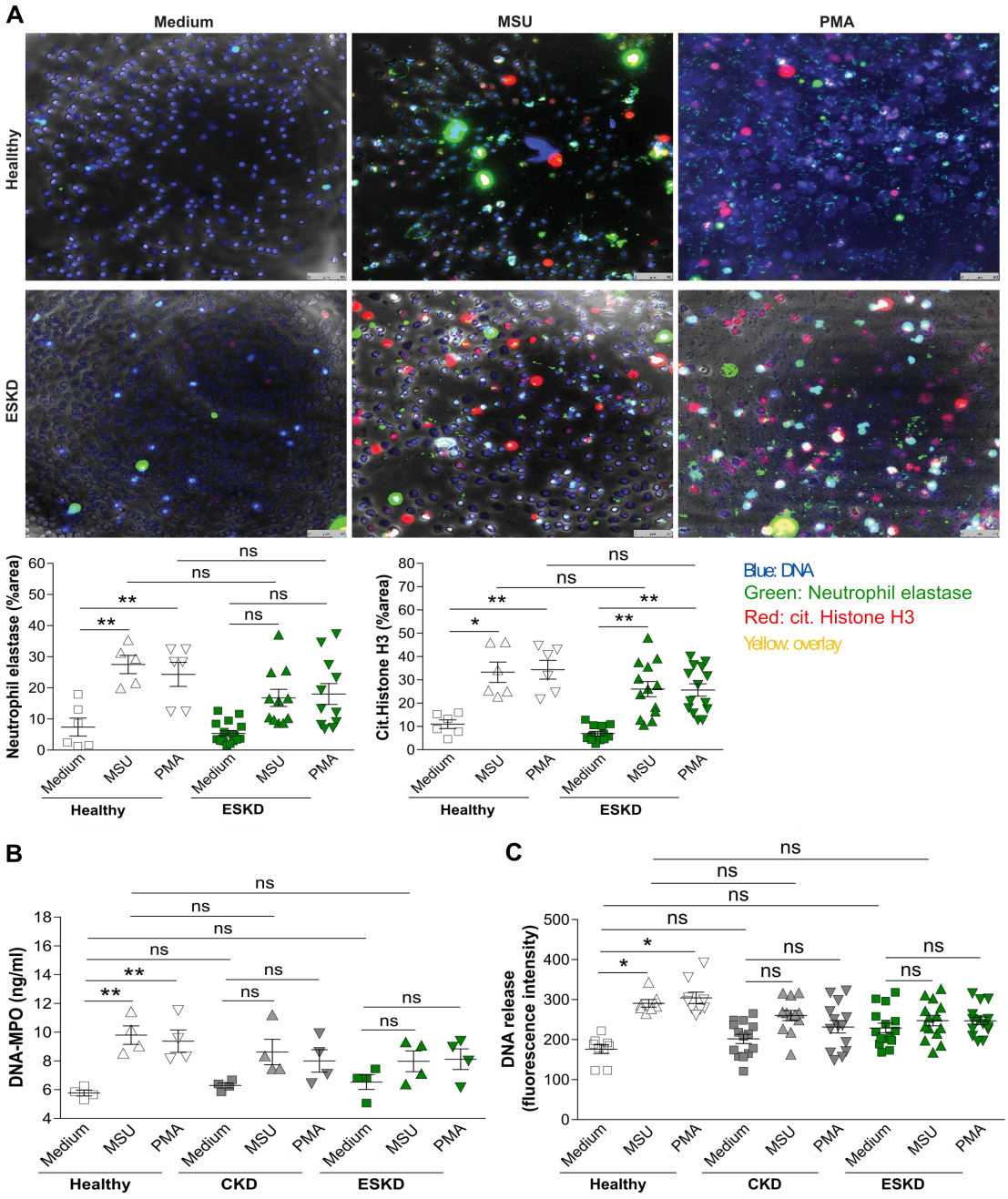

Figure 21: Uremia does not affect MSU crystal-induced NET formation in ESKD patients. Blood neutrophils were isolated from CKD and ESKD patients as well as healthy individuals, and stimulated with MSU crystals or PMA or left untreated (medium) for 3 hours. (**A**) NETs were stained with neutrophil elastase (NE), citrullinated histone H3 (cit. histone H3) and DAPI (for DNA release), and the % area of cit. histone H3 and NE quantified using the software ImageJ (healthy, n = 6; ESKD, n = 14). (**B** to **C**) Supernatants from MSU crystal- and PMA-stimulated neutrophils were collected and the DNA and MPO release determined using a DNA-MPO ELISA kit (n = 4) (**B**) and the fluorescence intensity of the dye PicoGreen (healthy, n = 8; CKD, n = 13; ESKD, n = 14) (**C**). Data are mean ± SEM. * $p<0.05$; ** $p<0.01$; ns = not significant by two-way ANOVA.

4.7 Soluble UA suppresses the monocyte function

Monocytes recruit in high numbers to the site of MSU crystal-induced inflammation (detailed information in section 1.3.3). HU and CKD also impaired monocyte recruitment in a mouse model of gout (section 4.2). However, previous reports demonstrated that monocytes isolated from uremic patients are hyporesponsive to *ex vivo* LPS or MSU crystal stimulation, indicating a reduced ability to synthesize pro-inflammatory cytokines[33].

4.7.1 Soluble UA suppresses LPS- and MSU crystal-induced pro-inflammatory cytokine expression in human monocytes

To examine the role of HU in this context, monocytes from CKD and ESKD patients as well as healthy subjects were isolated by $CD14^+$ bead separation. $CD14^+$ monocytes were identified as $CD15^-CD14^+CD16^-$ by flow cytometry (gating strategy) with a purity of 88.3% (Figure 22A). The number of isolated $CD14^+$ monocytes from CKD and ESKD patients as well as healthy individuals were shown as per/ml and there was no difference between the groups (Figure 22B).

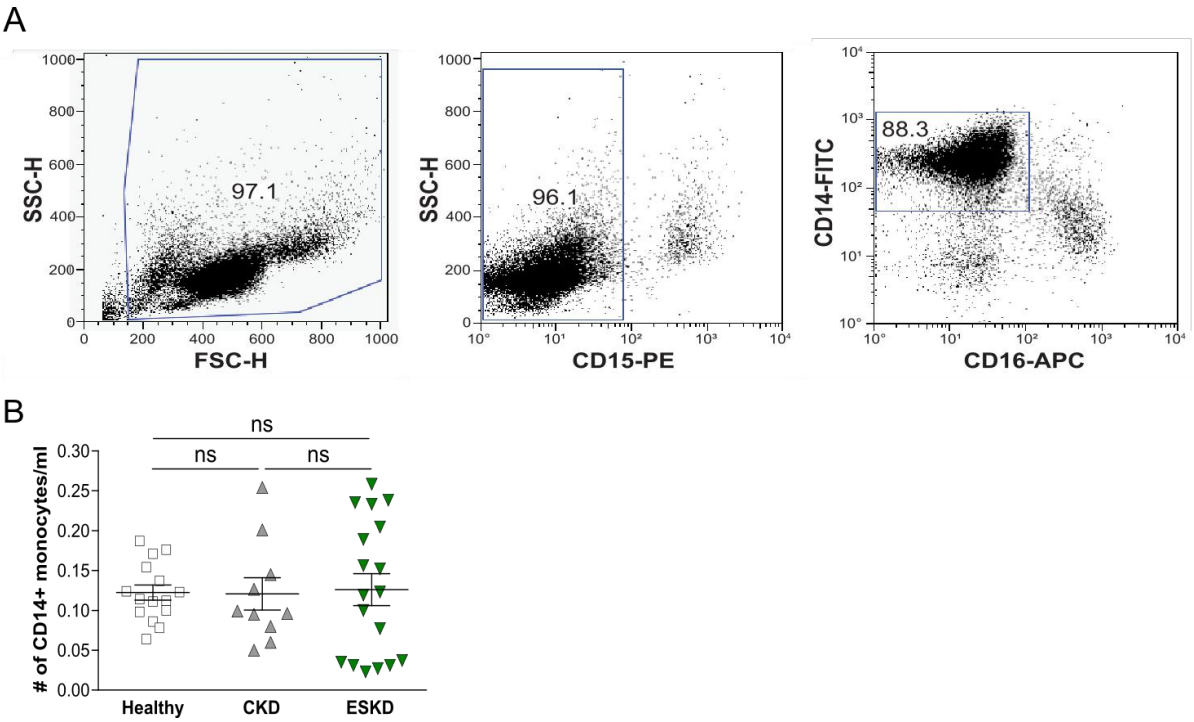

Figure 22: No difference in number of monocytes between uremic patients and healthy controls. (**A**) $CD14^+$ monocytes were isolated (see methods and materials) and identified as $CD15^-CD14^+CD16^-$ by flow cytometry (with gating strategy) with a purity of approximately 88%. (**B**) The number of isolated neutrophils per ml from CKD and ESKD patients as well as healthy individuals. Data are mean ± SEM (healthy, n = 15; CKD, n = 10; ESKD, n = 18; one-way ANOVA); ns = not significant.

To investigate the role of HU on the functional properties of monocytes from uremia patients, $CD14^+$ monocytes from healthy, CKD and ESKD patients were stimulated with LPS, MSU crystals or medium alone. Comparing LPS-stimulated healthy monocytes with LPS-stimulated monocytes from CKD patients, the mRNA expression levels of *NLRP3*, *ASC*, *NFκB*, *IL-6*, *TNF-alpha*, and *CCL2* were down-regulated but not the anti-inflammatory cytokine IL-10 (Figure 23A). This decreased inflammatory response to LPS was more pronounced in monocytes isolated from ESKD patients (Figure 23A). MSU crystal-stimulated monocytes showed a similar trend in the tested gene, although not all genes were significantly down regulated (Figure 23B).

In order to determine whether sUA accounted for the decreasing pro-inflammatory gene expression seen in monocytes from CKD and ESKD patients, monocytes from healthy individuals were next stimulated with LPS or MSU crystals in the presence or absence of 0.6 mM sUA. As shown in Figure 23C, the mRNA expression of *NLRP3*, *TNF-alpha* and *IL-6* increased in LPS- or MSU crystal-stimulated monocytes compared to medium control. However, sUA alone did not alter the gene expression. Interestingly, pre-incubation with 0.6 mM sUA significantly reduced the LPS- and MSU crystal-induced mRNA expression of these pro-inflammatory mediators (Figure 23C).

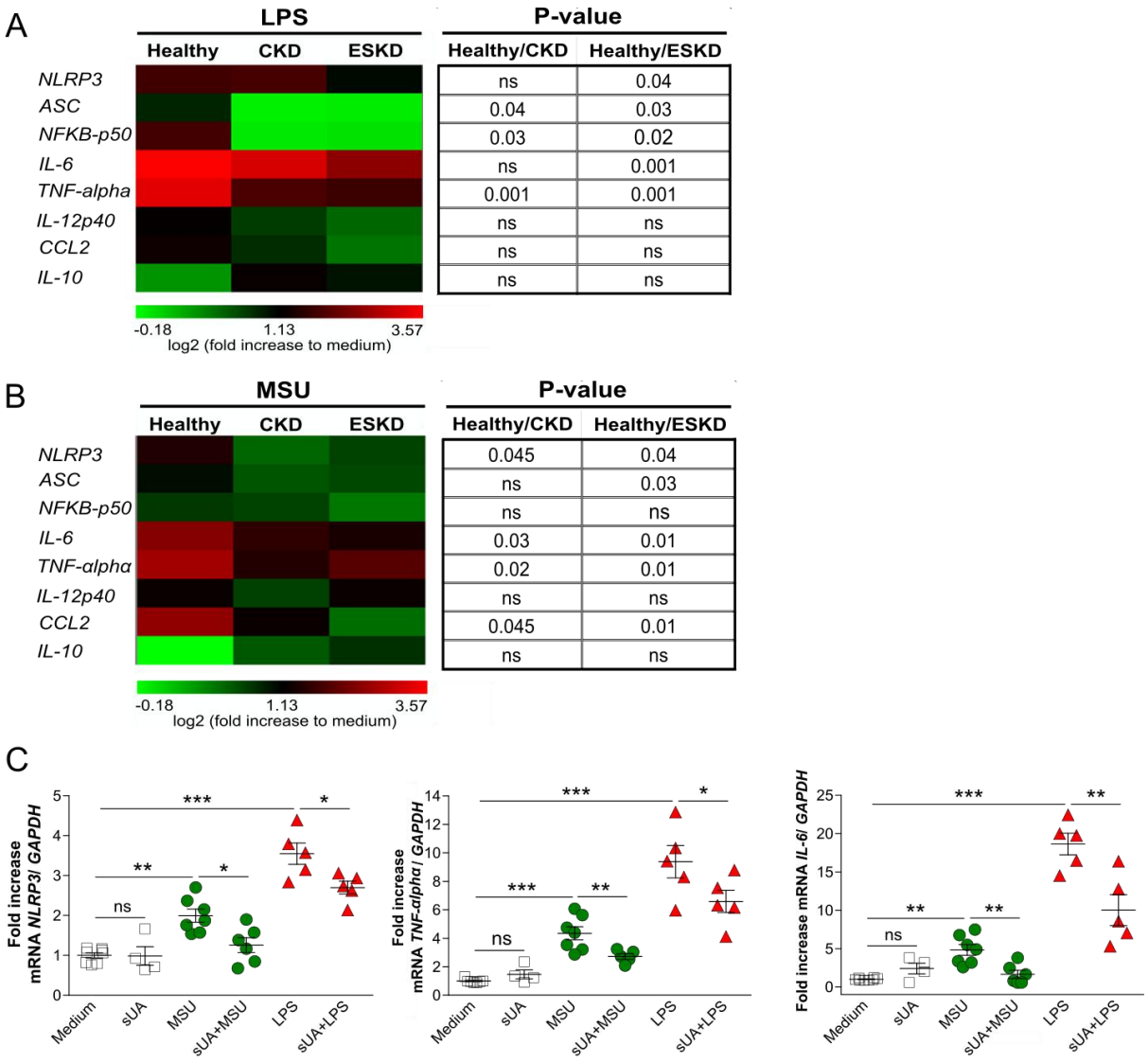

Figure 23: Soluble UA mediates the defective inflammatory function of monocytes in uremic patients. (**A** to **B**) $CD14^+$ monocytes were isolated from CKD and ESKD patients as well as healthy individuals, and stimulated with LPS or MSU crystals or left untreated (medium). After stimulation, RNA expression levels of the genes *NLRP3, ASC, NFKB-p50, IL-6, TNF-alpha, IL-12p40, CCL2* and *IL-10* determined via RT-PCR. Heat maps of gene expression data after LPS (**A**) and MSU crystal (**B**) stimulation. Color intensity represents the mean $\log_2$ fold change within each row (mean expression value of stimulated vs. medium control). P-values of genes were calculated between healthy vs. CKD or healthy vs. ESKD of stimulated monocytes (n = 4-10 per group, Student's *t*-test). (**C**) $CD14^+$ monocytes isolated from healthy individuals were pre-incubated with 0.6 mM sUA prior to stimulation with LPS or MSU crystals or left untreated (medium). After stimulation, RNA expression levels of the genes *NLRP3*, *TNF-alpha*, and *IL-6*, determined via RT-PCR (n = 4-7 per group; one-way ANOVA). Data are mean ± SEM and values are representative of two independent experiments. * $p<0.05$; ** $p<0.01$; *** $p<0.001$; ns = not significant.

4.7.2 Soluble UA suppresses intracellular cytokine expression in monocytes

The data in section 4.7.1 have shown that sUA suppressed LPS- and MSU crystal-induced pro-inflammatory cytokines mRNA expression in human monocytes. To look whether sUA also affected the intracellular protein levels, monocytes from healthy individuals were pre-incubated with 0.6 mM sUA prior to stimulation with LPS or MSU crystals or left untreated (medium) for 8 hours. After stimulation, the percentage of TNF-α^{+}IL-6^{-}, TNF-α^{-}IL-6^{+}, and TNF-α^{+}IL-6^{+} monocytes was determined by intracellular staining and quantified using flow cytometry. Flow cytometric analysis for the intracellular cytokines IL-6 and TNF-α confirmed that sUA significantly reduced the number of IL-6 and TNF-α single-positive as well as of IL-6/TNF-α double-positive activated monocytes compared to LPS or MSU crystal stimulation only, indicating that sUA suppressed the inflammatory function of monocytes (Figure 24 A to C).

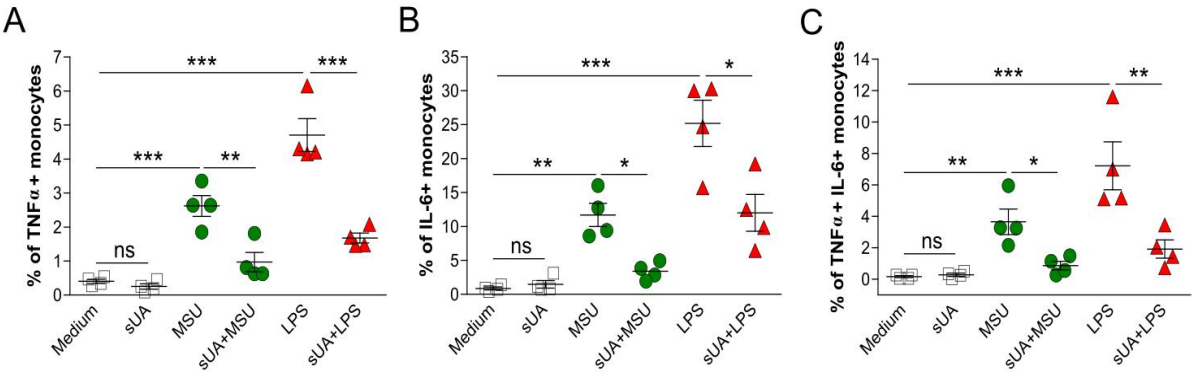

Figure 24: Soluble UA mediates the defective inflammatory function in monocytes (**A to C**) $CD14^{+}$ monocytes were isolated from healthy individuals, pre-incubated with 0.6 mM sUA and then stimulated with LPS or MSU crystals or left untreated (medium) for 8 hours. After stimulation, the percentage of TNF-α^{+}IL-6^{-} (**A**), TNF-α^{-}IL-6^{+} (**B**), and TNF-α^{+}IL-6^{+} (**C**) monocytes determined by intracellular staining and quantified using flow cytometry (n = 4 per group; one-way ANOVA). Data are mean ± SEM and values are representative of two independent experiments. * $p<0.05$; ** $p<0.01$; *** $p<0.001$; ns = not significant.

4.7.3 Soluble UA supresses PSGL-1 expression in monocytes

Monocytes migrate in lower numbers towards MSU crystal-induced inflammation under hyperuricemic conditions (see section 4.2.1). The recruitment of circulating monocytes to the site of inflammation requires P-selectins such as the glycoprotein ligand-1 (PSGL-1), which is important for monocyte rolling, as well as adhesion molecules such as the very late antigen 4 (VLA-4)[223,224]. To test whether sUA affected monocyte recruitment by inhibiting surface marker expression, monocytes from healthy individuals were isolated and pre-incubated with 0.6 mM sUA prior to stimulation with LPS. After stimulation, the expression of CD162 (PSGL-1) and CD49a (VLA-4a) were determined by flow cytometry. LPS stimulation increased the expression of PSGL-1 on monocytes, whereas sUA significantly decreased PSGL-1 expression (Figure 25A). However, LPS nor sUA had an effect on the expression levels of VLA-4 compared to unstimulated monocytes (Figure 25B).

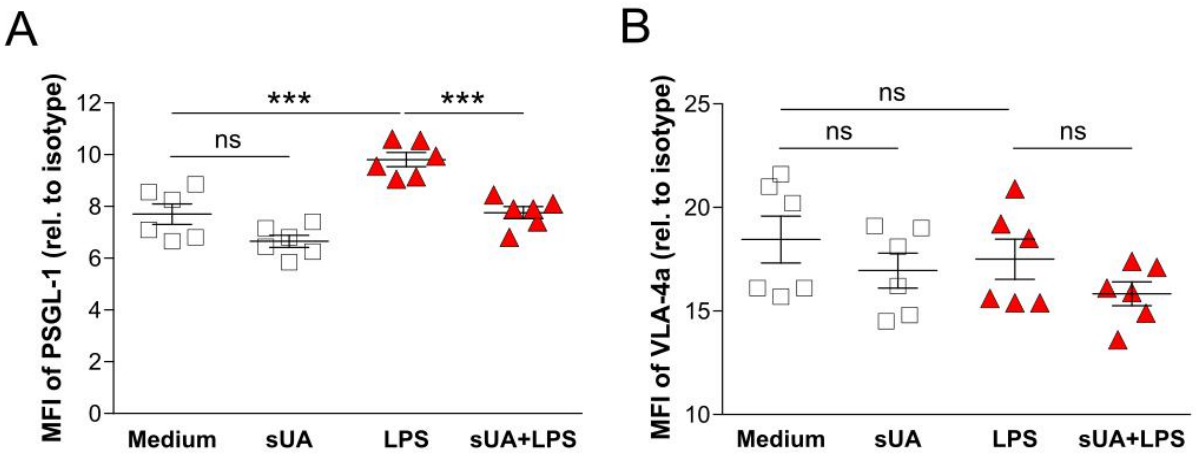

Figure 25: Soluble UA suppresses PSGL-1 expression in monocytes. $CD14^+$ monocytes isolated from healthy individuals were pre-incubated with 0.6mM sUA prior to stimulation with LPS or left untreated (medium). Expression (MFI) of CD162 (PSGL-1) (**A**) and CD49a (VLA-4a) (**B**) determined by flow cytometry (n = 6). Data are mean ± SEM and values are representative of two independent experiments. * $p<0.05$; ** $p<0.01$; *** $p<0.001$; ns = not significant by one-way ANOVA.

4.7.4 Soluble UA inhibits activated monocyte-induced formation of NETs

Previous studies including data within this thesis have shown that MSU crystals can directly induce NET formation[182]. However, soluble mediators, including IL-1β and TNF-α, released from activated macrophages can indirectly promote NETs release[225,226]. In order to investigate whether sUA can indirectly affect NET formation via monocyte-derived soluble mediators, healthy $CD14^+$ monocytes were pre-treated with sUA (0.6 mM) prior to stimulation with MSU crystals or LPS. After stimulation, supernatants from MSU crystal- and LPS-activated monocytes were collected and added to freshly isolated neutrophils from healthy subjects for three hours. As shown in Figure 26, soluble mediators released from LPS- or MSU crystal-activated monocytes induced NET release, as indicated by an increase in the % area of cit. histone H3 and NE. However, this effect was attenuated by adding supernatants that from sUA+LPS- or sUA+MSU crystal-stimulated monocytes (Figure 26). These data indicated that sUA suppressed the function and accordingly the release of pro-inflammatory mediators in monocytes; therefore altering secondary effects on other immune cells, specifically NET formation.

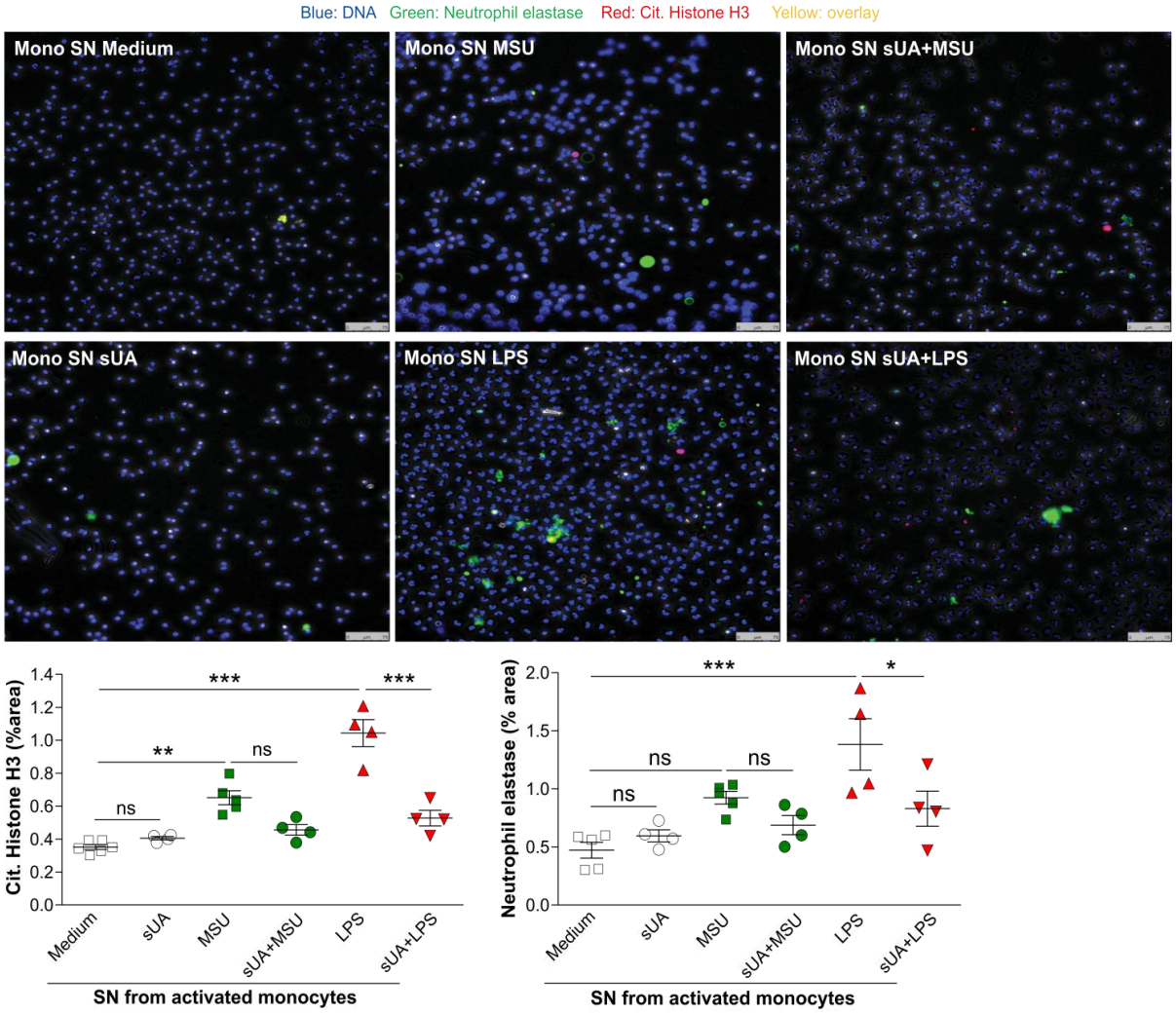

Figure 26: Soluble UA inhibits the release of inflammatory cytokines by activated monocyte-induced NET formation. Human blood CD14$^+$ monocytes and neutrophils were isolated from healthy individuals. CD14$^+$ monocytes were pre-incubated with or without sUA (0.6 mM) and then stimulated with MSU crystals or LPS or left untreated (medium). Supernatants (SN) from activated monocytes were collected and added to the neutrophil culture for 3 hours. NETs were stained with neutrophil elastase (NE), citrullinated histone H3 (cit. histone H3) and DAPI (for DNA release), and the % area of cit. histone H3 and NE quantified using the software ImageJ. Data are mean ± SEM and values are representative of two independent experiments. * $p<0.05$; ** $p<0.01$; *** $p<0.001$; ns = not significant by one-way ANOVA.

4.8 Soluble UA modulates monocyte function by intracellular uptake via SLC2A9/GLUT9

UA does not ligate specific surface receptors but can cross cellular membranes via a number of solute carrier (SLC) family members and multispecific 'drug' transporters in the kidney and intestine, including SLC2A9/GLUT9, SLC22A12/URAT1, OAT1, OAT3, and ABCG2[227] (see introduction 1.2.2). Multiple urate transporters have been reported to be expressed in human renal tubular cells[63]. Except for renal tubular cells, endothelial cells can also take up UA via GLUT9 leading to increased ROS production[228]. Unlike non-immune cells, immune cells only express GLUT9 according to the online gene atlas database. Currently, nothing is known about the functional role of urate transporters in immune cells, which raises the question: Does sUA enter and modulate the inflammatory function in monocytes?

4.8.1 Soluble UA suppresses LPS- or TNF-α-induced pro-inflammatory cytokines expression in human monocytic THP-1 cells

To explore this question, human monocytic THP-1 cells were used. THP-1 cells are a spontaneously immortalized monocyte-like cell line, which arrived from the blood of a boy with acute monocytic leukemia, and are widely used for investigating monocyte structure and function in both health and disease[229]. First, we tested whether sUA had similar effects on the pro-inflammatory cytokine production on THP-1 cells compared to human primary monocytes. There was a significant decrease in the mRNA expression of the inflammatory genes *NFκBp50, ASC, NLRP3, IL-6* and *TNF-alpha* when LPS- or TNF-α-activated THP-1 cells were pre-incubated with 0.6 mM sUA (Figure 27A and B). These data were consistent with the LPS-stimulated primary $CD14^+$ monocytes from healthy individuals (see Figure 23).

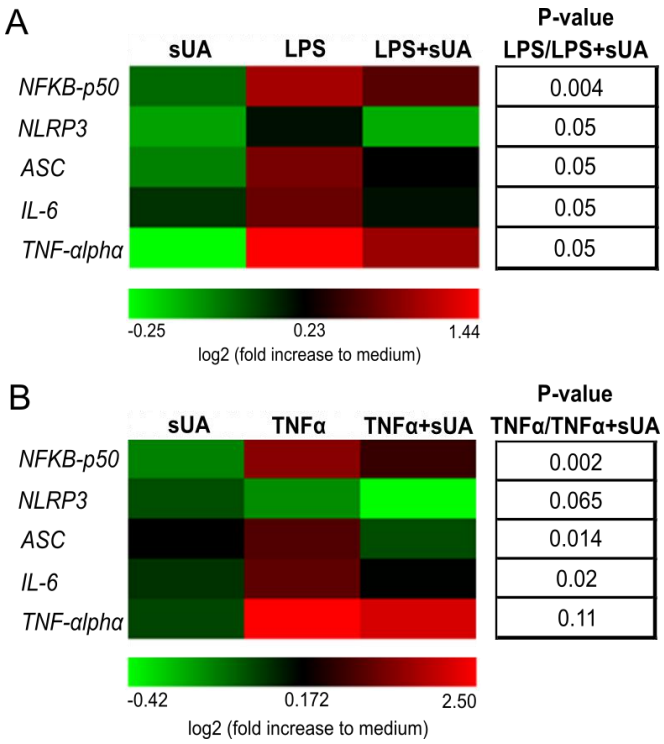

Figure 27: Soluble UA mediates the defective inflammatory function of human monocytic THP-1 cells. Human monocytic THP-1 cells were pre-incubated with 0.6mM sUA prior to stimulation with LPS, TNF-α or left untreated (medium) for 4 hours. After LPS (**A**) or TNF-α (**B**) stimulation, mRNA expression levels of the inflammatory genes *NFκBp50, NLRP3, ASC, IL-6* and *TNF-alpha* were determined via RT-PCR and illustrated as heat map (n = 6 per group; Student's t-test). Data are representative of three independent experiments.

4.8.2 THP-1 cells take up uric acid upon stimulation of LPS via GLUT9

Whether human monocytes also express GLUT9 or other UA transporters that could mediate uptake of sUA, THP-1 cells were pre-incubated with or without 0.6 mM sUA prior to stimulation with LPS for 4 hours, and we found that the presence of LPS significantly reduced the extracellular sUA levels but increased the intracellular levels of sUA (Figure 28A and B). Benzbromarone, an inhibitor of several urate transporters with uricosuric properties, attenuated the LPS-induced intracellular uptake of sUA (Figure 28B). This implied that LPS-induced intracellular sUA uptake in monocytes is mediated by one or several urate transporters and monocytes require activation signals for the SLC2A9-mediated uptake of sUA.

Renal tubular cells express a variety of urate transporters[230]. The expression of *SLC22A6, SLC22A9, SLC22A11, SLC22A12* and *SLC22A13* mRNA levels were tested in human renal progenitor cells by RT-PCR and they were all highly expressed. Next, to look for the expression of these urate transporters in THP-1 cells, we carried out RT-PCR and found that THP-1 cells only expressed *SLC2A9* but not *SLC22A6 (OAT1)*, *11 (OAT4)*, *12 (URAT1)* and *13 (OAT10)* as demonstrated in Figure 28C. However, stimulation of THP-1 cells with LPS did not affect the mRNA expression levels of *SLC2A9* in sUA-treated THP-1 cells (Figure 28D)

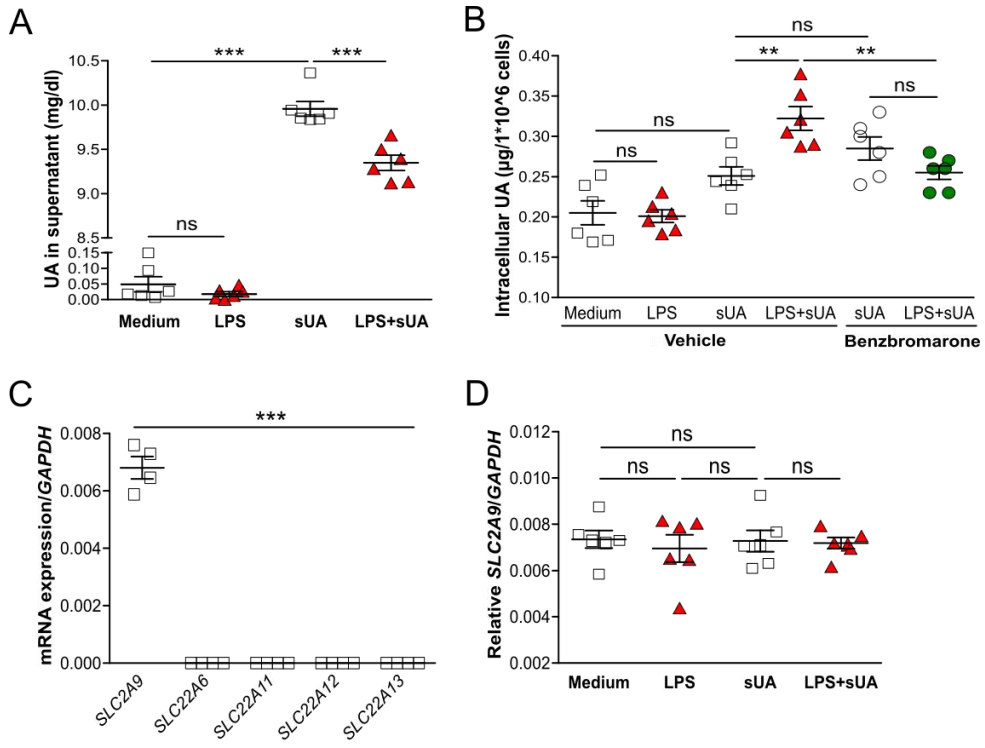

Fig. 28: Monocytes require activation signals for the SLC2A9-mediated uptake of sUA. Human monocytic THP-1 cells were pre-incubated with 0.6 mM sUA prior to stimulation with LPS or left untreated (medium) for 4 hours. (**A**) Culture supernatants were collected and the UA concentrations measured (n = 6 per group; one-way ANOVA). (**B**) LPS-activated THP-1 cells with or without 0.6mM sUA were digested after treatment with vehicle or benzbromarone, and the intracellular UA concentration measured (n = 6 per group; one-way ANOVA). (**C**) mRNA expression of *SLC2A9, SLC22A6, SLC22A11, SLC22A12, SLC22A13* from THP-1 cells determined by RT-PCR (n = 4 per group; one-way ANOVA). (**D**) mRNA expression levels of *SLC2A9* from LPS-treated THP-1 cells with the presence or without sUA determined via RT-PCR (n = 6 per group). Data are mean ± SEM and values are representative of three independent experiments. * $p<0.05$; ** $p<0.01$; *** $p<0.001$; ns = not significant by one-way ANOVA.

4.8.3 Knockdown of SLC2A9 in monocytes reverses the effect of sUA

To confirm that the impaired monocytes function due to sUA is regulated via Glut9, we performed knockdown experiments using SLC2A9-specific siRNA. The effective knockdown of SLC2A9 with siRNA in LPS-stimulated and untreated THP-1 cells was confirmed by RT-PCR for *SLC2A9* as compared to siRNA control (Figure 29A). SLC2A9 silencing significantly attenuated the suppressive effect of LPS on extracellular and intracellular sUA levels, indicating that the uptake of sUA in LPS-stimulated monocytes occurs via the urate transporter SLC2A9 (Figure 29B and C). The same effect on extracellular and intracellular sUA levels by THP-1 cells was observed in response to TNF-α (Figure 29D and E).

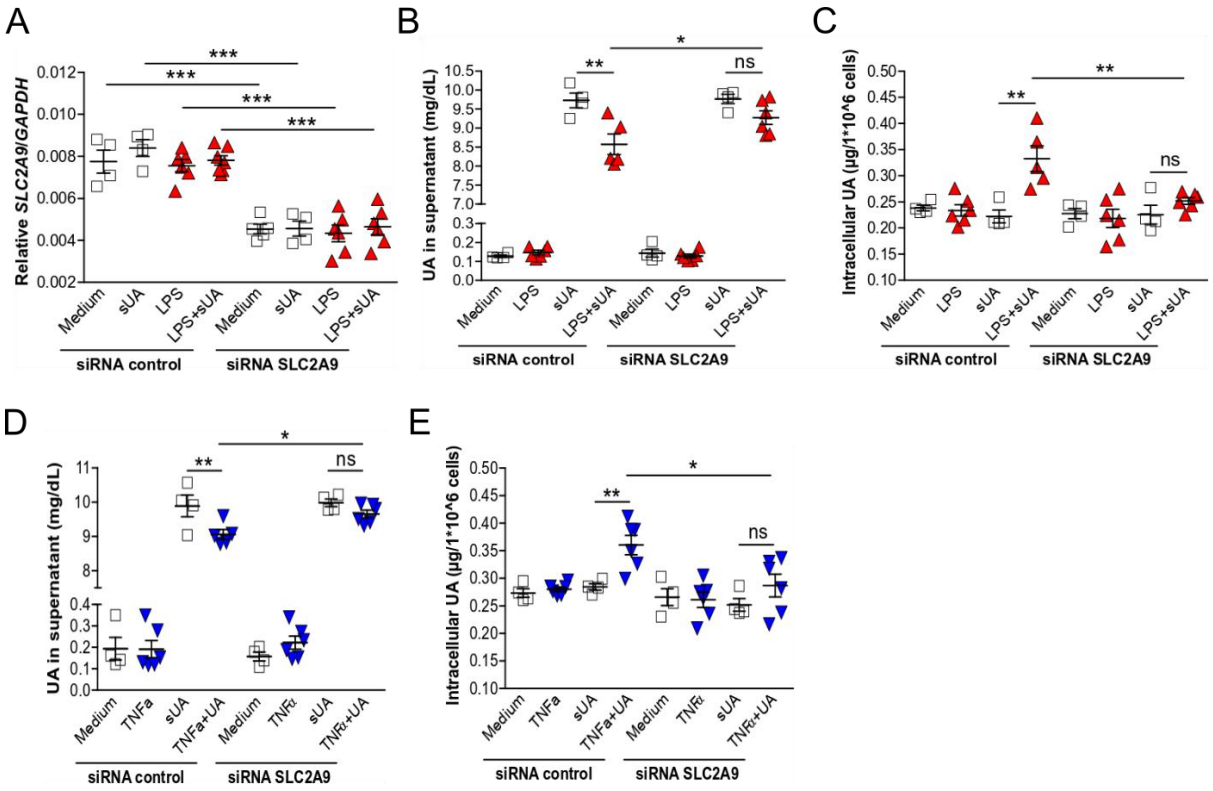

Figure 29: Knockdown of SLC2A9 in THP-1 cells abolished the uptake of sUA. Knockdown of SLC2A9 using specific siRNA (siRNA SLC2A9) or scrambled siRNA (siRNA control) in THP-1 cells. After transfection and LPS stimulation, relative mRNA expression levels of *SLC2A9* determined via RT-PCR (**A**) (n = 4-6 per group; two-way ANOVA); concentration of sUA in the supernatants (**B**) and intracellular sUA levels (**C**) determined using an UA assay kit (n = 4-6 per group; two-way ANOVA). (**D** to **E**) After transfection and TNF-α stimulation, concentration of sUA in the supernatants (**D**) and intracellular sUA levels (**E**) determined using an UA assay kit (n = 4-6 per group; two-way ANOVA). Data are mean ± SEM and values are representative of two independent experiments. * $p<0.05$; ** $p<0.01$; *** $p<0.001$; ns = not significant.

Using scambled control siRNA, the mRNA expression of the inflammatory genes *NFκBp50*, *IL-6*, and *TNF-alpha* significantly decreased in LPS+sUA-stimulated THP-1 cells compared to LPS-activated THP-1 cells alone (Figure 30 A to C). However, SLC2A9 knockdown did not alter the inflammatory gene expression in LPS+sUA-activated THP-1 cells compared to LPS-activated cells only (Figure 30A to C). The same effect of sUA on the inflammatory function in monocytes was also observed in response TNF-α independent after silencing SLC2A9 (Figure 30D and E). In summary, monocyte activation under hyperuricemic conditions leads to SLC2A9-mediated intracellular uptake of sUA, which inhibits the expression of pro-inflammatory cytokines.

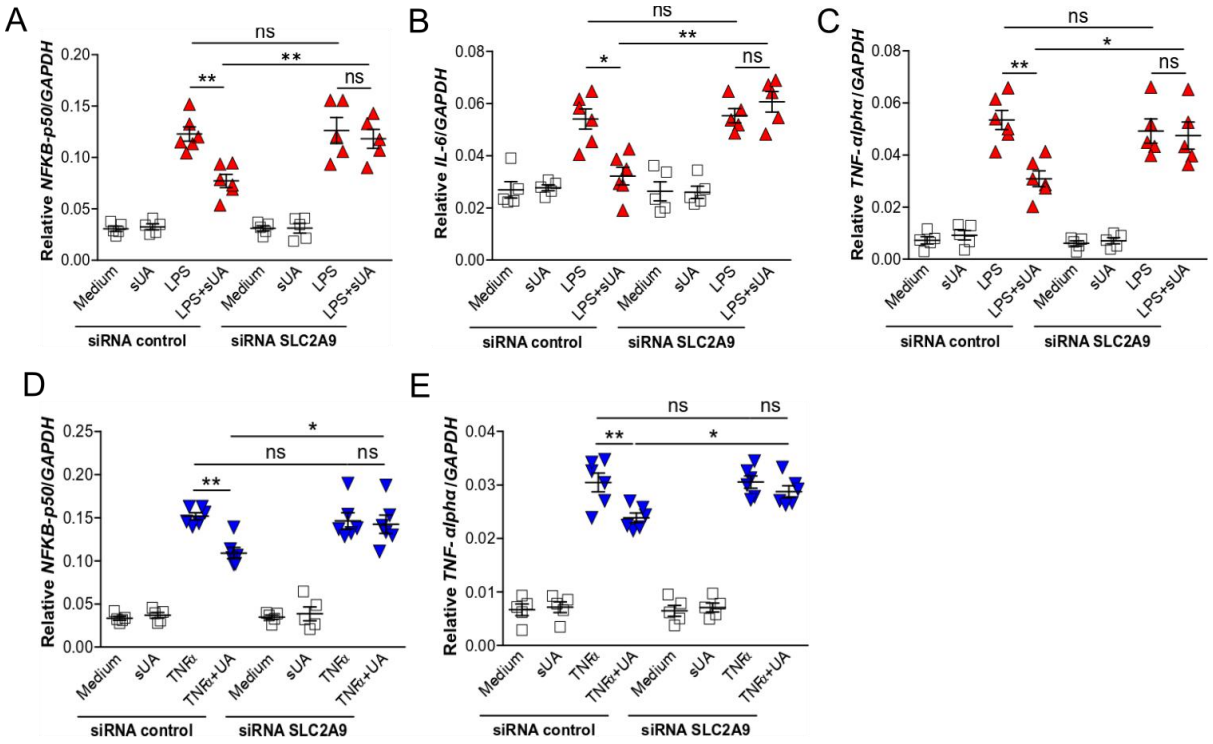

Figure 30: Knockdown of SLC2A9 in THP-1 cells reverses sUA effect. Knockdown of *SLC2A9* using specific siRNA (siRNA *SLC2A9*) or scrambled siRNA (siRNA control) in activated THP-1 cells. After transfection, relative mRNA expression levels of the inflammatory genes *NFKB-p50* (**A**), *IL-6* (**B**) and *TNF-alpha* (**C**) or TNF-α-stimulated THP-1 cells relative mRNA expression levels of the inflammatory genes *NFκBp50* (**D**) and *TNF-alpha* (**E**) determined via RT-PCR (n = 5-6 per group; two-way ANOVA). Data are mean ± SEM and values are representative of two independent experiments. * $p<0.05$; ** $p<0.01$; *** $p<0.001$; ns, not significant.

5 Discussion

5.1 Overview

There have been many studies exploring the potential causative role of UA in the association of HU with inflammatory disease states. This thesis provides further insights into this previously unknown function of HU involved in gout and CKD/ESKD. The aims of this thesis were to investigate: whether HU has immunomodulatory effects on the acute inflammatory response in vivo during experimental gouty arthritis in CKD; the effect of sUA on blood neutrophils from healthy volunteers and CKD/ESKD patients *ex vivo*, e.g. neutrophil activation and migration, as well as NET formation in response to MSU crystals; and the immunemodulatory role of sUA on the inflammatory function of CD14+ monocytes from healthy volunteers and CKD/ESKD patients *ex vivo* and on THP-1 cells *in vitro*.

Our *in vitro* and *in vivo* data provided evidence that sUA acts as an endogenous modulator of innate immunity. First, sUA regulated neutrophils recruitment by β2 integrin deactivation in sterile inflammation during CKD. Second, SLC2A9/GLUT9 facilitates the intracellular uptake of sUA by activated monocytes, which results in a suppressed inflammatory response. Beyond its known role as substrate for MSU crystal formation, sUA not always has adverse effects on other diseases.

5.2 The suppressive effect of hyperuricemia on sterile inflammation

There has been substantial interest in investigating the role of sUA as an anti-oxidant. A protective role for HU has been demonstrated in a prospective study by Lai, *et al.* showing that higher UA levels are associated with lower risks of all-cause, cardiovascular and infection-associated mortality in women treated with continuous ambulatory peritoneal dialysis[231]. *In vitro* studies also showed that sUA can act as a potent scavenger of singlet oxygen[232] and peroxynitite[233], inhibit Akt phosphorylation in endothelial cells[234], reduce intracellular ROS in cancer cell lines[235], and modulate the activity of extracellular superoxide dismutase in atherosclerotic vessels[236]. The results of this study now provide insight into how HU may influence the inflammatory response in gouty arthritis.

Our data show that HU suppresses the MSU crystals-induced sterile inflammatory response. This was supported in an *in vivo* mouse model of HU with and without CKD and *in vitro* experiments using human blood neutrophils and monocytes. First, HU suppressed β2 integrin activation in neutrophils and PSGL-1 expression in monocyte isolated from CKD and ESKD

patients compared to healthy subjects; second, HU impaired the migratory ability of leukocytes and therefore attenuated MSU crystal-induced inflammation, and even more pronounced in mice with HU and CKD by regulating leukocyte rolling, adhesion, and extravasation; third, sUA inhibited the inflammatory function of human monocytes in response to inflammatory stimuli via the urate transporter Glut9, which might be a potential mechanism for the suppressive effect of HU in ESKD patients.

In contrast to our study, many studies suggest that sUA directly contributes to oxidative stress and inflammation. For example, sUA has been identified as a dangerous signal that can alert the immune system to dying cells[121], activate TLRs and induced pro-inflammatory cytokine production in human peripheral blood mononuclear cells[122], and initiate the AKT-PRAS40 autophagy pathway in human monocytes[123], and trigger the activation of the NLRP3 inflammasome in bone marrow derived macrophages[120]. Apart from immune cells, sUA has the ability to activate MAP kinase signaling in adipocytes through increased ROS production and oxidative stress[124]. Soluble UA activates NFκB and MAPK signaling, cell proliferation in vascular smooth muscle cells[80,126,127], and induces endothelial dysfunction by activating the HMGB1/RAGE signaling pathway[237]. Furthermore, sUA also can reduce the production of nitric oxide (NO), a regulator molecule for cardiovascular system and hypertension[238,239], either by affecting NO biosynthesis, or by reducing NO bioavailability[126,240]. However, currently, the overall functional importance of HU *in vitro* and *in vivo* remains controversial.

UA is the end product of the purine metabolism in humans beings due to the loss of the enzyme uricase during evolution[61], in addition, the continuous UA production and the reabsorption during renal excretion together result in high serum UA level in humans[62]. However, rodents have uricase, therefore it is difficult to develop a mouse model with stable HU. Currently, most *in vivo* studies that investigate the function of UA are based on very low serum UA levels (2-5 mg/dl)[120,126,241–243], which would not even be considered clinically as HU. For example, when gavaging rats with the uricase inhibitor oxonic acid, the serum UA levels remain either below 2 mg/dl[126] or rise up to 4 mg/dl[241]. By using an high-fat diet-induced HU model of type 2 diabetes, rats will develop serum UA level of around 2 mg/dl[243]. And even when daily intraperitoneal injected mice with UA (250 mg/kg), the serum UA concentration will still be only around 180 µmol/l (3 mg/dl)[244]. GWAS found that Glut9 is a major urate transporter in humans and mice. Humans carrying the Glut9 loss-of-function mutation develop familial renal hypouricemia type 2, a condition characterized by hypouricemia. In mice, serum UA levels are controlled by the hepatic breakdown and renal

processes of reabsorption and secretion. A systemic knockout of Glut9 leads to moderate HU, massive hyperuricosuria and an early-onset of mild renal insufficiency; while the liver-specific inactivation of Glut9 causes severe HU and hyperuricosuria, in the absence of urate nephropathy or any structural abnormality of the kidney[207]. Kidney damage and inflammation was not observed in Alb-creERT2;*Glut9*$^{lox/lox}$ mice that only developed HU. On the other hand, Alb-creERT2;*Glut9*$^{lox/lox}$ mice fed a high-fat diet with inosine developed kidney injury due to the deposition of uric acid crystals. This mouse model may imply that HU itself may not be sufficient to cause CKD. However, argument about whether HU causes CKD and contributes to CKD progression have been a matter of debate for many years, but all clinical studies so far cannot fully conclude whether HU is just the cause or the consequence of CKD[245]. For judging the purpose of ULT in CKD patients, further studies are needed to clarify the contribution of HU on CKD progression.

5.3 Hyperuricemia mediates neutrophil migration but not NET formation

Using an *in vivo* and *in vitro* approach, our study shows for the first time that HU directly impairs leukocyte recruitment, specifically leukocyte rolling velocity, adhesion, and extravasation via β2 integrin deactivation, which diminished MSU crystal-related tissue inflammation, a model mimicking sterile inflammation in acute gouty arthritis. Meanwhile, when HU+CKD mice were treated with rasburicase to decline the serum UA level, the decreased neutrophils migration and reduced inflammatory cytokines were restored. Furthermore, rasburicase treated sera from CKD/ESKD patients also restored the capability of healthy neutrophils to migrate towards chemoattractants using transwell migration assays. This finding may explain why the initiation of ULT can trigger a new onset of acute gouty arthritis[246]. Current treatment guidelines recommend concomitant prophylaxis with colchicine[143], an inhibitor of neutrophil activation and migration[247].

Neutrophils express more than 30 surface receptors that are related to multi-functions, including G protein-coupled receptors, Fc receptors, adhesion receptors, chemokine receptors and pattern recognition receptors[248]. It is well-known that neutrophils from CKD/ESKD patients show changes in surface receptor expression leading to functional abnormalities due to numerous metabolic waste and toxic substances. For example, accelerated neutrophil apoptotic cell death[37], reduced chemotactic activity, lower cellular phagocytic response and reduced oxidative metabolism leading to intracellular killing[40,214]. CKD/ESKD patients suffer from a high incidence of recurrent bacterial infections and inflammation[35,37,249,250], which has

been linked to an unresponsiveness of neutrophils to further stimuli, accompanied by an impaired migratory behavior[251].

Neutrophils chemotaxis is critical for appropriate recruitment to sites of inflammation. Reports have also shown that leptin[43], resistin[45], modified ubiquitin[42] and granulocyte inhibitory proteins[41] can contribute to a disturbed neutrophil chemotactic ability in uremic patients. Rossaint *et al*. identified a role for the fibroblast growth factor 23, which is highly elevated in uremic patients, to deactivate neutrophil integrins and thereby inhibiting neutrophil rolling, adhesion and transmigration in infection and inflammation during CKD[250,252]. Several other endogenous regulators of neutrophil integrin activation and transmigration have been identified, including growth and differentiation factor 15 after myocardial infarction[253], developmental endothelial locus-1 during periodontitis[254], and AnnexinA1 during the pathogenesis of artherosclerosis[255]. In our study, neutrophils from CKD/ESKD patients showed decreased expression of CD62L and Mac-1, both are adhesion molecules important for leukocyte-endothelial cell interactions and slowing leukocyte trafficking through the blood. This decreased expression of selectin and integrins on neutrophils, as well as the impaired neutrophil recruitment is partly due to HU, and provides further insights into the novel function of HU (Figure 31).

Neutrophils require stimulatory signaling events such as chemokines for the activation of integrins, a process called inside-out signaling[256]. Once an increase in affinity or ‘activation’ has been achieved, integrins such as LFA-1 will bind firmly to the ligand and signal back into the cell on which it is expressed. This is termed outside-in signaling, and the effector functions of adhesion and cell migration depends on this signaling[256]. Besides these known endogenous regulators, our present findings now demonstrate a previously unrecognized role of HU on the inside-out signaling in activated neutrophils in the context of CKD-related gout by impairing their migratory ability to the site of crystal-induced inflammation (Figure 31). However, the exact intracellular or receptor-mediated effects of sUA on the inside-out and outside-in signaling cascade need to be addressed in future studies.

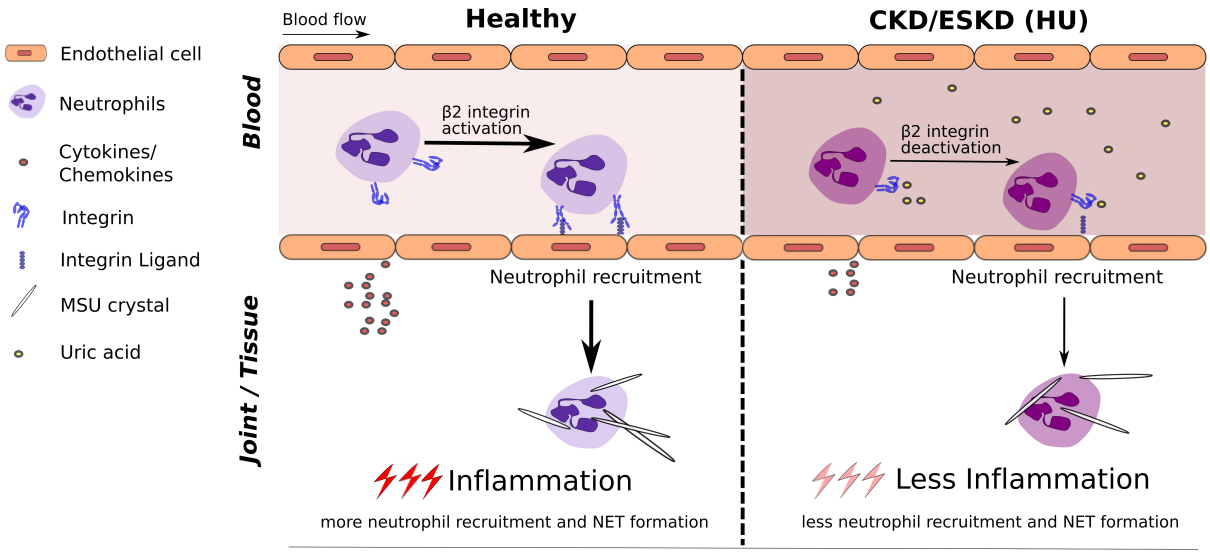

Figure 31: Schematic showing neutrophils recruitment from the vasculature into the inflamed tissue is impaired in CKD/ESKD. In the healthy stage, MSU crystals trigger a joint inflammation, which induces the release of inflammatory cytokines and chemokines, and leads to the activation of endothelial cells to express selectins. Circulating neutrophils are captured by selectins, which is followed by the activation of integrins from the inactive bend form to the open conformation with high affinity. After integrin activation, neutrophils undergoing integrin-mediated crawling and finally transmigrate to the site of inflammation. In ESKD, HU impaired neutrophil's integrin activation, leading to weakened adhesion ability and less transmigration into the inflamed joint/tissue, a mechanism responsible for a diminished MSU crystal-induced inflammatory response less inflammation. CKD, chronic kidney disease; ESKD, end-stage kidney disease; MSU, monosodium urate; HU, hyperuricemia; GLUT9, glucose transporter 9.

Many papers show that NETs play an important role in gout attack as mentioned in the introduction[162,257]. After neutrophils recruit to the site of MSU crystals deposits, they can release NETs. It was reported that neutrophils from gout patients spontaneously release NETs, meanwhile NETs also can be induced by serum from gout patients when cultured with healthy neutrophils[258].These NETs can be visualized by detecting DNA, MPO and NE in the synovium of gout patients. In our study, we found that neutrophils from CKD/ESKD patients had no difference on NET formation compared to neutrophils from healthy individuals. This suggested that uremic toxins do not relate to impaired NET formation. However, studies have shown an increased NET formation in CKD patients (CKD stage G1-3)[40] as well as in hemodialysis patients which related to chronic inflammation and cardiovascular disease[259]. Meanwhile, the impaired NETs degradation was reported to be associated with SLE[260], ANCA-associated vasculitis[205,218] and rheumatoid arthritis[216]. In contrast, a recent study showed that aggregated NETs due to a high density of neutrophils can have a positive role in favoring the resolution of MSU crystal-induced inflammation by degrading cytokines and chemokines, indicating a role for aggregated NETs in dampening chronic inflammation[162].

5.4 Hyperuricemia mediates the inflammatory function of monocytes

Our data show that HU and CKD impair monocyte recruitment in a mouse model of gouty arthritis and that HU also suppresses LPS- and MSU crystal-induced pro-inflammatory cytokine expression in monocytes from CKD/ESKD patients. The suppressed function of monocytes is consistent with previous reports demonstrating that monocytes isolated from uremic patients are hyporesponsive to *ex vivo* LPS or MSU crystal stimulation, indicating a reduced ability to synthesize pro-inflammatory cytokines[33]. It is also well-known that HU seems to be associated with Parkinson's disease because higher levels of serum UA are related to a decreased risk of this neurogenerative disease[261]. On the other hand, monocytes from Parkinson' disease patients are hyperactive in response to LPS stimulation, and that this hyperactivity correlates with the disease severity[262]. HU itself did not change gene expression of monocytes but only suppressed the hyperactivity to a "second stimuli", which may explain the suppressed function of monocytes in Parkinson's disease as well as our data in ESKD patients.

In contrast, other studies suggest that sUA directly contributes to oxidative stress and inflammation in monocytes. For example, sUA has been identified as a dangerous signal that can alert the immune system to dying cells[121], activate TLRs and induced pro-inflammatory

cytokine production in human peripheral blood mononuclear cells[122], and initiate the AKT-PRAS40 autophagy pathway in human monocytes[123], trigger the NLRP3 inflammasome in bone marrow derived macrophages[120]. However, the overall functional importance of HU *in vitro* and *in vivo* remains controversial due to the use of clinically irrelevant sUA concentrations of 12 to 50 mg/dl for *in vitro* experiments[120,123,241,243]. These UA concentrations exceed the saturation point of solubility and form microcrystals that in turn induce the activation of the NLRP3 inflammasome and other inflammatory signaling pathways in monocytes[156,169]. Further studies to investigate the mechanisms of UA's effect on monocyte are still needed.

The exact intracellular mechanism how sUA suppresses the inflammatory function of human monocytes in response to LPS- or MSU crystal is not known. These intracellular processes may occur following uptake of sUA via urate transporters[63]. Although many of these urate transporters are highly expressed in the kidney and intestine, recent studies found SLC22A12 and SLC2A9 to be expressed in human endothelial cells, leukocytes and chondrocytes[263–265]. The urate transporters SLC2A9 and BCRP/ABCG2[234] can regulate the sUA uptake in human umbilical vascular endothelial cells, which further triggers cell injury and inflammation. Unlike in endothelial[264], pancreatic beta[86] and vascular smooth muscle cells[241], our data show that the sUA uptake by monocytes occurs via SLC2A9 leading to this suppressed monocyte phenotype. Interestingly, this uptake only seems to happen in the presence of stimuli, such as LPS and TNF-α, indicating that monocytes require a second signaling event for the intracellular uptake of sUA. Whether other transporters apply to other cell types, e.g. urate transporters or selective organic anion channels[266], remain to be investigated in future studies.

Although, there was no difference in the MSU crystal-induced formation of NETs between neutrophils from healthy individuals and ESKD patients, interesting was to observe that soluble inflammatory mediators released from UA-treated activated monocytes induced less NET formation. This is consistent with data showing that apart from the direct NET formation by MSU crystals, soluble mediators, such as IL-1β and TNF-α, released from activated macrophages can indirectly promote NET release[225,226]. Our data indicated that sUA suppresses the function and accordingly the release of pro-inflammatory mediators in monocytes; therefore altering secondary effects on other immune cells, specifically NET formation. As shown previously, NETs can contribute to the resolution phase of an acute gout attack[162]. Now, we identified another possible mechanism of shutting down sterile inflammation showing that HU induces secondary effects on NET formation and might

therefore explain why many patients have lower serum UA levels during an acute gout flare[189,267].

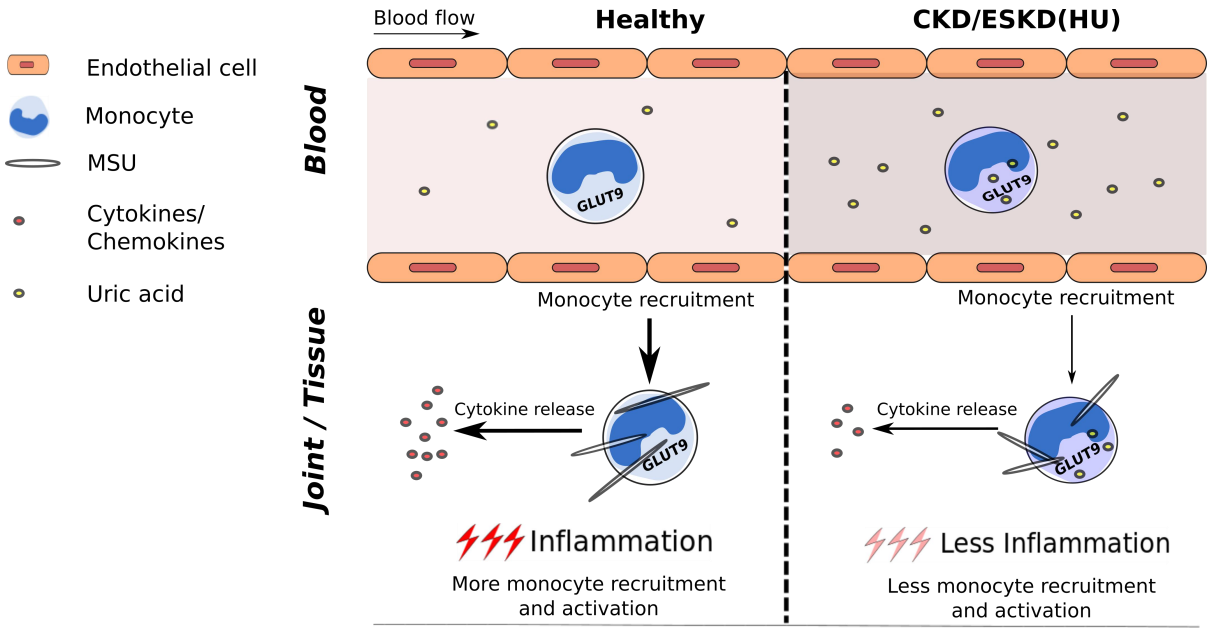

Figure 32: Schematic illustrating the immunomodulatory effects of HU on monocyte function in sterile inflammation during CKD/ESKD. Under healthy conditions, monocytes migrate from the blood into the inflamed joint. Once monocytes enter the inflamed joint space, they get activated by MSU crystals leading to the release of pro-inflammatory cytokines and chemokines, characteristic features for an acute inflammatory response. In the setting of HU and CKD/ESKD, monocytes take up sUA via GLUT9 which results in impaired monocyte recruitment from the blood into the joint and a suppressed GLUT9-mediated inflammatory monocyte phenotype in response to MSU crystals. CKD, chronic kidney disease; ESKD, end-stage kidney disease; MSU, monosodium urate; HU, hyperuricemia; GLUT9, glucose transporter 9.

5.5 Limitations of this study

One limitation of this study is that we lack information on whether the enrolled CKD and ESKD patients had a previous history of gouty arthritis. Only patients that did not receive ULT or immunosuppressive drugs were included into the study. However, this does not rule out the presence of MSU crystal deposits within the joints of CKD and ESKD patients. Prospective studies have shown that MSU crystals can also be found in the joint space of ESKD patients, despite the absence of active inflammatory gout attacks[268]. Whether the formation of MSU crystals within joints might also be altered in ESKD patients remains elusive.

The pathophysiology of an acute gout attack in humans is complex and to get more insights into the cellular response one would need to retrieve synovial fluid from patients before and after an acute gout attack has occurred. However, this is ethically not possible. Therefore, animal models have been developed for studying gouty inflammation in more detail. The established mouse models of gout that are widely used in the literature are: the joint model[269], the peritoneal model[169] and the air pouch model[162]. All mouse models do have some limitations including the small size of murine joints limits the range of investigations that can be performed, and the absence of osteoclasts and chondrocytes in the bone niche as well as the absence of cartilage and bone. Within this thesis, the air pouch model and the previously unknown intravital microcopy model of the cremaster muscle were used as inflammatory mouse models for acute gout. The air pouch model is beneficial due to the easy access to get enough recruited leukocytes and lavage fluid to study the inflammatory response induced by MSU crystals. In addition, using the cremaster muscle as the inflammatory model for acute gout makes it possible for us to study and virtualize the leukocyte recruitment under the microscope in the different stages of rolling, adhesion and transmigration. Except for the shortages mentioned above, these two models do not include the joint structure.

THP-1 cells are a monocyte-like cell line and derived from the peripheral blood of a boy with acute monocytic leukemia[229]. Using THP-1 cells for *in vitro* studies are widely appreciated in the literature to investigate function of human monocytes and THP-1-differentiated macrophages. Here, we used THP-1 cells because they are easier to obtain and to handle with less variation in cell culture compared to human primary monocytes. These cells are also non-adherent cells, which is convenient when performing sUA uptake experiments and siRNA knockdown assays. However, unlike primary human blood monocytes, THP-1 cells

only express low levels of CD14 accompanied with reduced responsiveness to LPS. It would be still of importance to investigate the effects of sUA on human primary monocytes in the future.

6 Conclusions

The results provide new insights into a potential immune-suppressive function of HU. Our *in vitro* and *in vivo* data demonstrate that sUA has immunomodulatory effects during sterile inflammation, e.g. on the immune response induced by MSU crystals, beyond its known role as substrate for MSU crystal formation.

The findings of the current study have multiple implications that are listed as followed and summarized in Figure 32:

- HU contributes to CKD-related suppression of MSU crystal-induced gouty arthritis-like sterile inflammation.
- Rasburicase treatment reversed the suppressive effect HU.
- HU and CKD attenuate MSU-crystal-induced leukocyte rolling, adhesion, and extravasation in vivo.
- sUA regulated neutrophils recruitment by supressing β2 integrin expression and activation in sterile inflammation during CKD.
- SLC2A9/GLUT9 facilitates the intracellular uptake of sUA by activated monocytes, which results in a suppressed inflammatory response.
- HU does not directly affect MSU crystal-induced NET formation in ESKD patients, but indirectly though soluble mediators released form suppressed monocyte.

Taken together, our research provides new insights on the immunomodulatory effects of HU and gives possible clinical explanations for the unexpectedly low incidence of acute gouty arthritis in CKD/ESKD patients as well as the increased risk for acute gout attacks in patients upon starting ULT, highlighting that soluble and crystalline UA have opposite effects on innate immunity.

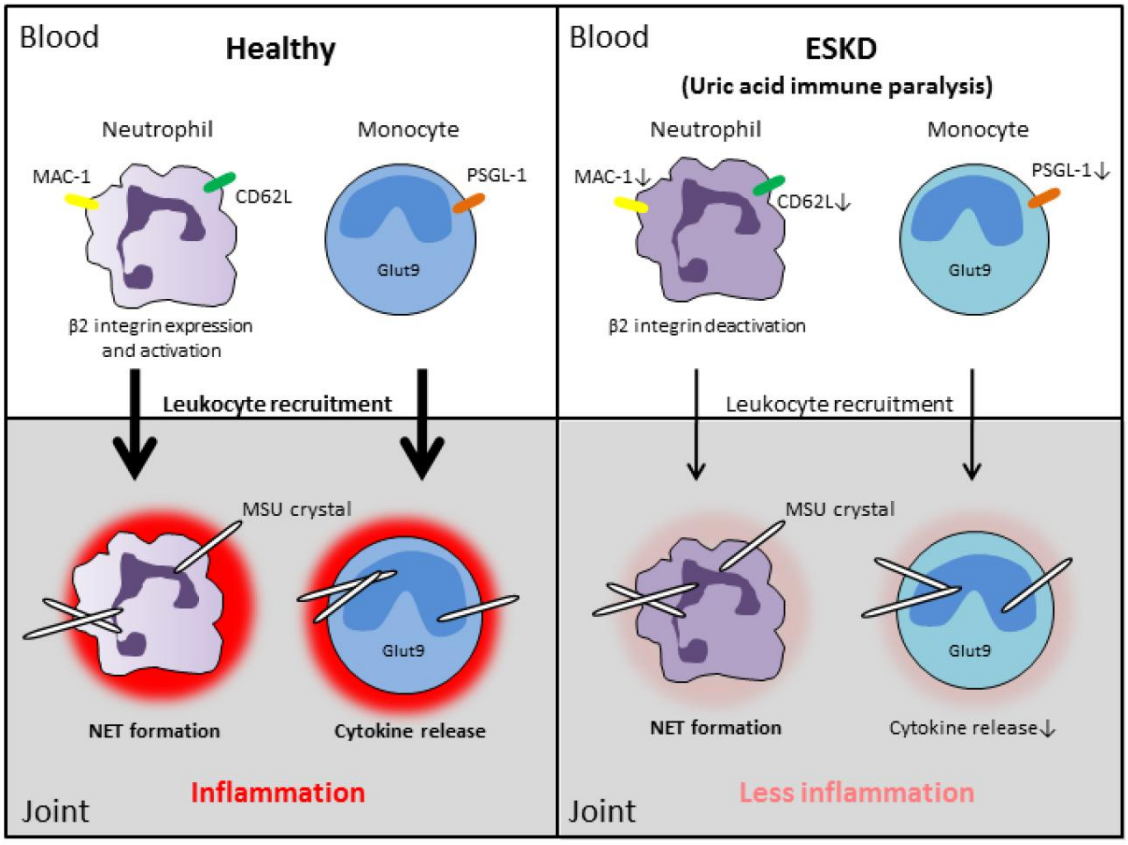

Figure 33: Schematic illustrating the immunomodulatory effects of HU on neutrophil migration and monocyte function in sterile inflammation during ESKD.

7 Future directions in the context of hyperuricemia

Integrin signaling through the leukocyte membrane is bidirectional, known as “inside-out” and “outside-in” signaling, which mediates cell migration and activation. Our present findings now demonstrate a previously unrecognized role of HU on neutrophil recruitment by inhibiting β2 integrin activation (“inside-out” signaling) in sterile inflammation during CKD. Future experiments are needed to also investigate the exact intracellular or receptor-mediated effects of sUA on the outside-in signaling cascade to clarify the mechanism.

Our *in vitro* study shows SLC2A9/GLUT9 facilitates the intracellular uptake of sUA in LPS and TNF-α-activated monocytes, which results in a suppressed inflammatory response. Currently it is not known how exactly GLUT9 mediates intracellular sUA uptake and which downstream signaling events other than TNF-α, IL-6, NFκB and the NLRP3 inflammasome are involved in inhibiting activated monocytes. We found that human monocytes only express GLUT9 but not the previously reported urate transporters in tubular cells, including OAT1, OAT4, OAT12 URAT1 and OAT10. Future studies could be undertaken to determine whether membrane channels that mediate the sUA transport in activated monocytes are involved.

We have identified sUA as an endogenous modulator of innate immunity, especially neutrophils and monocytes. Whether HU can directly affect other cell types in the context of gouty arthritis is currently not known. For example, endothelial cells are important for the transmigration of neutrophils and monocytes and are in direct contact via adhesion molecules. It is known that CKD patients suffer from endothelial cells dysfunction[270]. However, whether this is due to HU and contributes to the impaired neutrophil recruitment still needs to be investigated.

Besides the immunosuppressive role of HU in sterile inflammation, it would be of interest to investigate whether HU can modulate the immune response during infection. CKD/ESKD patients suffer from a high incidence of recurrent bacterial infections and inflammation, which has been linked to an unresponsiveness of neutrophils to further stimuli, accompanied by an impaired migratory behavior.

The findings reported in this thesis are vital for advocacy among doctors and researchers to help patients to improve the treatment of gout care, especially patients with CKD and ESKD.

It is tempting to speculate on a role of HU also in CKD/ESKD-related secondary immunodeficiency and that correcting HU in CKD/ESKD may restore host defense. This remains to be addressed in future experiments. Furthermore, more nationwide clinical studies and patients registries are needed in order to predict the burden of gouty arthritis in the general population of individuals with HU as well as in ESKD patients stage G5D.

8 References

1. Hill, N. R. *et al.* Global prevalence of chronic kidney disease - A systematic review and meta-analysis. *PLoS ONE* (2016). doi:10.1371/journal.pone.0158765
2. ISN. Global Kidney Health Atlas.
3. Zoccali, C. *et al.* The systemic nature of CKD. *Nat. Rev. Nephrol.* **13**, 344–358 (2017).
4. Levin, A. & Stevens, P. E. Summary of KDIGO 2012 CKD Guideline: Behind the scenes, need for guidance, and a framework for moving forward. *Kidney International* (2014). doi:10.1038/ki.2013.444
5. Judd, E. & Calhoun, D. A. Management of Hypertension in CKD: Beyond the Guidelines. *Adv. Chronic Kidney Dis.* **22**, 116–122 (2015).
6. Kearney, P. M. *et al.* Global burden of hypertension: Analysis of worldwide data. *Lancet* (2005). doi:10.1016/S0140-6736(05)70151-3
7. Tozawa, M. *et al.* Blood pressure predicts risk of developing end-stage renal disease in men and women. *Hypertension* (2003). doi:10.1161/01.HYP.0000069699.92349.8C
8. Lash, J. P. *et al.* Chronic renal insufficiency cohort (CRIC) study: Baseline characteristics and associations with kidney function. *Clin. J. Am. Soc. Nephrol.* (2009). doi:10.2215/CJN.00070109
9. Perkovic, V. *et al.* Management of patients with diabetes and CKD: conclusions from a “Kidney Disease: Improving Global Outcomes” (KDIGO) Controversies Conference. *Kidney Int.* **90**, 1175–1183 (2016).
10. Forouzanfar, M. H. *et al.* Global, regional, and national comparative risk assessment of 79 behavioural, environmental and occupational, and metabolic risks or clusters of risks, 1990–2015: a systematic analysis for the Global Burden of Disease Study 2015. *Lancet* (2016). doi:10.1016/S0140-6736(16)31679-8
11. Kramer, H. J. Increasing Body Mass Index and Obesity in the Incident ESRD Population. *J. Am. Soc. Nephrol.* **17**, 1453–1459 (2006).
12. Obermayr, R. P. *et al.* Predictors of new-onset decline in kidney function in a general middle-european population. *Nephrol. Dial. Transplant.* (2008). doi:10.1093/ndt/gfm790
13. Kovesdy, C. P., Furth, S. & Zoccali, C. Obesity and kidney disease: Hidden consequences of the epidemic. *Brunei Int. Med. J.* (2017). doi:10.1080/16089677.2017.1299975
14. Maric-Bilkan, C. Obesity and Diabetic Kidney Disease. *Medical Clinics of North America* (2013). doi:10.1016/j.mcna.2012.10.010
15. Câmara, N. O. S., Iseki, K., Kramer, H., Liu, Z. H. & Sharma, K. Kidney disease and obesity: Epidemiology, mechanisms and treatment. *Nat. Rev. Nephrol.* **13**, 181–190 (2017).
16. D’Agati, V. D. *et al.* Obesity-related glomerulopathy: Clinical and pathologic characteristics and pathogenesis. *Nat. Rev. Nephrol.* **12**, 453–471 (2016).
17. Chacko, E. C., Surrun, S. K., Mubarack Sani, T. P. & Pappachan, J. M. Chronic viral hepatitis and chronic kidney disease. *Postgraduate Medical Journal* (2010). doi:10.1136/pgmj.2009.092775
18. Komenda, P. *et al.* The Prevalence of CKD in Rural Canadian Indigenous Peoples: Results From the First Nations Community Based Screening to Improve Kidney Health and Prevent Dialysis (FINISHED) Screen, Triage, and Treat Program. *Am. J. Kidney Dis.* (2016). doi:10.1053/j.ajkd.2016.04.014
19. Genovese, G. *et al.* Association of trypanolytic ApoL1 variants with kidney disease in African Americans. *Science (80-.).* (2010). doi:10.1126/science.1193032
20. Kopp, J. B. *et al.* APOL1 Genetic Variants in Focal Segmental Glomerulosclerosis and HIV-Associated Nephropathy . *J. Am. Soc. Nephrol.* (2011). doi:10.1681/asn.2011040388
21. Gifford, F. J., Gifford, R. M., Eddleston, M. & Dhaun, N. Endemic Nephropathy Around the World. *Kidney International Reports* (2017). doi:10.1016/j.ekir.2016.11.003
22. Bowe, B. *et al.* Particulate Matter Air Pollution and the Risk of Incident CKD and Progression to ESRD. *J. Am. Soc. Nephrol.* ASN.2017030253 (2017). doi:10.1681/ASN.2017030253
23. Bello, A. K. *et al.* Complications of chronic kidney disease: current state, knowledge gaps, and strategy

for action. *Kidney Int. Suppl.* **7**, 122–129 (2017).

24. Liu, M. *et al.* Cardiovascular disease and its relationship with chronic kidney disease. *Eur. Rev. Med. Pharmacol. Sci.* (2014).

25. Disthabanchong, S. Vascular calcification in chronic kidney disease: Pathogenesis and clinical implication. *World J Nephrol* (2012). doi:10.5527/wjn.v1.i2.43

26. Matsushita, K. *et al.* Association of estimated glomerular filtration rate and albuminuria with all-cause and cardiovascular mortality in general population cohorts: a collaborative meta-analysis. *Lancet* (2010). doi:10.1016/S0140-6736(10)60674-5

27. Gansevoort, R. T. *et al.* Lower estimated GFR and higher albuminuria are associated with adverse kidney outcomes. A collaborative meta-analysis of general and high-risk population cohorts. *Kidney Int.* (2011). doi:10.1038/ki.2010.531

28. Masson, P. *et al.* Chronic kidney disease and the risk of stroke: A systematic review and meta-analysis. *Nephrol. Dial. Transplant.* **30**, 1162–1169 (2015).

29. Thomas, R., Kanso, A. & Sedor, J. R. Chronic Kidney Disease and Its Complications. *Prim. Care - Clin. Off. Pract.* **35**, 329–344 (2008).

30. McClellan, W. *et al.* The prevalence of anemia in patients with chronic kidney disease. *Curr. Med. Res. Opin.* (2004). doi:10.1185/030079904X2763

31. Alem, A. M. *et al.* Increased risk of hip fracture among patients with end-stage renal disease. *Kidney Int.* (2000). doi:10.1046/j.1523-1755.2000.00178.x

32. Kato, S. *et al.* Aspects of immune dysfunction in end-stage renal disease. *Clinical Journal of the American Society of Nephrology* (2008). doi:10.2215/CJN.00950208

33. Ando, M. *et al.* Impairment of innate cellular response to in vitro stimuli in patients on continuous ambulatory peritoneal dialysis. *Nephrol. Dial. Transplant.* (2005). doi:10.1093/ndt/gfi048

34. Stenvinkel, P. *et al.* IL-10, IL-6, and TNF-α: Central factors in the altered cytokine network of uremia - The good, the bad, and the ugly. *Kidney International* (2005). doi:10.1111/j.1523-1755.2005.00200.x

35. Cohen, G. & Hörl, W. Immune Dysfunction in Uremia—An Update. *Toxins (Basel).* (2012). doi:10.3390/toxins4110962

36. Fernández-Fresnedo, G. *et al.* B lymphopenia in uraemia is related to an accelerated in vitro apoptosis and dysregulation of Bcl-2. *Nephrol. Dial. Transplant.* (2000). doi:10.1093/ndt/15.4.502

37. Cohen, G., Rudnicki, M. & Hörl, W. H. Uremic toxins modulate the spontaneous apoptotic cell death and essential functions of neutrophils. *Kidney Int.* (2001). doi:10.1046/j.1523-1755.2001.59780048.x

38. Galli, S. J., Borregaard, N. & Wynn, T. A. Phenotypic and functional plasticity of cells of innate immunity: Macrophages, mast cells and neutrophils. *Nature Immunology* (2011). doi:10.1038/ni.2109

39. Summers, C. *et al.* Neutrophil kinetics in health and disease. *Trends in Immunology* (2010). doi:10.1016/j.it.2010.05.006

40. Yevgenyevna Muravlyova, L. *et al.* The alteration in peripheral neutrophils of patients with chronic kidney disease. *Curr. Issues Pharm. Med. Sci.* **28**, 17–20 (2015).

41. Haag-Weber, M. & Hörl, W. H. Are granulocyte inhibitory proteins contributing to enhanced susceptibility to infections in uraemia? *Nephrol. Dial. Transplant* (1996).

42. Cohen, G., Rudnicki, M. & Hörl, W. H. Isolation of modified ubiquitin as a neutrophil chemotaxis inhibitor from uremic patients. *Journal of the American Society of Nephrology : JASN* (1998). doi:10.1021/ic302168g

43. Ottonello, L. *et al.* Leptin as a uremic toxin interferes with neutrophil chemotaxis. *J. Am. Soc. Nephrol.* (2004). doi:10.1097/01.ASN.0000139321.98029.40

44. Cohen, G., Rudnicki, M., Walter, F., Niwa, T. & Hörl, W. H. Glucose-modified proteins modulate essential functions and apoptosis of polymorphonuclear leukocytes. *J. Am. Soc. Nephrol.* (2001).

45. Cohen, G., Ilic, D., Raupachova, J., Hörl, H. & Ho, W. H. Resistin inhibits essential functions of polymorphonuclear leukocytes. *J. Immunol.* (2008). doi:181/6/3761 [pii]

46. Miyagi, M., Aoyama, H., Morishita, M. & Iwamoto, Y. Effects of sex hormones on chemotaxis of human peripheral polymorphonuclear leukocytes and monocytes. *J. Periodontol.* (1992).

doi:10.1902/jop.1992.63.1.28

47. Cohen, G., Rudnicki, M., Deicher, R. & Hörl, W. H. Immunoglobulin light chains modulate polymorphonuclear leucocyte apoptosis. *Eur. J. Clin. Invest.* (2003). doi:10.1046/j.1365-2362.2003.01191.x

48. Galle, J. *et al.* Lp(a) and LDL induce apoptosis in human endothelial cells and in rabbit aorta: Role of oxidative stress. *Kidney Int.* (1999). doi:10.1046/j.1523-1755.1999.00351.x

49. Kettritz, R., Falk, R. J., Jennette, J. C. & Gaido, M. L. Neutrophil superoxide release is required for spontaneous and FMLP-mediated but not for TNF-alpha-mediated apoptosis. *J. Am. Soc. Nephrol.* (1997).

50. Glorieux, G., Vanholder, R. & Lameire, N. Uraemic retention and apoptosis: what is the balance for the inflammatory status in uraemia? *Eur. J. Clin. Invest.* (2003). doi:10.1046/j.1365-2362.2003.01204.x

51. Ingersoll, M. A., Platt, A. M., Potteaux, S. & Randolph, G. J. Monocyte trafficking in acute and chronic inflammation. *Trends in Immunology* (2011). doi:10.1016/j.it.2011.05.001

52. Hill, L. M., Gavala, M. L., Lenertz, L. Y. & Bertics, P. J. Extracellular ATP May Contribute to Tissue Repair by Rapidly Stimulating Purinergic Receptor X7-Dependent Vascular Endothelial Growth Factor Release from Primary Human Monocytes. *J. Immunol.* (2010). doi:10.4049/jimmunol.1001298

53. Ziegler-Heitbrock, L. Monocyte subsets in man and other species. *Cell. Immunol.* (2014). doi:10.1016/j.cellimm.2014.06.008

54. Rogacev, K. S. & Heine, G. H. Human monocyte heterogeneity-a nephrological perspective. *Nephrologie et Therapeutique* (2010). doi:10.1016/j.nephro.2010.01.008

55. Stenvinkel, P. *et al.* IL-10 , IL-6 , and TNF- a : Central factors in the altered cytokine network of uremia — The good , the bad , and the ugly. *Kidney Int.* **67**, 1216–1233 (2005).

56. Kimmel, P. L. *et al.* Immunologic function and survival in hemodialysis patients. *Kidney Int.* (1998). doi:10.1046/j.1523-1755.1998.00981.x

57. WH, L., Kireta, S., Leedham, E., GR, R. & PT, C. Uremia impairs monocyte and monocyte-derived dendritic cell function in hemodialysis patients. *Kidney Int.* (2007). doi:5002425 [pii]\r10.1038/sj.ki.5002425

58. Meyer zum Büschenfelde, K. H., Kurz, P., Hauer, M., Köhler, H. & Meuer, S. C. Selective blockade of the antigen-receptor-mediated pathway of T cell activation in patients with impaired primary immune responses. *J. Clin. Invest.* **80**, 743–749 (2008).

59. Ando, M., Shibuya, A., Tsuchiya, K., Akiba, T. & Nitta, K. Reduced expression of Toll-like receptor 4 contributes to impaired cytokine response of monocytes in uremic patients. *Kidney Int.* (2006). doi:10.1038/sj.ki.5001548

60. Mandal, A. K. & Mount, D. B. The Molecular Physiology of Uric Acid Homeostasis. *Annu. Rev. Physiol.* (2015). doi:10.1146/annurev-physiol-021113-170343

61. Álvarez-Lario, B. & Macarrón-Vicente, J. Uric acid and evolution. *Rheumatology* **49**, 2010–2015 (2010).

62. Ames, B. N., Cathcart, R., Schwiers, E. & Hochstein, P. Uric acid provides an antioxidant defense in humans against oxidant- and radical-caused aging and cancer: a hypothesis. *Proc. Natl. Acad. Sci.* (1981). doi:10.1073/pnas.78.11.6858

63. So, A. & Thorens, B. Uric acid transport and disease. *J. Clin. Invest.* **120**, 1791–1799 (2010).

64. Pascual, E. & Perdiguero, M. Gout, diuretics and the kidney. *Ann. Rheum. Dis.* **65**, 981–982 (2006).

65. Handler, J. S. THE ROLE OF LACTIC ACID IN THE REDUCED EXCRETION OF URIC ACID IN TOXEMIA OF PREGNANCY. *J Clin Invest* 1526–1532 (1960).

66. Firwana, B. M. *et al.* Tumor lysis syndrome: A systematic review of case series and case reports. *Postgraduate Medicine* (2012). doi:10.3810/pgm.2012.03.2540

67. Peixoto, M. do R. G. *et al.* Diet and medication in the treatment of hyperuricemia in hypertensive patients. *Arq. Bras. Cardiol.* (2001). doi:10.1590/S0066-782X2001000600004

68. Tseitlin, H. Tumor lysis syndrome. in *Emergencies in Pediatric Oncology* (2012). doi:10.1007/978-1-4614-1174-1_3

69. Davidson, M. B. *et al.* Pathophysiology, clinical consequences, and treatment of tumor lysis syndrome. *American Journal of Medicine* (2004). doi:10.1016/j.amjmed.2003.09.045

70. Coiffier, B. *et al.* Efficacy and safety of rasburicase (recombinant urate oxidase) for the prevention and treatment of hyperuricemia during induction chemotherapy of aggressive non-Hodgkin's lymphoma: Results of the GRAAL1 (Groupe d'Etude des Lymphomes de l'Adulte Trial on R. *J. Clin. Oncol.* (2003). doi:10.1200/JCO.2003.04.115

71. Cheuk, D. K. L., Chiang, A. K. S., Chan, G. C. F. & Ha, S. Y. Urate oxidase for the prevention and treatment of tumour lysis syndrome in children with cancer. *Cochrane Database of Systematic Reviews* (2017). doi:10.1002/14651858.CD006945.pub4

72. Shekarriz, B. & Stoller, M. L. Uric acid nephrolithiasis: current concepts and controversies. *J. Urol.* (2002). doi:10.1097/01.ju.0000028481.80787.d6

73. Johnson, R. J. *et al.* Uric acid and chronic kidney disease: Which is chasing which? *Nephrology Dialysis Transplantation* (2013). doi:10.1093/ndt/gft029

74. Torres, R. J. Lesch-Nyhan Syndrome. in *Brenner's Encyclopedia of Genetics: Second Edition* (2013). doi:10.1016/B978-0-12-374984-0.00856-1

75. Guo, L. Interpretation of the Chinese expert consensus: Recommendations for diagnosis and treatment of asymptomatic hyperuricemia complicated with cardiovascular diseases. *J. Transl. Intern. Med.* **2**, 93 (2014).

76. Feig, D. I., Soletsky, B. & Johnson, R. J. Effect of allopurinol on blood pressure of adolescents with newly diagnosed essential hypertension: A randomized trial. *JAMA - J. Am. Med. Assoc.* (2008). doi:10.1001/jama.300.8.924

77. Soletsky, B. & Feig, D. I. Uric acid reduction rectifies prehypertension in obese adolescents. *Hypertension* (2012). doi:10.1161/HYPERTENSIONAHA.112.196980

78. McMullan, C. J., Borgi, L., Fisher, N., Curhan, G. & Forman, J. Effect of uric acid lowering on renin-angiotensin-system activation and ambulatory BP: A randomized controlled trial. *Clin. J. Am. Soc. Nephrol.* (2017). doi:10.2215/CJN.10771016

79. Thanassoulis, G., Brophy, J. M., Richard, H. & Pilote, L. Gout, allopurinol use, and heart failure outcomes. *Arch. Intern. Med.* (2010). doi:10.1001/archinternmed.2010.198

80. Choi, Y. J. *et al.* Uric acid induces endothelial dysfunction by vascular insulin resistance associated with the impairment of nitric oxide synthesis. *FASEB J.* (2014). doi:10.1096/fj.13-247148

81. Chhabra, N. Endothelial dysfunction – A predictor of atherosclerosis. *Internet J Med Updat.* (2009). doi:10.5830/CVJA-2011-068

82. Alderman, M. H. Uric acid and cardiovascular risk. *Curr. Opin. Pharmacol.* (2002). doi:10.1016/S1471-4892(02)00143-1

83. Ioachimescu, A. G., Brennan, D. M., Hoar, B. M., Hazen, S. L. & Hoogwerf, B. J. Serum Uric Acid Is an Independent Predictor of All-Cause Mortality in Patients at High Risk of Cardiovascular Disease A Preventive Cardiology Information System (PreCIS) Database Cohort Study. **58**, 623–630 (2008).

84. Johnson, R. J. *et al.* Potential role of sugar (fructose) in the epidemic of hypertension, obesity and the metabolic syndrome, diabetes, kidney disease, and cardiovascular disease1-3. *American Journal of Clinical Nutrition* (2007). doi:86/4/899 [pii]

85. Chang, H. Y. *et al.* Hyperuricemia Is an Independent Risk Factor for New Onset Micro-Albuminuria in a Middle-Aged and Elderly Population: A Prospective Cohort Study in Taiwan. *PLoS One* (2013). doi:10.1371/journal.pone.0061450

86. Zhang, Y. *et al.* Uric acid induces oxidative stress and growth inhibition by activating adenosine monophosphate-activated protein kinase and extracellular signal-regulated kinase signal pathways in pancreatic β cells. *Mol. Cell. Endocrinol.* (2013). doi:10.1016/j.mce.2013.04.027

87. Yadav, D. *et al.* Hyperuricemia as a Potential Determinant of Metabolic Syndrome. *J. lifestyle Med.* (2013).

88. Samocha-Bonet, D. *et al.* Metabolically healthy and unhealthy obese - The 2013 stock conference report. *Obesity Reviews* (2014). doi:10.1111/obr.12199

89. Tsushima, Y. *et al.* Uric acid secretion from adipose tissue and its increase in obesity. *J. Biol. Chem.* (2013). doi:10.1074/jbc.M113.485094

90. Terkeltaub, R. A. Gout. 1647–1655 (2003).

91. So, A. K. & Martinon, F. Inflammation in gout: Mechanisms and therapeutic targets. *Nat. Rev. Rheumatol.* **13**, 639–647 (2017).

92. Riches, P. L., Wright, A. F. & Ralston, S. H. Recent insights into the pathogenesis of hyperuricaemia and gout. *Hum. Mol. Genet.* (2009). doi:10.1093/hmg/ddp369

93. Annemans, L. *et al.* Gout in the UK and Germany: Prevalence, comorbidities and management in general practice 2000-2005. *Ann. Rheum. Dis.* (2008). doi:10.1136/ard.2007.076232

94. Doherty, M. New insights into the epidemiology of gout. in *Rheumatology* (2009). doi:10.1093/rheumatology/kep086

95. Richette, P. & Bardin, T. Gout. *Lancet* **375**, 318–328 (2010).

96. Perez-Ruiz, F., Calabozo, M., Erauskin, G. G., Ruibal, A. & Herrero-Beites, A. M. Renal underexcretion of uric acid is present in patients with apparent high urinary uric acid output. *Arthritis Rheum.* (2002). doi:10.1002/art.10792

97. Mandal, A. K. & Mount, D. B. The Molecular Physiology of Uric Acid Homeostasis. *Annu. Rev. Physiol.* **77**, 323–345 (2015).

98. Joost, H. G. & Thorens, B. The extended GLUT-family of sugar/polyol transport facilitators: Nomenclature, sequence characteristics, and potential function of its novel members. *Molecular Membrane Biology* (2001). doi:10.1080/09687680110090456

99. Li, S. *et al.* The GLUT9 gene is associated with serum uric acid levels in sardinia and chianti cohorts. *PLoS Genet.* (2007). doi:10.1371/journal.pgen.0030194

100. Döring, A. *et al.* SLC2A9 influences uric acid concentrations with pronounced sex-specific effects. *Nat. Genet.* (2008). doi:10.1038/ng.107

101. Vitart, V. *et al.* SLC2A9 is a newly identified urate transporter influencing serum urate concentration, urate excretion and gout. *Nat. Genet.* (2008). doi:10.1038/ng.106

102. Wallace, C. *et al.* Genome-wide Association Study Identifies Genes for Biomarkers of Cardiovascular Disease: Serum Urate and Dyslipidemia. *Am. J. Hum. Genet.* (2008). doi:10.1016/j.ajhg.2007.11.001

103. Augustin, R. *et al.* Identification and characterization of human glucose transporter-like protein-9 (GLUT9): Alternative splicing alters trafficking. *J. Biol. Chem.* (2004). doi:10.1074/jbc.M312226200

104. Enomoto, A. *et al.* Molecular identification of a renal urate-anion exchanger that regulates blood urate levels. *Nature* (2002). doi:10.1038/nature742

105. Nigam, S. K. *et al.* The Organic Anion Transporter (OAT) Family: A Systems Biology Perspective. *Physiol. Rev.* (2015). doi:10.1152/physrev.00025.2013

106. Xu, X., Li, C., Zhou, P. & Jiang, T. Uric acid transporters hiding in the intestine. *Pharmaceutical Biology* (2016). doi:10.1080/13880209.2016.1195847

107. Ichida, K. *et al.* Decreased extra-renal urate excretion is a common cause of hyperuricemia. *Nat. Commun.* (2012). doi:10.1038/ncomms1756

108. Miner, J. *et al.* Lesinurad, a novel, oral compound for gout, acts to decrease serum uric acid through inhibition of urate transporters in the kidney. *Arthritis Res. Ther.* (2016). doi:10.1186/s13075-016-1107-x

109. Shen, Z. *et al.* Pharmacokinetics, pharmacodynamics, and safety of lesinurad, a selective uric acid reabsorption inhibitor, in healthy adult males. *Drug Des. Devel. Ther.* (2015). doi:10.2147/DDDT.S85193

110. Kydd, A. S. *et al.* Urate-lowering therapy for the management of gout: Summary of 2 cochrane reviews. *Journal of Rheumatology* (2014). doi:10.3899/jrheum.140460

111. Martinon, F., Pétrilli, V., Mayor, A., Tardivel, A. & Tschopp, J. Gout-associated uric acid crystals activate the NALP3 inflammasome. *Nature* **440**, 237–241 (2006).

112. Kang, D. H. & Nakagawa, T. Uric acid and chronic renal disease: Possible implication of hyperuricemia on progression of renal disease. *Seminars in Nephrology* (2005). doi:10.1016/j.semnephrol.2004.10.001

113. Shi, Y., Evans, J. E. & Rock, K. L. Molecular identification of a danger signal that alerts the immune system to dying cells. *Nature* (2003). doi:10.1038/nature01991

114. Kuhn, S. *et al.* Increased Numbers of Monocyte-Derived Dendritic Cells during Successful Tumor Immunotherapy with Immune-Activating Agents. *J. Immunol.* (2013). doi:10.4049/jimmunol.1301135

115. Davies, K. J. A., Sevanian, A., Muakkassah-Kelly, S. F. & Hochstein, P. Uric acid-iron ion complexes. A new aspect of the antioxidant functions of uric acid. *Biochem. J.* (1986). doi:10.1042/bj2350747

116. Einsele, H., Clemens, M. R., Wegner, U. & Waller, H. D. Effect of free radical scavengers and metal ion chelators on hydrogen peroxide and phenylhydrazine induced red blood cell lipid peroxidation. *Free Radic. Res.* (1987). doi:10.3109/10715768709069791

117. Schwarzschild, M. A. *et al.* Inosine to increase serum and cerebrospinal fluid urate in parkinson disease a randomized clinical trial. *JAMA Neurol.* (2014). doi:10.1001/jamaneurol.2013.5528

118. Ascherio, A. *et al.* Urate as a predictor of the rate of clinical decline in Parkinson disease. *Arch. Neurol.* (2009). doi:10.1001/archneurol.2009.247

119. Abraham, A. & Drory, V. E. Influence of serum uric acid levels on prognosis and survival in amyotrophic lateral sclerosis: A meta-analysis. *J. Neurol.* (2014). doi:10.1007/s00415-014-7331-x

120. Braga, T. T. *et al.* Soluble Uric Acid Activates the NLRP3 Inflammasome. *Sci. Rep.* **7**, 1–14 (2017).

121. Shi, Y., Evans, J. & Rock, K. Molecular identification of a danger\rsignal that alerts the immune\rsystem to dying cells. *Nature* **425**, 516–521 (2003).

122. Cri, T. O. *et al.* Soluble uric acid primes TLR-induced proin fl ammatory cytokine production by human primary cells via inhibition of IL-1Ra. 755–762 (2016). doi:10.1136/annrheumdis-2014-206564

123. Cris, T. O. Uric acid priming in human monocytes is driven by the AKT – PRAS40 autophagy pathway. (2017). doi:10.1073/pnas.1620910114

124. Sautin, Y. Y., Nakagawa, T., Zharikov, S. & Johnson, R. J. Adverse effects of the classic antioxidant uric acid in adipocytes: NADPH oxidase-mediated oxidative/nitrosative stress. *AJP Cell Physiol.* (2007). doi:10.1152/ajpcell.00600.2006

125. Luo, N. *et al.* Macrophage adiponectin expression improves insulin sensitivity and protects against inflammation and atherosclerosis. *Diabetes* (2010). doi:10.2337/db09-1338

126. Khosla, U. M. *et al.* Hyperuricemia induces endothelial dysfunction. *Kidney Int.* (2005). doi:10.1111/j.1523-1755.2005.00273.x

127. Park, J. H. *et al.* Uric acid attenuates nitric oxide production by decreasing the interaction between endothelial nitric oxide synthase and calmodulin in human umbilical vein endothelial cells: A mechanism for uric acid-induced cardiovascular disease development. *Nitric Oxide - Biol. Chem.* (2013). doi:10.1016/j.niox.2013.04.003

128. Dalbeth, N., Merriman, T. R. & Stamp, L. K. Gout. *Lancet* **388**, 2039–2052 (2016).

129. Harris, C. M., Lloyd, D. C. E. F. & Lewis, J. The prevalence and prophylaxis of gout in England. *J. Clin. Epidemiol.* (1995). doi:10.1016/0895-4356(94)00244-K

130. Wallace, K. L., Riedel, A. A., Joseph-Ridge, N. & Wortmann, R. Increasing prevalence of gout and hyperuricemia over 10 years among older adults in a managed care population. *J. Rheumatol.* (2004). doi:0315162X-31-1582 [pii]

131. Miao, Z. *et al.* Dietary and lifestyle changes associated with high prevalence of hyperuricemia and gout in the Shandong coastal cities of Eastern China. *J. Rheumatol.* (2008).

132. Singh, J. A., Reddy, S. G. & Kundukulam, J. Risk factors for gout and prevention: A systematic review of the literature. *Current Opinion in Rheumatology* (2011). doi:10.1097/BOR.0b013e3283438e13

133. Zhang, Y. *et al.* Alcohol Consumption as a Trigger of Recurrent Gout Attacks. *Am. J. Med.* (2006). doi:10.1016/j.amjmed.2006.01.020

134. Zhang, Y. *et al.* Purine-rich foods intake and recurrent gout attacks. *Ann. Rheum. Dis.* (2012). doi:10.1136/annrheumdis-2011-201215

135. Witkowska, K. *et al.* Human SLC2A9a and SLC2A9b isoforms mediate electrogenic transport of urate with different characteristics in the presence of hexoses. *AJP Ren. Physiol.* (2012). doi:10.1152/ajprenal.00134.2012

136. Choi, H. K., Liu, S. & Curhan, G. Intake of purine-rich foods, protein, and dairy products and relationship to serum levels of uric acid: The third national health and nutrition examination survey. *Arthritis Rheum.* (2005). doi:10.1002/art.20761

137. Choi, H. K. & Curhan, G. Coffee, tea, and caffeine consumption and serum uric acid level: The Third National Health and Nutrition Examination Survey. *Arthritis Care Res.* (2007). doi:10.1002/art.22762

138. Faller, J. & Fox, I. H. Ethanol-induced hyperuricemia: evidence for increased urate production by activation of adenine nucleotide turnover. *N. Engl. J. Med.* (1982). doi:10.1056/NEJM198212233072602

139. Kumar, S., Gupta, R. & Suppiah, R. Gout in women: Differences in risk factors in young and older women. *N. Z. Med. J.* **125**, 39–45 (2012).

140. Ljubojević, M. *et al.* Rat renal cortical OAT1 and OAT3 exhibit gender differences determined by both androgen stimulation and estrogen inhibition. *Am. J. Physiol. Physiol.* (2004). doi:10.1152/ajprenal.00029.2004

141. Roddy, E. Revisiting the pathogenesis of podagra: Why does gout target the foot? *Journal of Foot and Ankle Research* (2011). doi:10.1186/1757-1146-4-13

142. Merriman, T. R. An update on the genetic architecture of hyperuricemia and gout. *Arthritis Res. Ther.* **17**, (2015).

143. Richette, P. *et al.* 2016 updated EULAR evidence-based recommendations for the management of gout. *Ann. Rheum. Dis.* **76**, 29–42 (2017).

144. Ottaviani, S. *et al.* Efficacy of anakinra in gouty arthritis: A retrospective study of 40 cases. *Arthritis Res. Ther.* (2013). doi:10.1186/ar4303

145. Dubois, E. A., Rissmann, R. & Cohen, A. F. Rilonacept and canakinumab. *Br. J. Clin. Pharmacol.* (2011). doi:10.1111/j.1365-2125.2011.03958.x

146. Khanna, D. *et al.* 2012 American college of rheumatology guidelines for management of gout. part 2: Therapy and antiinflammatory prophylaxis of acute gouty arthritis. *Arthritis Care Res.* (2012). doi:10.1002/acr.21773

147. Dessein, P. H., Shipton, E. A., Stanwix, A. E., Joffe, B. I. & Ramokgadi, J. Beneficial effects of weight loss associated with moderate calorie/carbohydrate restriction, and increased proportional intake of protein and unsaturated fat on serum urate and lipoprotein levels in gout: A pilot study. *Ann. Rheum. Dis.* (2000). doi:10.1136/ard.59.7.539

148. BARLAND, P., NOVIKOFF, A. B. & HAMERMAN, D. Electron microscopy of the human synovial membrane. *J. Cell Biol.* (1962). doi:10.1083/jcb.14.2.207

149. Edwards, J. C. W. The Origin of Type A Synovial Lining Cells. *Immunobiology* **161**, 227–231 (1982).

150. Edwards, J. C. W. Fibroblast biology. Development and differentiation of synovial fibroblasts in arthritis. *Arthritis Research* (2000). doi:10.1186/ar110

151. Nelson, E. E. & Guyer, A. E. The role of uric acid as an endogenous danger signal in immunity and inflammation. **1**, 233–245 (2012).

152. Chhana, A., Lee, G. & Dalbeth, N. Factors influencing the crystallization of monosodium urate: a systematic literature review. *BMC Musculoskelet. Disord.* (2015). doi:10.1186/s12891-015-0762-4

153. Dorner, R. W., Weiss, T. D., Baldassare, A. R., Moore, T. L. & Zuckner, J. Plasma and synovial fluid as solvents for monosodium urate. *Ann. Rheum. Dis.* 70–74 (1981).

154. Martillo, M. A., Nazzal, L. & Crittenden, D. B. The crystallization of monosodium urate. *Curr. Rheumatol. Rep.* (2014). doi:10.1007/s11926-013-0400-9

155. Busso;, N. & So, A. Mechanisms of inflammation in gout. *Arthritis Res. Ther.* **42**, 479–479 (2010).

156. Chung, Y. H., Kim, D. H. & Lee, W. W. Monosodium urate crystal-induced pro-interleukin-1β production is post-transcriptionally regulated via the p38 signaling pathway in human monocytes. *Sci. Rep.* **6**, 1–15 (2016).

157. Schiltz, C. *et al.* Monosodium urate monohydrate crystal-induced inflammation in vivo: Quantitative histomorphometric analysis of cellular events. *Arthritis Rheum.* (2002). doi:10.1002/art.10326

158. Khameneh, H. J. *et al.* C5a regulates IL-1β production and leukocyte recruitment in a murine model of monosodium urate crystal-induced peritonitis. *Front. Pharmacol.* (2017). doi:10.3389/fphar.2017.00010

159. Muller, W. A. Leukocyte-endothelial-cell interactions in leukocyte transmigration and the inflammatory response. *Trends in Immunology* (2003). doi:10.1016/S1471-4906(03)00117-0

160. Ragab, G., Elshahaly, M. & Bardin, T. Gout: An old disease in new perspective – A review. *J. Adv. Res.* **8**, 495–511 (2017).

161. Chen, Y. H. *et al.* Spontaneous resolution of acute gouty arthritis is associated with rapid induction of the anti-inflammatory factors TGFβ1, IL-10 and soluble TNF receptors and the intracellular cytokine negative regulators CIS and SOCS3. *Ann. Rheum. Dis.* (2011). doi:10.1136/ard.2010.145821

162. Schauer, C. *et al.* Aggregated neutrophil extracellular traps limit inflammation by degrading cytokines and chemokines. *Nat. Med.* (2014). doi:10.1038/nm.3547

163. Empson, V. G., McQueen, F. M. & Dalbeth, N. The natural killer cell: A further innate mediator of gouty inflammation. *Immunology and Cell Biology* (2010). doi:10.1038/icb.2009.91

164. Lai, S. Inflammatory Cells in Tissues of Gout Patients and Their Correlations with Comorbidities. *Open Rheumatol. J.* (2013). doi:10.2174/1874312901307010026

165. Dinarello, C. A. How interleukin-1β induces gouty arthritis. *Arthritis and Rheumatism* (2010). doi:10.1002/art.27663

166. Z Brown, M. E. G. W. W. C. R. M. S. S. L. K. J. W. Chemokine gene expression and secretion by cytokine-activated human microvascular endothelial cells. Differential regulation of monocyte chemoattractant protein-1 and interleukin-8 in response to interferon-gamma. *Am. J. Pathol.* (1994).

167. Pouliot, M. *et al.* Monosodium Urate Microcrystals Induce Cyclooxygenase-2 in Human Monocytes. *Blood* (1998).

168. Robinson, D. R. *Gout: Basic Science and Clinical Practice*. (2013).

169. Martin, W. J., Shaw, O., Liu, X., Steiger, S. & Harper, J. L. Monosodium urate monohydrate crystal-recruited noninflammatory monocytes differentiate into M1-like proinflammatory macrophages in a peritoneal murine model of gout. *Arthritis Rheum.* **63**, 1322–1332 (2011).

170. Landis, R. C. *et al.* Safe disposal of inflammatory monosodium urate monohydrate crystals by differentiated macrophages. *Arthritis Rheum.* **46**, 3026–3033 (2002).

171. Yagnik, D. R. *et al.* Macrophage release of transforming growth factor β1 during resolution of monosodium urate monohydrate crystal-induced inflammation. *Arthritis Rheum.* (2004). doi:10.1002/art.20317

172. Martin, W. J. & Harper, J. L. Innate inflammation and resolution in acute gout. *Immunol. Cell Biol.* **88**, 15–19 (2009).

173. Dalbeth, N. *et al.* Cellular characterization of the gouty tophus: A quantitative analysis. *Arthritis Rheum.* (2010). doi:10.1002/art.27356

174. Chapman, P. T. *et al.* Endothelial activation in monosodium urate monohydrate crystal-induced inflammation: In vitro and in vivo studies on the roles of tumor necrosis factor α and interleukin-1. *Arthritis Rheum.* (1997). doi:10.1002/art.1780400525

175. Kim, M.-H., Curry, F.-R. E. & Simon, S. I. Dynamics of neutrophil extravasation and vascular permeability are uncoupled during aseptic cutaneous wounding. *Am. J. Physiol. Physiol.* (2009). doi:10.1152/ajpcell.00520.2008

176. Middleton, J., Patterson, A. M., Gardner, L., Schmutz, C. & Ashton, B. A. Leukocyte extravasation: Chemokine transport and presentation by the endothelium. *Blood* (2002). doi:10.1182/blood.V100.12.3853

177. Rich, A. M., Giedd, K. N., Cristello, P. & Weissmann, G. Granules are necessary for death of neutrophils after phagocytosis of crystalline monosodium urate. *Inflammation* (1985). doi:10.1007/BF00916273

178. Dalbeth, N. & Haskard, D. O. Mechanisms of inflammation in gout. 1090–1096 (2005). doi:10.1093/rheumatology/keh640

179. Akahoshi, T., Nagaoka, T., Namai, R., Sekiyama, N. & Kondo, H. Prevention of neutrophil apoptosis by monosodium urate crystals. *Rheumatol. Int.* **16**, 231–235 (1997).

180. Papayannopoulos, V., Metzler, K. D., Hakkim, A. & Zychlinsky, A. Neutrophil elastase and myeloperoxidase regulate the formation of neutrophil extracellular traps. *J. Cell Biol.* (2010). doi:10.1083/jcb.201006052

181. Park, S. Y. *et al.* Autophagy primes neutrophils for neutrophil extracellular trap formation during sepsis.

Am. J. Respir. Crit. Care Med. (2017). doi:10.1164/rccm.201603-0596OC

182. Desai, J. *et al.* PMA and crystal-induced neutrophil extracellular trap formation involves RIPK1-RIPK3-MLKL signaling. *Eur. J. Immunol.* (2016). doi:10.1002/eji.201545605

183. Steiger, S. & Harper, J. L. Neutrophil cannibalism triggers transforming growth factor β1 production and self regulation of neutrophil inflammatory function in monosodium urate monohydrate crystal-induced inflammation in mice. *Arthritis Rheum.* (2013). doi:10.1002/art.37822

184. Schett, G., Schauer, C., Hoffmann, M. & Herrmann, M. Why does the gout attack stop? A roadmap for the immune pathogenesis of gout. *RMD Open* **1**, 1–5 (2015).

185. Gagné, V. *et al.* Modulation of monosodium urate crystal-induced responses in neutrophils by the myeloid inhibitory C-type lectin-like receptor: Potential therapeutic implications. *Arthritis Res. Ther.* (2013). doi:10.1186/ar4250

186. Duskin-Bitan, H. *et al.* The degree of asymptomatic hyperuricemia and the risk of gout. A retrospective analysis of a large cohort. *Clin. Rheumatol.* **33**, 549–553 (2014).

187. Dalbeth, N. *et al.* Relationship between serum urate concentration and clinically evident incident gout: An individual participant data analysis. *Ann. Rheum. Dis.* **77**, 1048–1052 (2018).

188. Schumacher, H. R. *et al.* Effects of febuxostat versus allopurinol and placebo in reducing serum urate in subjects with hyperuricemia and gout: A 28-week, phase III, randomized, double-blind, parallel-group trial. *Arthritis Care Res.* (2008). doi:10.1002/art.24209

189. Schlesinger, N., Norquist, J. M. & Watson, D. J. Serum urate during acute gout. *J. Rheumatol.* **36**, 1287–1289 (2009).

190. Vargas-Santos, A. B. & Neogi, T. Management of Gout and Hyperuricemia in CKD. *Am. J. Kidney Dis.* **70**, 422–439 (2017).

191. Prasad Sah, O. S. & Qing, Y. X. Associations between Hyperuricemia and Chronic Kidney Disease: A Review. *Nephrourol. Mon.* (2015). doi:10.5812/numonthly.7(3)2015.27233

192. Juraschek, S. P., Kovell, L. C., Miller, E. R. & Gelber, A. C. Association of kidney disease with prevalent gout in the United States in 1988–1994 and 2007–2010. **42**, 551–561 (2013).

193. Jing, J. *et al.* Prevalence and correlates of gout in a large cohort of patients with chronic kidney disease: the German Chronic Kidney Disease (GCKD) study. *Nephrol. Dial. Transplant.* **30**, 613–621 (2015).

194. Ifudu, O., Tan, C. C., Dulin, A. L., Delano, B. G. & Friedman, E. A. Gouty Arthritis in End-Stage Renal Disease: Clinical Course and Rarity of New Cases. *Am. J. Kidney Dis.* (1994). doi:10.1016/S0272-6386(12)80995-4

195. Ohno, I. *et al.* Frequency of gouty arthritis in patients with end-stage renal disease in Japan. *Intern Med* (2005). doi:10.2169/internalmedicine.44.706

196. Ramirez, M. E. G. & Bargman, J. M. Treatment of asymptomatic hyperuricemia in chronic kidney disease: A new target in an old enemy – A review. *J. Adv. Res.* **8**, 551–554 (2017).

197. Roughley, M. *et al.* Risk of chronic kidney disease in patients with gout and the impact of urate lowering therapy: a population-based cohort study. *Arthritis Res. Ther.* **20**, 243 (2018).

198. Badve, S. V. *et al.* Challenges of conducting a trial of uric-acid-lowering therapy in CKD. *Nat. Rev. Nephrol.* **7**, 295–300 (2011).

199. KDIGO & CKD. KDIGO CPG for Evaluation & Management of CKD 2013. *Kidney Int. Suppl.* **3**, 4–4 (2013).

200. Preitner, F. *et al.* Urate-induced acute renal failure and chronic inflammation in liver-specific Glut9 knockout mice. *AJP Ren. Physiol.* **305**, F786–F795 (2013).

201. Sperandio, M., Pickard, J., Unnikrishnan, S., Acton, S. T. & Ley, K. Analysis of Leukocyte Rolling In Vivo and In Vitro. *Methods in Enzymology* (2006). doi:10.1016/S0076-6879(06)16023-1

202. Gorczynski, R. J., Klitzman, B. & Duling, B. R. Interrelations between contracting striated muscle and precapillary microvessels. *Am. J. Physiol. Circ. Physiol.* (2017). doi:10.1152/ajpheart.1978.235.5.h494

203. Ley, K. & Gaehtgens, P. Endothelial, not hemodynamic, differences are responsible for preferential leukocyte rolling in rat mesenteric vanules. *Circ. Res.* (1991). doi:10.1161/01.RES.69.4.1034

204. Nakazawa, D. *et al.* Histones and Neutrophil Extracellular Traps Enhance Tubular Necrosis and Remote

Organ Injury in Ischemic AKI. *J. Am. Soc. Nephrol.* **28**, 1753–1768 (2017).

205. Daigo, N. *et al.* Enhanced formation and disordered regulation of nets in MPO-ANCA-associated vasculitis. *Nephrology* (2014).

206. Pruenster, M. *et al.* Extracellular MRP8/14 is a regulator of β2 integrin-dependent neutrophil slow rolling and adhesion. *Nat. Commun.* (2015). doi:10.1038/ncomms7915

207. Preitner, F. *et al.* Glut9 is a major regulator of urate homeostasis and its genetic inactivation induces hyperuricosuria and urate nephropathy. *Proc. Natl. Acad. Sci.* **106**, 15501–15506 (2009).

208. Edwards, J. C. W., Sedgwick, A. D. & Willoughby, D. A. The formation of a structure with the features of synovial lining by subcutaneous injection of air: An in vivo tissue culture system. *J. Pathol.* (1981). doi:10.1002/path.1711340205

209. Vestweber, D. How leukocytes cross the vascular endothelium. *Nat. Rev. Immunol.* **15**, 692–704 (2015).

210. Merrill-Skoloff, G., Dubois, C., Atkinson, B. & Furie, B. Real Time In Vivo Imaging of Platelets During Thrombus Formation. in *Platelets* (2013). doi:10.1016/B978-0-12-387837-3.00031-6

211. Steeber, D. A., Campbell, M. A., Basit, A., Ley, K. & Tedder, T. F. Optimal selectin-mediated rolling of leukocytes during inflammation in vivo requires intercellular adhesion molecule-1 expression. *Proc. Natl. Acad. Sci.* **95**, 7562–7567 (1998).

212. Evans, R. *et al.* Integrins in immunity. *J. Cell Sci.* **122**, 215–225 (2009).

213. McDowall, A. *et al.* A novel form of integrin dysfunction involving β1, β2, and β3 integrins. *J. Clin. Invest.* (2003). doi:10.1172/JCI200314076

214. Rossaint, J. *et al.* FGF23 signaling impairs neutrophil recruitment and host defense during CKD. *J. Clin. Invest.* **126**, 962–974 (2016).

215. Papayannopoulos, V. Neutrophil extracellular traps in immunity and disease. *Nature Reviews Immunology* (2018). doi:10.1038/nri.2017.105

216. Khandpur, R. *et al.* NETs are a source of citrullinated autoantigens and stimulate inflammatory responses in rheumatoid arthritis. *Sci. Transl. Med.* (2013). doi:10.1126/scitranslmed.3005580

217. Pinegin, B., Vorobjeva, N. & Pinegin, V. Neutrophil extracellular traps and their role in the development of chronic inflammation and autoimmunity. *Autoimmunity Reviews* (2015). doi:10.1016/j.autrev.2015.03.002

218. Kessenbrock, K. *et al.* Netting neutrophils in autoimmune small-vessel vasculitis. *Nat. Med.* (2009). doi:10.1038/nm.1959

219. Garcia-Romo, G. S. *et al.* Netting neutrophils are major inducers of type I IFN production in pediatric systemic lupus erythematosus. *Sci. Transl. Med.* (2011). doi:10.1126/scitranslmed.3001201

220. Kim, J.-K. *et al.* Increased Neutrophil Extracellular Trap Formation in Uremia Is Associated with Chronic Inflammation and Prevalent Coronary Artery Disease. *J. Immunol. Res.* (2017). doi:10.1155/2017/8415179

221. Kenny, E. F. *et al.* Diverse stimuli engage different neutrophil extracellular trap pathways. *Elife* (2017). doi:10.7554/eLife.24437

222. Kano, H., Aminul Huq, M., Tsuda, M., Noguchi, H. & Takeyama, N. Sandwich ELISA for Circulating Myeloperoxidase- and Neutrophil Elastase-DNA Complexes Released from Neutrophil Extracellular Traps. *Adv. Tech. Biol. Med.* (2017). doi:10.4172/2379-1764.1000196

223. Yago, T., Tsukuda, M. & Minami, M. P-selectin binding promotes the adhesion of monocytes to VCAM-1 under flow conditions. *J. Immunol.* (1999).

224. Chuluyan, H. E. & Issekutz, A. C. VLA-4 integrin can mediate CD11/CD18-independent transendothelial migration of human monocytes. *J. Clin. Invest.* (1993). doi:10.1172/JCI116895

225. Sil, P., Wicklum, H., Surell, C. & Rada, B. Macrophage-derived IL-1β enhances monosodium urate crystal-triggered NET formation. *Inflamm. Res.* **66**, 227–237 (2017).

226. Kaplan, M. & Radic, M. Neutrophil extracellular traps (NETs): Double-edged swords of innate immunity. *J Immunol.* **189**, 2689–2695 (2012).

227. Wright, A. F., Rudan, I., Hastie, N. D. & Campbell, H. A complexity of urate transporters. *Kidney Int.* **78**, 446–452 (2010).

228. Liu, S. *et al.* Phloretin attenuates hyperuricemia-induced endothelial dysfunction through co-inhibiting inflammation and GLUT9-mediated uric acid uptake. *J. Cell. Mol. Med.* (2017). doi:10.1111/jcmm.13176

229. Bosshart, H. & Heinzelmann, M. THP-1 cells as a model for human monocytes. *Ann. Transl. Med.* **4**, 438–438 (2016).

230. Wright, A. F., Rudan, I., Hastie, N. D. & Campbell, H. A complexity of urate transporters. *Kidney Int.* **78**, 446–452 (2010).

231. Lai, K.-J., Kor, C.-T. & Hsieh, Y.-P. An Inverse Relationship between Hyperuricemia and Mortality in Patients Undergoing Continuous Ambulatory Peritoneal Dialysis. *J. Clin. Med.* **7**, 416 (2018).

232. Whiteman, M., Ketsawatsakul, U. & Halliwell, B. A reassessment of the peroxynitrite scavenging activity of uric acid. in *Annals of the New York Academy of Sciences* (2002). doi:10.1111/j.1749-6632.2002.tb04072.x

233. Kuzkaya, N., Weissmann, N., Harrison, D. G. & Dikalov, S. Interactions of peroxynitrite with uric acid in the presence of ascorbate and thiols: Implications for uncoupling endothelial nitric oxide synthase. *Biochem. Pharmacol.* (2005). doi:10.1016/j.bcp.2005.05.009

234. Komori, H., Yamada, K., Tamai, I., Yamada, K. & Tamai, I. Hyperuricemia enhances intracellular urate accumulation via down-regulation of cell-surface BCRP/ABCG2 expression in vascular endothelial cells. *Biochim Biophys Acta Biomembr* **1860(5)**, 973–980 (2018).

235. Itahana, Y. *et al.* The uric acid transporter SLC2A9 is a direct target gene of the tumor suppressor p53 contributing to antioxidant defense. *Oncogene* **34**, 1799–1810 (2014).

236. Hink, H. U. *et al.* Peroxidase properties of extracellular superoxide dismutase role of uric acid in modulating in vivo activity. *Arterioscler. Thromb. Vasc. Biol.* (2002). doi:10.1161/01.ATV.0000027524.86752.02

237. Cai, W. *et al.* Uric Acid Induces Endothelial Dysfunction by Activating the HMGB1/RAGE Signaling Pathway. *Biomed Res. Int.* **2017**, 1–11 (2017).

238. Cook, S. *et al.* Partial gene deletion of endothelial nitric oxide synthase predisposes to exaggerated high-fat diet - Induced insulin resistance and arterial hypertension. *Diabetes* (2004). doi:10.2337/diabetes.53.8.2067

239. Duplain, H. *et al.* Insulin resistance, hyperlipidemia, and hypertension in mice lacking endothelial nitric oxide synthase. *Circulation* (2001). doi:10.1161/01.CIR.104.3.342

240. Zharikov, S. *et al.* Uric acid decreases NO production and increases arginase activity in cultured pulmonary artery endothelial cells. *Am. J. Physiol. Physiol.* (2008). doi:10.1152/ajpcell.00075.2008

241. Liang, W. Y. *et al.* Uric acid promotes chemokine and adhesion molecule production in vascular endothelium via nuclear factor-kappa B signaling. *Nutr. Metab. Cardiovasc. Dis.* **25**, 187–194 (2015).

242. Shi, Y. *et al.* Blockade of Enhancer of Zeste Homolog 2 alleviates renal injury associated with hyperuricemia. *Am. J. Physiol. Physiol.* ajprenal.00234.2018 (2018). doi:10.1152/ajprenal.00234.2018

243. Kim, S.-M. *et al.* Hyperuricemia-induced NLRP3 activation of macrophages contributes to the progression of diabetic nephropathy. *Am. J. Physiol. - Ren. Physiol.* **308**, F993–F1003 (2015).

244. Wang, Y. *et al.* Blockade of Enhancer of Zeste Homolog 2 alleviates renal injury associated with hyperuricemia. *Am. J. Physiol. Physiol.* (2018). doi:10.1152/ajprenal.00234.2018

245. Badve, S. V. *et al.* Challenges of conducting a trial of uric-acid-lowering therapy in CKD. *Nat. Rev. Nephrol.* **7**, 295–300 (2011).

246. Latourte, A., Bardin, T. & Richette, P. Prophylaxis for acute gout flares after initiation of urate-lowering therapy. *Rheumatology (United Kingdom)* (2014). doi:10.1093/rheumatology/keu157

247. Slobodnick, A., Shah, B., Pillinger, M. H. & Krasnokutsky, S. Colchicine: Old and New. *American Journal of Medicine* (2015). doi:10.1016/j.amjmed.2014.12.010

248. Futosi, K., Fodor, S. & Mócsai, A. Neutrophil cell surface receptors and their intracellular signal transduction pathways. *Int. Immunopharmacol.* (2013). doi:10.1016/j.intimp.2013.11.010

249. Thompson, S. *et al.* Cause of Death in Patients with Reduced Kidney Function. *J. Am. Soc. Nephrol.* (2015). doi:10.1681/asn.2014070714

250. Rossaint, J. *et al.* Acute loss of renal function attenuates slow leukocyte rolling and transmigration by

interfering with intracellular signaling. *Kidney Int.* **80**, 493–503 (2011).

251. Clark, R. A., Hamory, B. H., Ford, G. H. & Kimball, H. R. Chemotaxis in acute renal failure. *J. Infect. Dis.* **126**, 460–463 (1972).

252. Rossaint, J., Unruh, M. & Zarbock, A. Fibroblast growth factor 23 actions in inflammation: A key factor in CKD outcomes. *Nephrol. Dial. Transplant.* (2017). doi:10.1093/ndt/gfw331

253. Kempf, T. *et al.* GDF-15 is an inhibitor of leukocyte integrin activation required for survival after myocardial infarction in mice. *Nat. Med.* (2011). doi:10.1038/nm.2354

254. Eskan, M. A. *et al.* The leukocyte integrin antagonist Del-1 inhibits IL-17-mediated inflammatory bone loss. *Nat. Immunol.* (2012). doi:10.1038/ni.2260

255. Drechsler, M. *et al.* Annexin A1 counteracts chemokine-induced arterial myeloid cell recruitment. *Circ. Res.* (2015). doi:10.1161/CIRCRESAHA.116.305825

256. Abram, C. L. & Lowell, C. a. The Ins and Outs of Leukocyte Integrin Signaling. *Annu. Rev. Immunol.* **27**, 339–362 (2009).

257. Desai, J., Steiger, S. & Anders, H. J. Molecular Pathophysiology of Gout. *Trends in Molecular Medicine* (2017). doi:10.1016/j.molmed.2017.06.005

258. Mitroulis, I. *et al.* Neutrophil extracellular trap formation is associated with IL-1β and autophagy-related signaling in gout. *PLoS One* (2011). doi:10.1371/journal.pone.0029318

259. Kim, J. K. *et al.* Increased Neutrophil Extracellular Trap Formation in Uremia Is Associated with Chronic Inflammation and Prevalent Coronary Artery Disease. *J. Immunol. Res.* (2017). doi:10.1155/2017/8415179

260. Hakkim, A. *et al.* Impairment of neutrophil extracellular trap degradation is associated with lupus nephritis. *Proc. Natl. Acad. Sci.* (2010). doi:10.1073/pnas.0909927107

261. Annanmaki, T., Muuronen, A. & Murros, K. Low plasma uric acid level in Parkinson's disease. *Mov. Disord.* (2007). doi:10.1002/mds.21502

262. Grozdanov, V. *et al.* Inflammatory dysregulation of blood monocytes in Parkinson's disease patients. *Acta Neuropathol.* **128**, 651–663 (2014).

263. Price, K. L. Human Vascular Smooth Muscle Cells Express a Urate Transporter. *J. Am. Soc. Nephrol.* (2006). doi:10.1681/asn.2006030264

264. Liu, S. *et al.* Phloretin attenuates hyperuricemia-induced endothelial dysfunction through co-inhibiting inflammation and GLUT9-mediated uric acid uptake. *J. Cell. Mol. Med.* **21**, 2553–2562 (2017).

265. Mobasheri, A. *et al.* Expression of the GLUT1 and GLUT9 facilitative glucose transporters in embryonic chondroblasts and mature chondrocytes in ovine articular cartilage. *Cell Biol. Int.* (2005). doi:10.1016/j.cellbi.2004.11.024

266. Sabirov, R. Z. *et al.* The organic anion transporter SLCO2A1 constitutes the core component of the Maxi-Cl channel. *EMBO J.* (2017). doi:10.15252/embj.201796685

267. Badulescu, M., Macovei, L. & Rezus, E. Acute gout attack with normal serum uric acid levels. *Rev Med Chir Soc Med Nat Iasi* (2014).

268. Rouault, T., Caldwell, D. S. & Holmes, E. W. Aspiration of the asymptomatic metatarsophalangeal joint in gout patients and hyperuricemic controls. *Arthritis Rheum.* (1982). doi:10.1002/art.1780250215

269. Galvao, I. *et al.* Macrophage migration inhibitory factor drives neutrophil accumulation by facilitating IL-1 production in a murine model of acute gout. *J. Leukoc. Biol.* **99**, 1035–1043 (2016).

270. Malyszko, J. Mechanism of endothelial dysfunction in chronic kidney disease. *Clinica Chimica Acta* (2010). doi:10.1016/j.cca.2010.06.019

9 Acknowledgements

Time flies! I still clearly remember the first day in the lab four years ago: everything was so fresh and attractive. This four-year PhD time has been a truly life-changing experience and it would not been possible without the support, guidance and encouragement that I received from many people.

First I would like to thank my supervisor Prof. Hans-Joachim Anders. Thank you very much for giving me the opportunity to work at the Medizinische Klinik und Poliklinik IV, Nephrologisches Zentrum, LMU Munich; providing encouragement, patience and professional advice for me to precede the doctoral program. I am really appreciative all of these.

I would express my special thank to my co-supervisor Dr. Stefanie Steiger for everything you have done for me both personal- and professional-wise, and for your constant support and guidance, which made my access simpler to the research. It wouldn't have been possible to conduct this research without your precious support.

I gratefully acknowledge the funding received towards my PhD from the China Scholarship Council (CSC) that provides enough funding for my four-year of living here.

I greatly appreciate the support received from Prof. Markus Sperandio, Dr. Monika Pruenster, Roland Immler at the Walter-Brendel-Center of Experimental Medicine Biomedical Center, Klinik III, LMU for sharing their knowledge about neutrophils and their cooperation to be able to complete this thesis.

I thank all my lab friends, Julian, Lidia, Lina, Luying, Moshen, Manga, Shangqing, Shishi, Shrikant, Santosh, Taka, Viviane, Wenkai, Yutian, Yao, Zhibo and all medical students including Bao Vi, Julia, Markus, Moritz, Nils, Tehyung, for the wonderful time we had together. And also thank Dan, Jana and Yvonne for providing skillful technical assistance to carry out the research work successfully.

I would like to thank all of my friends, Juanjuan, Ping Li, Chong Wang, Yanxin Fan, Yan Gu, Feng Yang, Mei Yang who supported me in my life and incented me to strive towards my goals.

A special thanks to my family and words cannot express how grateful I am to my grandmother, my mother, my father, and my brother who always encourage and support me spiritually through my PHD time and my life in general. At the end I would like express appreciation to my beloved boyfriend Fangzhou, for all your love and support.

Thanks for all your encouragement!

10 Appendix

Composition of buffers used in this thesis

PBS buffer:

NaCl	8 g
Na_2HPO_4	1.16 g
KH_2PO_4	0.2 g
KCl	0.2 g

Dissolved in 1l ddH_2O and adjust pH to 7.4 with HCl.

0.1M Sodium Carbonate buffer:

$NaHCO_3$	1.426 g
Na2CO3	0.318 g

Dissolved in 0.2 l ddH_2O and adjust pH to 9.5 with NaOH.

Red Blood Cell lysis buffer

NH_4Cl	0.829 g
$NaHCO_3$	0.1 g
EDTA	0.037 g

Dissolved in 100 ml ddH_2O, filtered with 0.2µm filter and storage at 4 °C.

FACS buffer :

D-PBS	500 ml
NaN_3	0.05 g (0.01 %)
BSA	0.5 g (0.1 %)

Storage at 4 °C.

0.01% Tamoxifen:

Tamoxifen	15 mg
100% Ethnol	0.15 ml
Sunflower oil	1.35 ml

Prepare freshly and preheated in 37 °C water bath to dissolve the power.

Magnetic separation buffer :

D-PBS	100 ml
0.5M EDTA	0.4 ml
BSA	0.5 g

Filtered with 0.2µm filter and storage at 4 °C.

Collagenase / DNAse solution:

Collagenase	10 mg
1mg/ml DNAse	0.2 ml
HBSS	9.8 ml

Always prepare freshly.